POLITECNICO DI MILANO

Scuola di Ingegneria Industriale

Corso di Laurea in Ingegneria Meccanica

Numerical analysis of the effect of Electronically Controlled Pneumatic braking on the longitudinal dynamics of freight train

Relatore: Prof. Stefano Melzi

Correlatore: Prof. A.A. Shabana

Tesi di Laurea di:

Martino Volpi   Mat. 770792

Anno Accademico 2012 – 2013

Table of Contents

List of Figures

List of Tables

ABSTRACT

The importance of braking forces in the longitudinal train dynamics and stability is well-known in the railway engineering. While, with current freight train braking systems originally developed in the nineteenth century, brakes on individual rail cars are applied sequentially at the speed of air pressure moving from car to car, along trains that are often well over a mile in length. As a result, there is a time delay in the braking of the neighboring cars; this causes the running of rear cars into front cars, thus producing large forces in couplers. The induced compression and tensile forces are mainly of longitudinal nature and considered to be responsible for large amount of expenses regarding rolling stock and track repairs as well as lower safety level of the trains, making also train handling more difficult, requiring longer stopping distances, and may prematurely deplete air brake reservoirs. Simulations of such phenomena are very important both for safety and economic reasons for long trains. From this investigation one can prove that the capability of the system to apply all brake forces simultaneously will reduce coupler impacts during brake applications and improve vehicle stability, therefore the development of ECP (Electronically controlled pneumatic) brake model. ECP braking uses electronic controls which make it possible to activate air-powered brakes on all the cars throughout the train at the same time. Applying the brakes uniformly and instantaneously in this way gives better train control, shortens the stopping distances, and leads to a lower risk of derailment or of coupling breakage. To this end a development of new ECP braking system should be modeled three-dimensional non-linear train car coupler model that takes into account the geometric nonlinearity due to the coupler and car body displacements is developed. Comparison between the new ECP brake model and the traditional air brake model should be done. Different braking scenarios for long train are presented and the effect of brake signal time delay will be discussed by comparing the results at using the traditional air brake system and the ECP braking system.

SOMMARIO

L'importanza dello studio della dinamica longitudinale nelle fasi di frenatura è ben nota nel settore ferroviario. Con i sistemi di frenatura per i treni merci, sviluppati originariamente nel XIX secolo, la frenata sulle singole vetture è applicata in seguito ad un calo di pressione nella condotta pneumatica che percorre l'intero treno. Come risultato, vi è un ritardo di tempo nella frenatura nelle vetture; questo provoca lo schiacciamento delle carrozze posteriori su quelle anteriori producendo così grandi forze sugli accoppiatori. Le forze di compressione e di trazione indotte sono principalmente di natura longitudinale e sono ritenute responsabili di grandi quantità di costi per quanto riguarda il materiale rotabile e le riparazioni dei binari inoltre rendono anche più difficile la manovrabilità il che si traduce nella necessità di maggiori distanze per fermare il treno. Simulazioni di tali fenomeni sono molto importanti sia per la sicurezza sia per ragioni economiche. In questa indagine si vuole mostrare come la capacità del sistema di applicare simultaneamente le forze frenanti su tutte le carrozze riduca le forze di trazione e compressione agenti sugli accoppiatori. Questo migliora la stabilità del veicolo, ne riduce la distanza necessaria per fermarsi, e porta a un minor rischio di deragliamento o di rottura degli accoppiatori. Il sistema di frenatura studiato in questo lavoro, noto come ECP (Electronically Controlled Pneumatic) si propone appunto di applicare la forza frenante in maniera simultanea su tutte le carrozze. Si svilupperà quindi un modello di un sistema ECP con le caratteristiche dei sistemi correntemente in uso e che rispetti la normativa vigente negli USA. La modellazione si concentrerà sul modello pneumatico e dinamico delle valvole e degli elementi del sistema. Il modello del sistema frenante ECP sarà quindi integrato all'interno di un modello multibody ferroviario sviluppato in precedenza, in modo da poter eseguire con esso un'analisi dinamica. Sarà di particolare importanza inoltre la presenza di un modello di accoppiatore non lineare che tenga conto della non linearità geometrica causata dalle caratteristiche dello stesso e dagli spostamenti relativi delle vetture.

ESTRATTO IN ITALIANO

I sistemi ferroviari sono tra i metodi di trasporto comunemente più utilizzati, sia per i passeggeri che per le merci. Il loro uso diffuso ha promosso, nel corso degli anni, continui sviluppi tecnologici, con l' obiettivo di raggiungere velocità operative maggiori al fine di minimizzare i costi e tempi di trasporto. Velocità operative più elevate, tuttavia, richiedono un approccio più sofisticato per la progettazione del veicolo ferroviario in modo tale da evitare deragliamenti e ridurre rumorosità e vibrazioni. Pertanto, sono necessari lo sviluppo e l'utilizzo di modelli computazionali maggiormente accurati per la simulazione di sistemi di veicoli ferroviari soggetti a diverse condizioni di carico, velocità di funzionamento, geometrie del tracciato, frenata e scenari di trazione.

Gli ultimi quindici anni hanno visto una diffusione sempre maggiore di una tecnologia relativamente nuova per il controllo del sistema frenante sui treni merci. La nuova tecnologia è nota “Electronically Controlled Pneumatic brake system” comunemente indicato come ECP.

Il sistema ECP consiste in un nuovo modo di controllare i freni pneumatici già in uso comunemente sui treni merci con l'aggiunta di un insieme di valvole a controllo elettronico a bordo di ogni vettura e di una rete cablata lungo il treno. In questo modo con una ragionevole modifica di un convenzionale sistema frenante ad aria, è possibile aumentare l'efficienza e la capacità di un treno merci.

I requisiti funzionali e le prestazioni del sistema frenante ECP sono indicati nello standard S-4200 " “Electronically Controlled Pneumatic (ECP) Cable-Based Brake Systems –Performance Requirements” (AAR Association of American Railroad) [1]. Il citato standard descrive un sistema di freno ECP come un "sistema di frenatura ferroviario ad aria compressa e controllata da segnali elettronici originati alla locomotiva per applicazioni di servizio e di emergenza” e aggiunge: “ Il sistema fornisce una risposta quasi istantanea ai comandi di frenata, rende possibili anche parziali rilasci dei freni e ricarica continua.”

Il sistema inoltre risponde adeguatamente alla separazione indesiderata o malfunzionamento di tubi o cavi. In caso di emergenza una rapida riduzione della pressione nella condotta pneumatica principale sarà causa di una frenatura di emergenza pneumatica lungo tutto il treno. Sia l'alimentazione elettrica sia il segnale di comunicazione tra le carrozze sono trasmessi tramite un cavo elettrico. Questo cavo, noto come “train line”, si sviluppa per l'intera lunghezza del treno [1],[2]. La condotta pneumatica principale viene ancora usata per fornire un'alimentazione continua di aria compressa da immagazzinare in un serbatoio su ogni carrozza

I principali vantaggi di ECP includono, ma non sono limitati a: ridurre lo spazio di arresto del treno, migliorando quindi i tempi del ciclo di servizio dei treni, aumentare la capacità della rete, migliorare la sicurezza ferroviaria, con un conseguente risparmio di carburante, e riduzione dell'usura del materiale rotabile [3].

Un sistema di frenatura ECP quindi può migliorare sia le operazioni di sicurezza ferroviaria che la manovrabilità riducendo le forze scambiate tra una carrozza e la sua limitrofa, rendendo la gestione dei tempi di fermata più semplice, ricaricando in maniera continua i serbatoi del sistema di frenatura di ogni carrozza del treno, e fornendo spazi di arresto ridotti indipendentemente dalla lunghezza del treno. Questo grazie alla modalità di trasmissione del comando di frenatura elettronico proprio del sistema ECP.

Il sistema ECP possiede diverse caratteristiche che possono aumentare significativamente la capacità di carico e ridurre i tempi di inattività. Le principali sono:

- Trasmissione istantanea del segnale del freno
- Ricarica continua dei serbatoi
- Le funzioni di auto- monitoraggio del sistema

Utilizzando un segnale elettronico invece che uno di pressione per trasmettere il segnale di frenatura si permette la trasmissione istantanea del comando di applicazione o di rilascio pressoché simultanea dei freni lungo l'intera lunghezza del treno.

È anche possibile caricare continuamente i serbatoi anche mentre vengono effettuata la frenata o il rilascio. L'uso di un cavo elettrico che percorre il treno permette anche la possibilità di sviluppare una rete per la raccolta delle informazioni di stato in tempo reale. Le informazioni raccolte permettono un controllo del buono stato del sistema, di auto-diagnosi che possono essere incorporati nel sistema frenante in modo da informare il personale del treno quando è necessaria la manutenzione o in caso di malfunzionamenti di qualunque tipo. Ognuna di queste caratteristiche saranno prese in considerazione per il loro impatto sulla capacità.

Trasmissione istantanea del segnale di frenata

Con i sistemi frenanti attuali c'è un ritardo durante la propagazione del segnale di frenatura mentre con ECP freni esso viene eliminato. Questo ridurrà la “stopping distance” (distanza necessaria al freno per fermarsi completamente) dal 40 al 60 per cento rispetto al convenzionale spazio di frenata. Poiché la distanza minima concessa tra due treni è legata, per motivi di sicurezza, alla “stopping distance”, se tutti i treni di una linea sono equipaggiati con un sistema ECP questo permetterà una maggiore vicinanza tra i treni. Supposto che il sistema di controllo del traffico sulla linea riesca a gestire questa maggiore frequenza, si avrà un aumento significativo della potenzialità di trasporto della linea. In secondo piano la trasmissione istantanea dei comandi di frenata (anche il segnale di rilascio è un “comando di frenata”) può essere utile per velocizzare il rilascio dopo una frenata, riducendo i tempi di ripartenza.

Ricarica continua dei serbatoi

La ricarica continua dei serbatoi e della condotta principale rende l'uso del sistema frenante molto più facile rispetto a quello convenzionale, infatti, per motivi di sicurezza, un treno non può riprendere la marcia se la pressione nei serbatoi è inferiore a una certa soglia e la pressione nella condotta principale pneumatica risulta inferiore alla pressione operativa. Con il sistema convenzionale, una volta che il conducente ha selezionato l'entità della frenata, essa non può essere ridotta a meno di non rilasciare completamente il freno ed eseguire nuovamente la frenata. Questo ha come conseguenza il fatto che spesso si utilizza una forza frenante eccessiva per la mancanza della possibilità di un rilascio parziale, con il risultato di rallentare significativamente le operazioni di ripartenza. La maggiore flessibilità offerta del sistema frenante ECP permette quindi a un treno di viaggiare a velocità maggiori a parità di condizioni della linea e, come già evidenziato, permette di ridurre significativamente il tempo di riavvio dopo l'arresto.

Le funzioni di auto- monitoraggio del sistema

Un segnale elettrico per il controllo dei freni ha il vantaggio di consentire la trasmissione dei dati sulla condizione dei componenti del sistema frenante alla locomotiva. Il conducente può monitorare le condizioni del freno ed essere immediatamente informato di qualsiasi guasto in qualsiasi carrozza del treno. Grazie a queste peculiari caratteristiche la FRA (Federal Railroad Administration) ha emesso un nuovo regolamento che permette che la manutenzione programmata dei freni debba essere eseguita ogni 3.500 miglia rispetto alle 1.000 miglia previste per un treno equipaggiato con freni convenzionali. Questo permette, per esempio, a un treno equipaggiato con un sistema frenante ECP provenienti dai porti di Los Angeles-Long Beach a viaggiare fino a Chicago senza fermarsi per le prove dei freni di routine. Questo non solo riduce i tempi di ciclo, ma può anche ridurre la congestione ai terminali in cui questi controlli attualmente si svolgono [4].

L'obiettivo di questa indagine è di introdurre un modello di sistema frenante ECP all'interno di un modello multibody per lo studio della dinamica longitudinale di veicoli ferroviari computazionalmente efficente, che si basa sulla scrittura delle equazioni dinamiche con riferimento alle "coordinate di traiettoria" sviluppate in [8] e [9]. Sarà sviluppato un modello che tenga conto delle specifiche e dei requisiti dell'AAR (Association of American Railroads), in quanto l'obiettivo di questa modellazione è di fornire un software multibody in grado di simulare quanto più fedelmente possibile il comportamento di un veicolo ferroviario. Sarà sviluppato un modello di rete pneumatica per il sistema frenante ECP basato sulla descrizione dei sistemi attualmente in uso. Nella formulazione sarà esposto come si è giunti a scrivere le equazioni dinamiche e le equazioni pneumatiche necessarie per descrivere pienamente il modello e saranno quindi introdotte alcune ipotesi semplificative al fine di risparmiare tempo di calcolo durante la simulazione.

Nel capitolo 1 verrà descritto un modello del freno pneumatico convenzionale sviluppata in [5] e [6] al fine di comprendere meglio la differenza tra i due sistemi, inoltre la modellazione di alcune componenti come il modello del cilindro freno sarà mantenuta sostanzialmente invariata nel nuovo modello.

Nel capitolo 2 verrà presentata una descrizione generale del sistema ECP seguita da una descrizione della nuova organizzazione dei componenti lungo il treno e in ogni carrozza sottolineando le analogia e le differenza rispetto al sistema convenzionale. Sarà inoltre fornita una descrizione dettagliata delle operazioni del sistema ECP, specificando cosa avviene in ogni possibile situazione operativa partendo dalla logica di controllo fino alla descrizione del meccanismo delle singole valvole coinvolte.

Nel capitolo 3 viene spiegato come vengono calcolate i flussi di massa all’interno della rete pneumatica e gli incrementi di pressione all’interno nei componenti del sistema frenante. Seguirà una formulazione matematica dettagliata delle valvole in modo da tenere in considerazione la dinamica interna e la loro influenza nel calcolo delle portate di aria. L'approccio seguito sarà quello di modellare il sistema in modo quanto più possibile fedele alle caratteristiche dei sistemi in uso (vedi [7]) e che rispetti le specifiche AAR di un sistema frenante ECP come descritto in [1].

Nei capitoli 4 e 5 saranno descritti in breve la formulazione multibody basata sulle “coordinate di traiettoria” sviluppata in [8] e il modello di accoppiatore tridimensionale utilizzato in questo studio e sviluppato in [9] e [10].

Nel capitolo 6 viene proposta una validazione del modello ECP sviluppato tramite il confronto con i risultati sperimentali di un test di conformità (“Safety Evaluation test”) eseguito dall’AAR su un prototipo di sistema ECP sviluppato da una azienda privata (TSM) trovato in letteratura [11] .

Infine sarà eseguita una simulazione di frenata su un treno di 75 carrozze viaggiante alla velocità di 29,1 m/s fino alla completa fermata su un tracciato rettilineo per mostrare le prestazioni del freno di ECP a confronto con quello pneumatico convenzionale, al fine di giustificare i benefici dichiarati del sistema ECP. Da questo confronto emergono in maniera chiara i benefici del sistema ECP come ad esempio la distanza percorsa prima della fermata completa, che risulta essere ridotta del 40% a parità di condizioni. Una successiva analisi delle forze scambiate dagli accoppiatori mostra che l’entità di tali forze si riduce notevolmente grazie alla applicazione simultanea delle forze frenanti lungo il treno. Si può notare inoltre come la distribuzione di queste stesse forze abbia un andamento pressoché costante nel caso del sistema ECP mentre col sistema convenzionale si abbia un andamento con un picco massimo a circa metà del treno che corrisponde a 4 o 5 volte la forza applicata a inizio o fine treno.

INTRODUCTION

Railroad vehicle systems are among the most commonly used methods of transportation, both for passengers and goods. Their widespread use has sparked, over the years, continuous technological developments, with the objective of achieving higher operating speeds in order to minimize cost and transportation time. Higher operating speeds, however, require a better and more sophisticated approach for the design of the rail vehicle system in order to avoid derailments and reduce the vibration and noise levels. Therefore, the development and use of accurate computer models for simulation of railroad vehicle systems subjected to different loading conditions, operating speeds, track geometries, braking and traction scenarios are necessary.

The last 15 years has seen a slow up-take in the use of a relatively new technology for controlling the brake system on freight trains. The new technology is called Electronically Controlled Pneumatic braking commonly referred to as ECP braking.

The ECP system consists in a new way to control pneumatics brakes with the addition of an electronically controlled valves manifold on board of each car and a cabled network along the train. In this way with a reasonable modification of a conventional air brake system, it is possible to increase efficiency and capacity of a freight train.

The functional and performance requirements of the ECP brake system are given in the AAR standard S-4200 “Electronically Controlled Pneumatic (ECP) Cable-Based Brake Systems –Performance Requirements” [1]. AAR standard S-4200 describes an ECP brake system as a “train power brake system actuated by compressed air and controlled by electronic signals originated at the locomotive for service and emergency applications.”, “The system provides almost instantaneous response to braking commands, including graduated brake releases and reapplications. The system responds appropriately to undesired separation or malfunction of hoses, cabling, or brake pipe.” The brake pipe is still used to provide a continuous supply of compressed air to be stored in a reservoir on each wagon.

A rapid reduction of brake pipe pressure to zero will still provide a pneumatic emergency brake application through the train. Both electrical power and communications are transmitted via an electric cable. This cable, known as the train line, spans the entire length of the train [1], [2].

The main advantages of ECP include, but are not limited to: providing shorter stopping distances, improving train service cycle times, increasing network capacity, enhancing rail safety, fuel savings as well as reducing wear and tear on rolling stock [3].

ECP braking can improve both train safety and operations by: reducing in-train forces, making train handling simpler, continuously recharging the train brake system, and providing shorter stopping distances independent of train length. This is because the ECP system communicates electronically with every vehicle in the train.

ECP brakes have also several characteristics that have the potential to affect capacity. These are:

- Instantaneous transmission of the brake signal
- Continuous charging of the brake line
- Self-monitoring capabilities

Using an electronic signal instead of air pressure to transmit the brake signal allows for instantaneous transmission enabling nearly simultaneous application or release of the brakes along the entire length of the train. It is also possible to continuously charge the brake line even while brakes are being applied. The use of a train line cable also allows real-time, self-diagnostic 'health check' functions to be incorporated into the brake system that inform the train crew when maintenance is needed. Each of these characteristics will be considered for their impact on capacity.

Instantaneous Transmission of Brake Signal

With current brake systems there is a delay during the propagation of the brake signal whereas with ECP brakes this is eliminated. This will reduce braking distance by about 40 to 60 percent compared to conventional braking distance. Since headway between trains is limited by safe braking distance, if ECP brakes are installed on all trains such a reduction will permit closer train spacing if the traffic control system can accommodate it. The instantaneous brake signal can be used for quicker brake release as well, reducing the time for a train to restart after a meet.

Continuous Charging of Train Brake Line

Continuous charging of the train brake line facilitates greater use of the braking system and reduces the time lost waiting to recharge brake pipe pressure after an application. With conventional freight train brakes, once the engineer has selected a brake level, it cannot be reduced without completely releasing and reapplying the brakes. Trains must sometimes travel with more applied braking force than necessary due to the lack of graduated release, resulting in slower operations. The continuous charging of the brake line enables graduated release of the brakes. The greater braking flexibility offered by ECP brakes allows a train to more closely conform to appropriate track speed limits. Another benefit is the shorter restarting time after stops. With current brake technology, in areas of descending grades, the auxiliary reservoirs on each car of the train must be recharged before restarting from a stop. With ECP brakes this is not necessary, reducing dwell time on routes with large grades.

Self-Monitoring Capabilities

An electrical signal to control the brakes has the added benefit of enabling transmission of brake condition data to the locomotive. The engineer can monitor brake condition and be immediately informed of any failure in any car on the train. In response to these capabilities the FRA (Federal Railroad Administration) issued a new regulation that permits intermediate brake inspections to be performed every 3,500 miles instead of the 1,000 miles that is required with conventional brakes. This allows an ECP brake-equipped intermodal train originating from the ports of Los Angeles-Long Beach to travel all the way to Chicago without stopping for routine brake tests. Similarly, ECP brake-equipped coal trains will be able to make quicker deliveries from western coal fields to power plants in the eastern and southern states. This not only decreases cycle times but may also reduce congestion at terminals where these inspections currently take place [4].

The objective of this investigation is to introduce a dynamic ECP brake model with efficient nonlinear train longitudinal force algorithms based on trajectory coordinate formulations. It will be developed a model which keep in consideration the AAR specification and requirements. A pneumatic network model for the ECP brake system will be developed. In the formulation will be exposed the dynamics equation of motions and the pneumatic equations that are necessary to fully described the model, then it will be proposed some assumption in order to save computation time during the simulation.

In chapter 1 will be described a model of the conventional air brake developed in [5] and [6] in order to better understand the difference between the two system and also because some part of the model like the brake cylinder model will be held identical in the ECP model.

In chapter 2 will be presented the ECP overview followed by a description of train and car layout underlining the analogy and difference with the conventional system. It will be also provided a detailed description of the operations of ECP system, specifying what happens in each possible operating situation starting from the logic of the CCD until the mechanism of the individual valves involved.

In chapter 3 will be explained how the mass flow rates in the pneumatic network and the pressure rates in the components of brake system are calculated. It will follow a detailed mathematical formulation of the valves considering their dynamics and their influence in the calculation of the mass flow rates. The followed approach will be to model the system as much as possible similar to the AAR specification about ECP brake system described in [1] and the detailed description of the ECP controlled valves founded in [7].

In chapter 4 and 5 will be described in brief the trajectory coordinates formulation developed in [8] and a three-dimensional coupler model as in [9], [10].

In chapter 6 will be proposed as a validation of the ECP model and will be also executed a simulation on a 75-car train to show the performance of the ECP brake and compared with the air brake model, in order to justify the claimed benefits of ECP brake. Numerical results achieved with the aforementioned model will be compared with experimental results provided to an AAR Test found in literature [11].

1. AIR BRAKE SYSTEM

In this section will be exposed the air brake model previously developed and implemented in order to make clear the differences and the similarity with the new model which is the main topic of this investigation. The model that is here exposed was developed in [5] and [6]. The air brake model, presented in this paper, consists of the *locomotive automatic brake valve*, *air brake pipe*, and *car control unit* (CCU) (Fig.1).

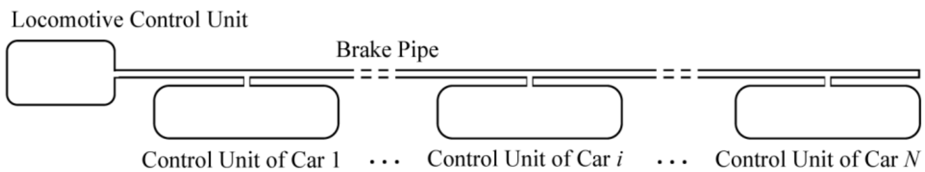

Figure 1 Main air brake components

The proposed air brake force model accounts for the effect of the air flow in long train pipes as well as the effect of leakage and branch pipe flows. For the air brake pipe model the governing equations of the air pressure flow are developed using the general fluid continuity and momentum equations, simplified using the assumptions of one dimensional isothermal flow. Using these assumptions, one obtains two coupled air velocity/pressure partial differential equations that depend on time and the longitudinal coordinate of the brake pipes. The partial differential equations are converted to a set of first order ordinary differential equations using the finite element method. The resulting air brake ordinary differential equations are solved simultaneously with the train second order nonlinear dynamic differential equations of motion that are based on the trajectory coordinates.

The air pressure in the brake pipe system is controlled by the brake locomotive automatic brake valve. The mathematical model of the 26C locomotive valve developed in [13] is used in this investigation. The valve and its main components are shown in Fig. 2. The primary function of the automatic brake valve is to control air pressure in the brake pipe allowing for the application or release of the train and locomotive brakes.

The main components of the 26C automatic brake valve are the *regulating valve*, *relay valve*, *brake pipe cut-off valve*, *vent* and *emergency valves*, and *suppression valve*.

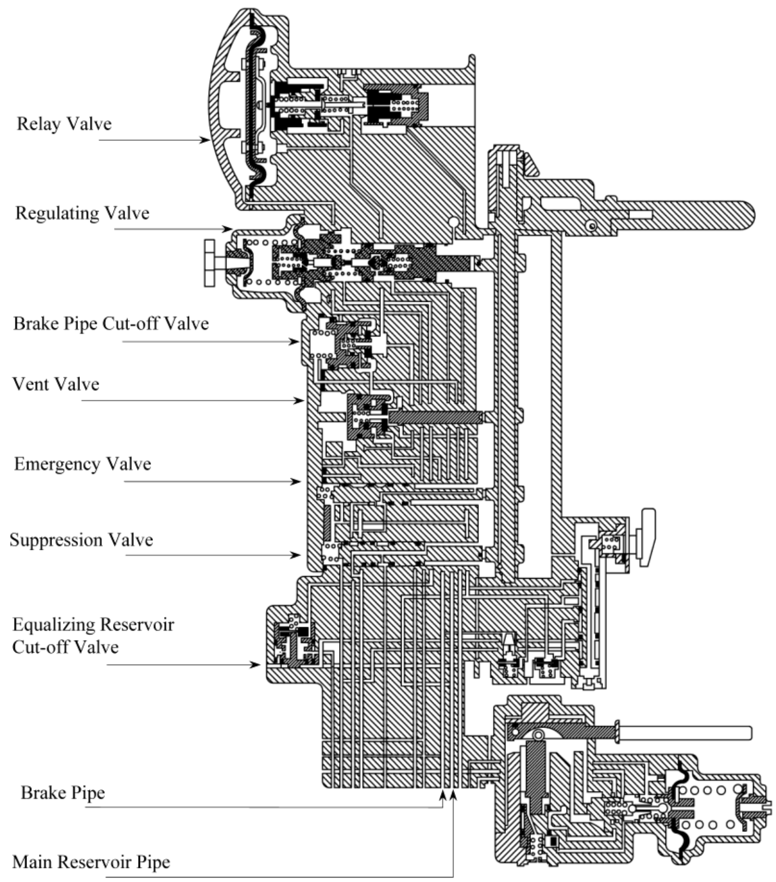

Figure 2 26C valve

The main function of the *regulating valve* is to control the *equalizing reservoir* pressure which has a value that depends on the position assumed by the automatic brake valve handle. This pressure controls the *relay valve* which controls the air pressure along the brake pipe for the purpose of brake application or release. The *brake pipe cut-off valve* is located between the relay valve and the brake pipe, and its function is to allow communication with the pipe only when a threshold pressure value is reached.

In the studies of Specchia [5] and Afshari [6], only the mathematical models of the first three valves are developed; relay valve, regulating valve, and brake pipe cut-off valve, are developed. The mathematical models are not included in this work.

1.1 BRAKE PIPE MODEL

In this section, the basic continuum mechanics equations used in this investigation to study the air flow dynamics in train brake pipes are presented. These equations include the momentum, continuity, and constitutive equations. Using the divergence theorem, the continuity equation can be written as

$$\frac{\partial \rho}{\partial t} + \nabla(\rho \mathbf{v}) = 0 \tag{1}$$

In this equation, ρ is the mass density, $\mathbf{v}$ is the velocity vector, ∇ is the divergence operator. Since air flow is considered in this study, the density ρ cannot be treated as a constant, and therefore, the assumption of incompressibility is not used in this study.

The momentum equation or the partial differential equation of equilibrium can be written in the following form as in [5]:

$$\frac{\partial(\rho \mathbf{v})}{\partial t} + \left(\rho(\nabla \mathbf{v}) + \nabla(\rho \mathbf{v})\right)\mathbf{v} = (\nabla \boldsymbol{\sigma})^T + \mathbf{f}_b \tag{2}$$

In this equation, $\mathbf{v}$ is the velocity vector, $\boldsymbol{\sigma}$ is the symmetric Cauchy stress tensor, and $\mathbf{f}_b$ is the vector of body forces per unit volume.

For the fluid constitutive equation, in the case of isotropic fluids, the constitutive equations that differentiate one fluid from another and define the fluid characteristics can be written as

$$\boldsymbol{\sigma} = \left\{-p(\rho,T) + \lambda(\rho,T)\mathrm{tr}(\mathbf{D})\right\}\mathbf{I} + 2\mu(\rho,T)\mathbf{D} \tag{3}$$

where p is the hydrostatic pressure, ρ is the mass density, T is the temperature, $\mathbf{D}$ is the rate of deformation tensor, λ and μ are viscosity coefficients that depend on the fluid density and temperature. In order to obtain the fluid equations of motion, the constitutive equations of Eq. 3 are substituted into the partial differential equations of equilibrium of Eq. 2. This leads to general three-dimensional partial differential equations of motion for isotropic fluids. If the fluid is assumed to be Newtonian, that is the shear stress is proportional to the rate of the shear strain, this leads to:

$$\frac{\partial(\rho \mathbf{v})}{\partial t} + \left(\rho(\nabla \mathbf{v}) + \nabla(\rho \mathbf{v})\right)\mathbf{v} = \left\{-\nabla(p\mathbf{I}) + \lambda\nabla\left(\mathrm{tr}(\mathbf{D})\mathbf{I}\right) + 2\mu\nabla(\mathbf{D})\right\}^T + \mathbf{f}_b \tag{4}$$

Equation 4 governs the motion of general isotropic fluid in the special case of Newtonian fluid.

1.1.1 ONE-DIMENSIONAL MODEL

The assumption of one-dimensional air flow used in this study implies that the flow, at any cross section, has only one direction along the longitudinal axis of the pipe, that is, the velocity components in the other directions are not considered. Furthermore, the magnitude of the flow velocity is assumed to be uniform at any cross section. Consequently, shear stresses are neglected, and as a result, the off-diagonal elements of the Cauchy stress tensor are assumed to be zero. Using the assumption of isothermal flow, one has the following relationship:

$$\frac{p}{\rho} = R_g \Theta \tag{5}$$

In this equation, R_g is the gas constant which has units J/(Kg°K), and Θ is the local temperature (°K). The relationship of Eq. 5 can be used to eliminate the air density ρ from the continuity and momentum equations leading to the following system of pressure/velocity coupled equations [5]:

$$\left.\begin{aligned} &\frac{\partial p}{\partial t} + \frac{\partial (pu)}{\partial x} + \gamma_t L = 0 \\ &\frac{\partial (pu)}{\partial t} + \frac{\partial (pu^2)}{\partial x} + \gamma_t \frac{\partial p}{\partial x} = \gamma_t f_b \end{aligned}\right\} \tag{6}$$

In this equation, $\gamma_t = R_g \Theta$. Given the boundary and initial conditions, the preceding system of coupled partial differential equations can be solved for the pressure and velocity distributions using numerical methods as discussed in the following section.

1.1.2 FINITE ELEMENT FORMULATION

In this study, a finite element procedure is used to transform the partial differential equations of Eq. 6 to a set of coupled first order ordinary differential equations. These ordinary differential equations can be solved using the method of numerical integration to determine the pressure and velocity for different braking scenarios. Let $q = pu$ be a new variable. Using this definition, Eq. 6 can be rewritten as

$$\left.\begin{aligned} &\frac{\partial p}{\partial t} + \frac{\partial q}{\partial x} = -\gamma_t L \\ &\frac{\partial q}{\partial t} + \frac{\partial (qu)}{\partial x} + \gamma_t \frac{\partial p}{\partial x} = \gamma_t f_b \end{aligned}\right\} \tag{7}$$

In the finite element analysis, the brake pipe is assumed to consist of m finite elements. The domain of the element is defined by the spatial coordinate

$x = x^e, 0 < x^e < l^e$, where l^e is the length of the finite element. Over the domain of the finite element, the variables p and q are interpolated using the following field:

$$p^e(x,t) = \mathbf{S}_p^e \mathbf{p}^e, \qquad q^e(x,t) = \mathbf{S}_q^e \mathbf{q}^e, \qquad e = 1, 2, \cdots, m \tag{8}$$

Where $\mathbf{S}_p^e$ and $\mathbf{S}_q^e$ are appropriate shape functions, and $\mathbf{p}^e$ and $\mathbf{q}^e$ are the vectors of nodal coordinates. Multiplying the first equation in Eq. 7 by the virtual change δp^e and the second equation by the virtual change δq^e, integrating over the volume, using the relationship $dV^e = A^e dx^e$, where A^e is the cross section area; and using Eq. 8; one obtains the following system of first order ordinary differential equations for the finite element e:

$$\mathbf{M}^e \dot{\mathbf{e}}^e = \mathbf{Q}^e, \qquad e = 1, 2, \cdots, m \tag{9}$$

In this equation,

$$\mathbf{e}^e = \begin{bmatrix} \mathbf{p}^e \\ \mathbf{q}^e \end{bmatrix}, \qquad \mathbf{Q}^e = \begin{bmatrix} \mathbf{Q}_p^e \\ \mathbf{Q}_q^e \end{bmatrix}, \qquad \mathbf{M}^e = \begin{bmatrix} \mathbf{M}_{pp}^e & \mathbf{M}_{pq}^e \\ \mathbf{M}_{qp}^e & \mathbf{M}_{qq}^e \end{bmatrix} \tag{10}$$

The components of the mass matrix and the Q vector are calculated by the substitution of the linear interpolation shown in Eq. 8 in the Eq. 7. More details are included in [5]. The finite element equations of Eq. 9 can be assembled using a standard finite element assembly procedure. This leads to the first order ordinary differential equations of the brake pipe system which can be written in the following matrix form:

$$\mathbf{M}\dot{\mathbf{e}} = \mathbf{Q} \tag{11}$$

In this equation, $\mathbf{e}$ is the vector of nodal coordinates, $\mathbf{M}$ is the brake pipe global coefficient matrix that results from assembling the $\mathbf{M}^e$ element matrices, and $\mathbf{Q}$ is the right hand side vector that results from the assembly of the $\mathbf{Q}^e$ element vectors.

The effect of the air leakage in the finite element formulation presented in this section can be considered by introducing this effect at the nodal points using the *isotropic approach* or the *average density approach* used in [13].

1.2 LOCOMOTIVE VALVE MODEL

The air pressure in the brake pipe system is controlled by the brake locomotive automatic brake valve. The mathematical model of the 26C locomotive valve developed in [13] is used in this investigation. The primary function of the automatic brake valve is to control air pressure in the brake pipe allowing for the application or release of the train and locomotive brakes. By changing the position of the handle of this valve, the air pressure can be reduced (venting air to the atmosphere) or increased (recharging) at a controlled rate to *apply* or *release* the brakes, respectively. The main components of the 26C automatic brake valve are the *regulating valve*, *relay valve*, *brake pipe cut-off valve*, *vent* and *emergency valves*, and *suppression valve*. The main function of the *regulating valve* is to control the *equalizing reservoir* pressure which has a value that depends on the position assumed by the automatic brake valve handle. This pressure controls the *relay valve* which controls the air pressure along the brake pipe for the purpose of brake application or release. The *brake pipe cut-off valve* is located between the relay valve and the brake pipe, and its function is to allow communication with the pipe only when a threshold pressure value is reached.

1.2.1 REGULATING VALVE

The main function of the regulating valve, shown in Fig. 3, is to control the equalizing reservoir pressure which controls the operation of the relay valve that regulates the air pressure in the brake pipes.

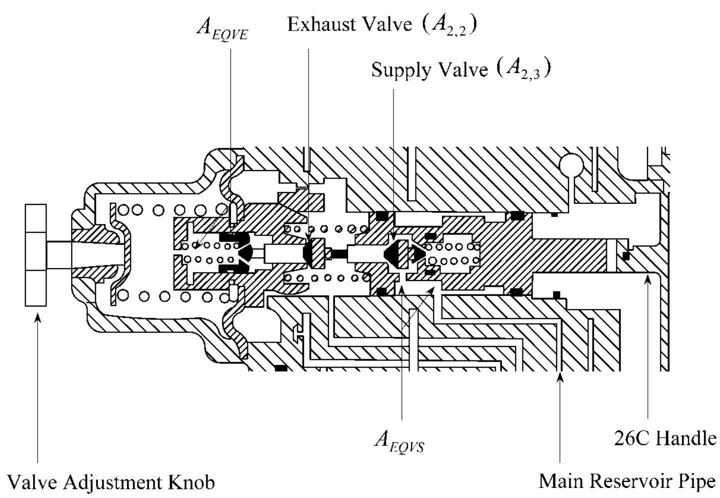

Figure 3 Regulating Valve Scheme

When the automatic brake valve handle is in the *Release/Recharge position*, the air pressure of the brake pipe P_{bp} must increase and the equalizing reservoir must be recharged. In this scenario, the cam rotates to a higher position allowing the supply valve seat to move left away from the handle, and causing the exhaust valve to be sealed. As a result, the air from the main reservoir with pressure P_{mr} flows through the supply valve and supply orifice reaching the inner diaphragm chamber, through the equalizing reservoir cut-off valve to, finally, the equalizing reservoir. The equalizing reservoir pressure P_{eq} increases causing the supply valve to start closing. When the handle is within the *service mode sector*, the air pressure of the brake pipe P_{bp} has to decrease in order to apply the car brakes. The regulating valve has to reduce the equalizing reservoir pressure P_{eq} which controls the relay valve that regulates the air flow to and from the brake pipe. The pressure reduction depends on the automatic brake valve handle position from the full service position. In the case of brake application, the cam rotates to a lower position allowing the regulating valve spool to move towards the handle (right), while the supply valve is sealed and the exhaust valve is opened. At the same time, the air pressure P_{mr} from the main reservoir is removed, causing the equalizing reservoir cut-off valve to close. This allows the air to flow only from the equalizing reservoir to the regulating valve to reach the atmosphere. As the equalizing reservoir pressure P_{eq} decreases, the exhaust valve seat moves right, causing the exhaust valve to start closing. The equalizing reservoir is connected to the outer chamber of the relay valve, and therefore, the pressure $P_{1,1}$ inside the relay valve outer chamber can be controlled by the equalizing reservoir pressure P_{eq}. The pressure $P_{1,1}$ is used to control the operations of the relay valve which controls the pressure in the brake pipe. The relay valve operations are discussed in more detail in the following section. For the detail mathematical model of the regulating valve see [5].

1.2.2 RELAY VALVE

Figure 4 shows a schematic diagram of the relay valve and its components. The *relay valve* controls the air pressure along the brake pipe for the purpose of brake application or release.

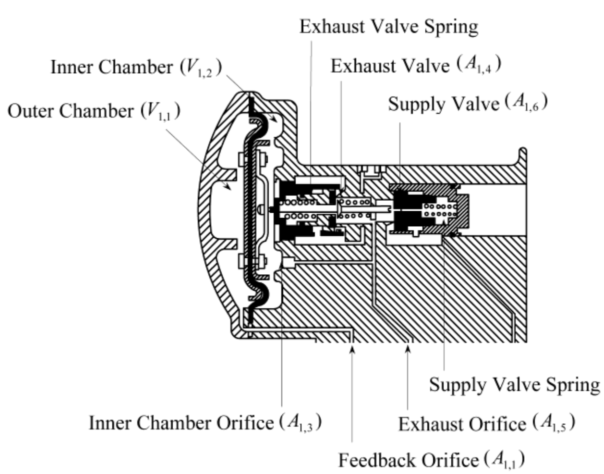

Figure 4 26C Relay valve

The relay valve is composed by two chambers called in this study inner and outer chamber with a diaphragm between them to which is fixed a rod that controls the opening or closing of two orifices. The outer chamber is connected to the regulating valve and the pressure $P_{1,1}$ consequently is almost equal to that of the equalizing reservoir P_{eq}, the inner chamber is instead connected with an intermediate chamber which in turn is connected to the brake pipe through the cut-off valve. Depending on the difference in pressure between the two chambers diaphragm rod moves to the right or to the left. When the diaphragm rod moves to the right opens, via a valve called supply valve, an orifice which connects the main reservoir to the intermediate chamber causing the increase of the pressure $P_{1,3}$ in said chamber to which then will follow charging the brake pipe. If instead the diaphragm rod moves to the left the intermediate chamber is placed in communication via the exhaust chamber to the atmosphere, in this way the pressure $P_{1,3}$ is decreased abruptly in the brake pipe and is application of a braking force according to size of the drop. As for the regulating valve, for a detail mathematical model refer to [5].

1.2.3 CUT-OFF VALVE

The *brake pipe cut-off valve* is located between the relay valve and the brake pipe, and its function is to allow communication with the pipe only when a threshold pressure value is reached. This function is made by a valve controlled by a spring which allow the opening only if the pressure of the intermediate chamber of the relay valve ($P_{3,1}$) overcomes the resultant of the pressure P_a force and the spring preload force. The brake pipe cut-off valve is shown in Fig. 5. As for the regulating valve and relay valve, for a detail mathematical model refer to [5].

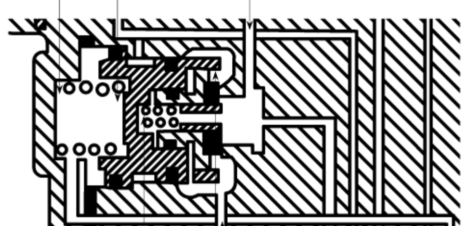

Figure 5 Brake Pipe Cut-Off valve

1.3 CAR CONTROL UNIT

As discussed in the precedent section and shown in Fig. 1, the air brake system of a freight train consists of three main units; the *locomotive control unit*, the *brake pipe*, and the *car control unit* (CCU). A common train brake has one locomotive control unit and one brake pipe. The number of the car control units, however, depends on the number of cars in the train, as depicted in Fig. 1. The CCU consists of different pneumatic and mechanical components that control the brake application or release. These brake modes depend on the brake pipe pressure and the automatic brake valve handle position that is controlled by the train operator. A CCU, which is installed on each train car, consists of different pneumatic and mechanical components. The simplified CCU model considered in this investigation is assumed to have the basic components; the *control valve*, the *auxiliary reservoir*, the *brake cylinder*, the *brake rigging*, and the *brake shoes*, as well as a component called the *emergency reservoir* that is only used in the case of emergency brake application. The control valve acts as a pressure sensor that operates based on the local brake pipe pressure (the pressure at the control valve connection point with the brake pipe) and its time rate of change. The control valve function is to connect different CCU parts and to control the air transfer between them. In the model used in this paper, it is assumed that the control valve has the *triple valve* that controls the communication between the brake pipe, the auxiliary reservoir, the brake cylinder, and the atmosphere. Furthermore, the emergency portion of the CCU controls the communication between the emergency reservoir and the brake cylinder. The auxiliary reservoir, the most frequently used CCU storage reservoir, supplies the pressurized air required for service brake application. The brake cylinder is the component where the pressurized air can push the cylinder piston to produce an axial force required to apply the brake. The brake rigging is a leverage mechanism that transmits the piston axial force and converts it to a normal force applied to the brake shoes on the car wheels; it is also used to magnify the normal brake shoe force magnitude. The brake shoe is the part that is pressed against the wheel by the normal force to produce the frictional brake retarding force. The magnitude of the normal brake force produced on the brake shoes depends on the automatic brake valve handle position that is controlled by the train operator. In this description, it is assumed that the train operator can apply three main brake operation modes; the *brake release*, *service brake*, and *emergency brake* modes. In the case of the emergency brake mode, both the emergency reservoir and the auxiliary reservoir are connected to the brake cylinder to produce higher brake cylinder pressure. It is presented the mathematical model developed in [6] for the simplified CCU components, including the auxiliary reservoir, the emergency reservoir, and the brake cylinder. A scheme with the components of a CCU is shown in Fig. 6.

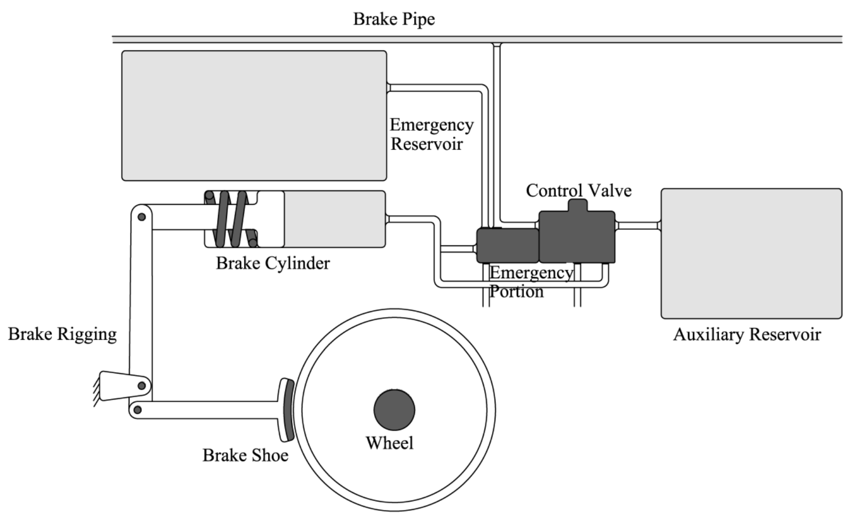

Figure 6 Car control unit components

For different operation modes of the brake, the air flow between different CCU sections is modeled. This leads to a set of first order ordinary differential equations that are combined with the automatic brake valve and the brake pipe differential equations in order to define the air brake mathematical model. This model will be integrated with the nonlinear train dynamic model that employs the trajectory coordinates. As fully explained in the Appendix attached at the end of this work, the total mass flow rate to component e is denoted by $dm_e/dt = \dot{m}_e$, while the mass flow rate from component f to component e is denoted by $\dot{m}_{e-f}$. In this paper, the letters *bp*, *x*, *c*, *u*, *em*, and *a* denote, respectively, the brake pipe, the auxiliary reservoir, the brake cylinder, the control unit, emergency reservoir, and the atmosphere. The schematic of the airflow between the above- mentioned parts are shown in Fig. 7.

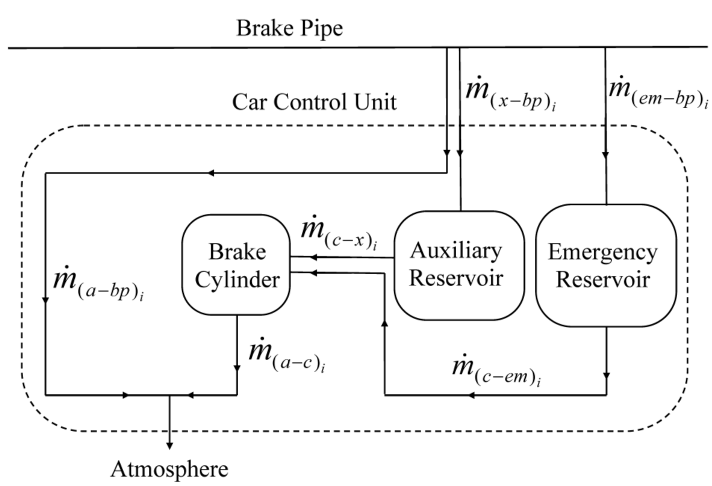

Figure 7 The mass flow rate between the brake pipe, atmosphere, and the control unit components of car

The air flow to the auxiliary and emergency reservoirs of Car i from the brake pipe ($e = x, em$ and $f = bp$) is obtained from the following equation:

$$\begin{cases} \dot{m}_{(x-bp)_i} = 0.6 A_{(x-bp)_i} P_{x_i} \sqrt{\dfrac{\left| r_i^{\,2} - 1 \right|}{R_g \Theta}} \dfrac{\left| r_i - 1 \right|}{r_i - 1} & \text{(a)} \\ \dot{m}_{(em-bp)_i} = 0.6 A_{(em-bp)_i} P_{em_i} \sqrt{\dfrac{\left| r_i^{\,2} - 1 \right|}{R_g \Theta}} \dfrac{\left| r_i - 1 \right|}{r_i - 1} & \text{(b)} \end{cases} \tag{12}$$

where $r_i = P_{bp}(x_{u_i}, t) / P_{e_i}$ $(e = x, em)$, $P_{bp}(x_{u_i}, t)$ is the local brake pipe pressure that is function of the location of the CCU connection point with the pipe x_{u_i} and time t, $A_{(x-bp)_i}$ and $A_{(em-bp)_i}$ are the equivalent areas connecting the pertinent components [6]. Similarly, the air flow from the auxiliary and emergency reservoirs to the brake cylinder ($e = c$ and $f = x, em$) can be obtained from the following equation:

$$\begin{cases} \dot{m}_{(c-x)_i} = 0.6 A_{(c-x)_i} P_{c_i} \sqrt{\dfrac{\left| r_i^{\,2} - 1 \right|}{R_g \Theta}} \dfrac{\left| r_i - 1 \right|}{r_i - 1} & \text{(a)} \\ \dot{m}_{(c-em)_i} = 0.6 A_{(c-em)_i} P_{c_i} \sqrt{\dfrac{\left| r_i^{\,2} - 1 \right|}{R_g \Theta}} \dfrac{\left| r_i - 1 \right|}{r_i - 1} & \text{(b)} \end{cases} \tag{13}$$

where $r_i = P_{f_i} / P_{c_i}$ $(f = x, em)$, $A_{(c-x)_i}$ and $A_{(c-em)_i}$ are the equivalent of the connecting areas. In addition, the air vented to the atmosphere ($e = a$) from the brake cylinder ($f = c$) or from the brake pipe ($f = bp$) is governed by the following equation:

$$\begin{cases} \dot{m}_{(a-c)_i} = 0.6 A_{(a-c)_i} P_a \sqrt{\dfrac{\left| r_i^{\,2} - 1 \right|}{R_g \Theta}} \dfrac{\left| r_i - 1 \right|}{r_i - 1} & \text{(a)} \\ \dot{m}_{(a-bp)_i} = 0.6 A_{(a-bp)_i} P_a \sqrt{\dfrac{\left| r_i^{\,2} - 1 \right|}{R_g \Theta}} \dfrac{\left| r_i - 1 \right|}{r_i - 1} & \text{(b)} \end{cases} \tag{14}$$

Where, $r_i = P_{f_i} / P_a$ $(f = bp, c)$, $A_{(a-c)_i}$ and $A_{(a-bp)_i}$ are the equivalent areas of the pertinent components of car i.

Assuming that all the processes taking place in the CCU are isothermal (Θ is constant), one can obtains the time rate of the auxiliary reservoir pressure of car i. Using the fact that the volumes of the auxiliary and emergency reservoirs are constant, one can write as:

$$\begin{cases} \dfrac{dP_{x_i}}{dt} = \dfrac{1}{V_{x_i}}\left(R_g \Theta \dfrac{dm_{x_i}}{dt} - P_{x_i} \dfrac{dV_{x_i}}{dt} \right) = \dfrac{R_g \Theta}{V_{x_i}} \dot{m}_{x_i} & \text{(a)} \\ \dfrac{dP_{em_i}}{dt} = \dfrac{1}{V_{em_i}}\left(R_g \Theta \dfrac{dm_{em_i}}{dt} - P_{em_i} \dfrac{dV_{em_i}}{dt} \right) = \dfrac{R_g \Theta}{V_{em_i}} \dot{m}_{em_i} & \text{(b)} \end{cases} \tag{15}$$

Similarly, the time rate of the brake cylinder pressure as:

$$\frac{dP_{c_i}}{dt} = \frac{1}{V_{c_i}}\left(R_g \Theta \frac{dm_{c_i}}{dt} - P_{c_i} \frac{dV_{c_i}}{dt} \right) \tag{16}$$

Unlike the auxiliary reservoir, the brake cylinder, in general, does not have a constant volume because of the piston movement. However, during the brake shoe force application, one can assume that the cylinder volume remains constant. The CCU parameters previously discussed, depending on the brake mode, can be function of time, the car location in the train, and other air brake parameters.

In this investigation, $\dot{m}_{bp_i}$ is the rate of the pipe mass flow through the CCU of car i to its auxiliary reservoir, to emergency reservoir or to the atmosphere. In the model developed in this study, $\dot{m}_{bp_i}$ is the parameter that links the brake pipe FE model to the CCU of car i. In order to include the effect of $\dot{m}_{bp_i}$ in the FE model, the element where the car control valve is connected to the brake pipe is determined. Then, $\dot{m}_{bp_i}$ is distributed between the two nodes of the element and is considered as the element leakage in the equations presented in [5].

1.3.1 BRAKE FORCE MODEL

In order to determine the brake force, the brake cylinder piston axial force has to be calculated. In general, in order to obtain the piston displacement u_{p_i} and the brake cylinder pressure, a set of two coupled differential equations needs to be solved; the piston equation of motion and the time rate of the cylinder pressure equation. These two equations are

$$\left.\begin{aligned} & m_{p_i}\frac{d^2u_{p_i}(t)}{dt^2} = \left(P_{c_i}(t) - P_a\right)S_{p_i} - K_{c_i}u_{p_i}(t) - f_{f_i} - F_{p_i}h(u_{p_i}(t) - u_{con._i}) \\ & \frac{dP_{c_i}(t)}{dt} = \frac{1}{V_{0_i} + S_{c_i}u_{p_i}(t)}\left(R_g\Theta\frac{dm_{c_i}(t)}{dt} - P_{c_i}(t)S_{c_i}\frac{du_{p_i}(t)}{dt}\right) \end{aligned}\right\} \tag{17}$$

where m_{p_i} is the piston mass, S_{p_i} is the piston cross-section area, K_{c_i} is the stiffness constant of the cylinder spring, f_{f_i} is the friction force, F_{p_i} is the axial force of the piston, $u_{con._i}$ is the piston displacement when the brake shoes contact the wheels, $h(u_{p_i})$ is the Heaviside step function, V_{0_i} is the initial volume of the brake cylinder, S_{c_i} is the cross-section area of the cylinder that is assumed to be approximately equal to that of the piston (i.e. $S_{c_i} \cong S_{p_i}$), and $\dot{m}_{c_i}(t)$ is the cylinder mass flow rate that is obtained as presented in the previous section , depending on the brake mode. After the brake shoes contact the wheels, one can assume that $d^2u_{p_i}(t)/dt^2 \cong du_{p_i}(t)/dt \approx 0$, and $u_{p_i}(t) \cong u_{con._i}, u_{p_i}(t) > u_{con._i}$ which leads to $h\left(u_{p_i}(t) - u_{con._i}\right) = 1$. Using these assumptions, the piston axial force can be calculated as

$$F_{p_i}(t) = \left(P_{c_i}(t) - P_a\right)S_{p_i} - K_{c_i}u_{con._i} - f_{f_i} \tag{18}$$

Furthermore, with the assumption of small piston acceleration and velocity, when $u_{p_i}(t) \le u_{con._i}$, one can obtain the spring displacement using the following equation:

$$u_{p_i}(t) = \left(\left(P_{c_i}(t) - P_a\right)S_{p_i} - f_{f_i}\right)/K_{c_i} \tag{19}$$

It should be noted that an ideal brake rigging transfers the entire normal force to the wheels without any loss. In reality, however, this is not the case. In other words, some fraction of the force is used to move the brake rigging components and to overcome the friction in its joints and connections. In order to take into account such an energy loss without considering the complicated equations of motion, joint constraints, etc. of the brake rigging, a rigging efficiency can be used when the brake force is calculated. Figure 8 shows the schematic of the brake force applied on one car wheel.

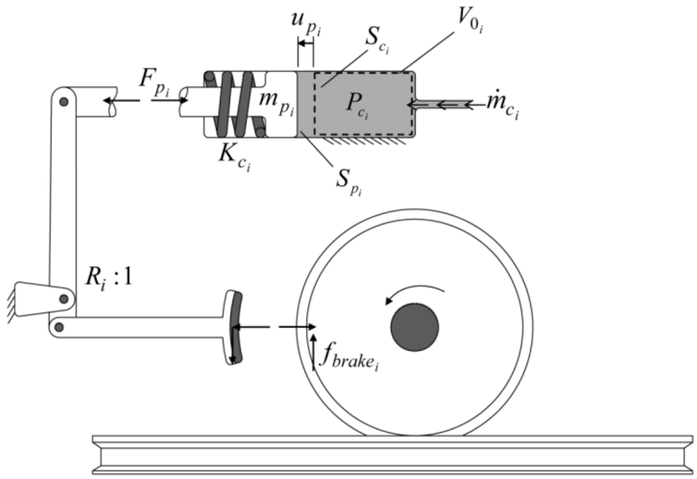

Figure 8 The brake force applied on a car wheel

If it is assumed that each car has one brake cylinder and the normal force resulting from the brake cylinder pressure is equally distributed to all brake shoes, the frictional tangential or retarding brake force for each shoe can be calculated as follows (Sanborn et al., 2007):

$$f_{brake_i}(t) = \eta_i \frac{\mu_i}{N_{s_i}} R_i F_{p_i}(t) = \eta_i \frac{\mu_i}{N_{s_i}} R_i \left\{ \left(P_{c_i}(t) - P_a \right) S_{p_i} - K_{c_i} u_{con._i} - f_{f_i} \right\} \qquad (20)$$

where η_i is the rigging efficiency (which is often considered as a function of the brake cylinder pressure), μ_i is the friction coefficient between the wheel tread and the brake shoe, R_i is the brake rigging leverage ratio, and N_{s_i} is the total number of the brake shoes of the car. The brake shoe retarding friction force obtained from Eq. 20 enters into the formulation of the generalized forces acting on the car.

2. ECP BRAKING SYSTEM

As an overview, cable-based ECP systems provide for brake commands to be received on each car simultaneously. Pneumatics is still used as the braking “muscle”, but the brake pipe is no longer used to signal brake level commands. A key attribute is to allow “graduated release” capability, as opposed to “direct release” as in conventional freight brakes. This allows increased flexibility in train handling, much as is commonly provided in transit rail braking systems. In addition to improved control, brake health and critical status information is monitored, with exceptions reported to the locomotive. This capability can be extended with a variety of “smart car” sensors to report unreleased hand brakes, excessive vibrations, or other fault conditions.

Target benefits of ECP braking systems include: reduced wheel and brake shoe wear, from even distribution of braking and better pressure control, reduced fuel consumption, from use of graduated release capability to eliminate power braking, increased safety from shorter stopping distances (typically over 50% reduction), reduced in-train forces, wear on equipment, and derailment risks, car system alarm reporting and diagnostics to aid maintenance.

ECP braking represents the largest change in North American freight train brake standards in over 100 years. Cable-based systems have matured to the point where the specifications have stabilized and been demonstrated to be practical.

2.1 ECP TRAIN LAYOUT

As a prelude to the discussion on the layout of ECP system equipped train layout is necessary to make a distinction between stand-alone systems and overlays. The ECP called stand-alone systems, expect to have on board the train only the components necessary for the operation of the ECP system described without the presence of elements such as control valve (triple valve) and the locomotive automatic valve described in Chapter 1. The systems called overlay instead are those in which the two systems are simultaneously present on board the locomotive and on each car, the latter have no doubt an overabundance of components, but can take advantage of both the failsafe logic of the conventional system and the benefits ECP system. The overlay systems are definitely the most popular because of increased security of the system and because most of the trains are equipped with the ECP car or locomotive built with the conventional system on board, and subsequently modify. For that reason the kind of system described here is the overlay.

The functional and performance requirements of the ECP brake system are given in the AAR standard S-4200 “Electronically Controlled Pneumatic (ECP) Cable-Based Brake Systems - Performance Requirement” [1] AAR standard S-4200 describes an ECP brake system as a train power brake system actuated by compressed air and controlled by electronic signals originated at the locomotive for service and emergency applications. The system provides almost instantaneous response to braking commands, including graduated brake releases and reapplications. The system responds appropriately to undesired separation or malfunction of hoses, cabling, or brake pipe. The brake pipe provides a continuous supply of compressed air to be stored in a reservoir on each wagon. A rapid reduction of brake pipe pressure to zero will still provide a pneumatic emergency brake application through the train. Both electrical power and communications are transmitted via an electric cable. This cable, known as the train line, spans the entire length of the train. AAR standard S-4200 provides a detailed explanation of all devices which make-up an ECP brake system. A brief description of each major component is given here providing their purpose and functions. A schematic drawing of the train layout is shown in Fig. 9.

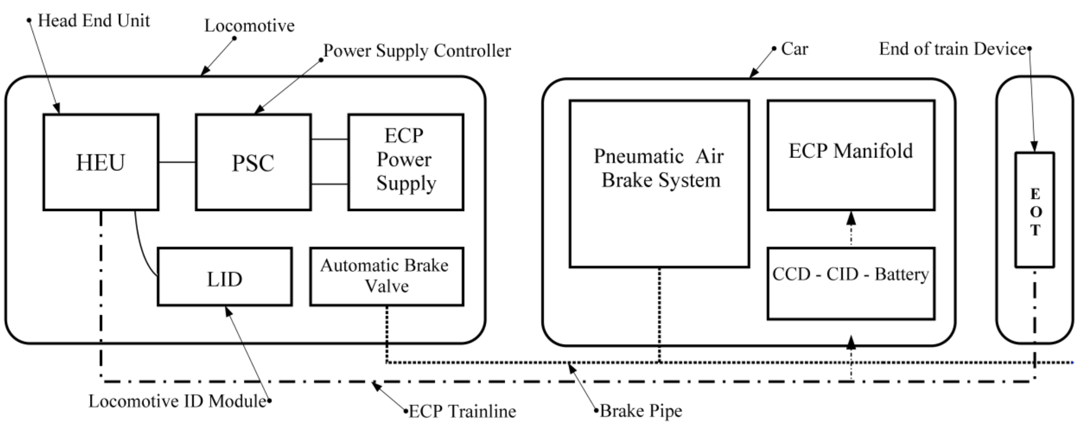

Figure 9 ECP train layout

The Head End Unit (HEU) is mounted within the locomotive cab and it is the ECP brake system control device. It consists in an interface to the driver to enable the application and release of train brakes, and to various ECP components within the train. It provides a display for showing the of the ECP system reporting such as: current braking effort, faults, trainline power, and EOT status. The End-of-Train (EOT) Device is a device connected to the train line at the end of the train. It contains a means of communicating with the HEU. The EOT is physically the last network node in the train and transmits a status message at a rate of once per second as a beacon to state the train is intact.

The Power Supply Controller (PSC) interfaces with the train line communication network and controls the train line power supply as commanded by the HEU. The power supply operates at nominally 230 VDC. It provides electrical power to all connected CCDs and EOT devices.

The Locomotive ID Module (LID) contains the locomotive and brake system specific data. The data is provided to the HEU and PSC during ECP operation. These components, the HEU, the PSC and the LID are interconnected with each other and constitute the control centre of the ECP brake system. Together these components are capable of generating and communicating through the ECP trainline signal braking or brake release the whole train. The ECP trainline is a two wired electric cable that runs along all the train, in a similar way to the brake pipe, which brings the signal generated from the HEU to all the car control units as well as the alimentation necessary for control system of the brake.

2.2 ECP CAR LAYOUT

On each car of a train equipped with ECP brake system, as shown in Fig. 10, in addiction of the usual equipment for the conventional air brake system as: auxiliary and emergency reservoir, brake cylinder there are other several components: car control device (CCD), an ECP manifold which contain the pneumatic valves, batteries, car ID module (CID) and pressure transducers.

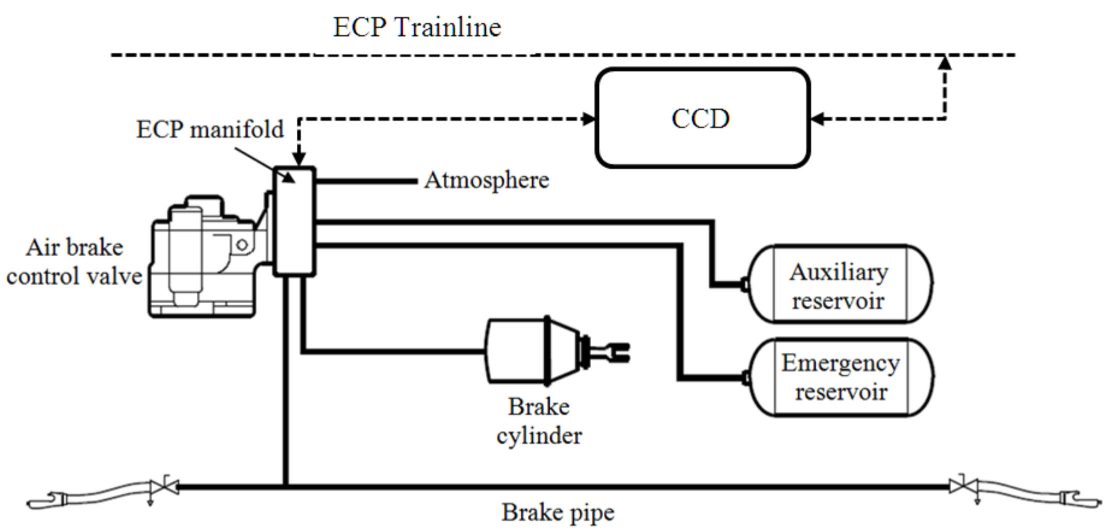

Figure 10 ECP equipped car layout

The car control device (CCD) is a device used to control all the functions for the application and release of brakes on a wagon in accordance with the commanded brake requirement from the HEU. It contains a microprocessor that control four solenoids located in the ECP manifold. Each of these solenoids has the function to open or close a passage area that leads to the upper chamber of a specified valve, the function and the task of each valve will be shown further on in this work.

Similar to the LID it stores wagon specific data called Car ID Module (CID) for use by the CCD which uses the information for controlling the brakes on a vehicle correctly. The pressure transducers are fundamental elements in ECP brake systems, for example the information of pressure in the brake cylinder is critical for proper operation of the CCD. The control logic of the CCD, which will be discussed extensively later in this work, provides for a continuous comparison between the pressure in the brake cylinder and the pressure desired by the operator. Other pressure transducers are present on the car, depending on the manufacturer, for example to monitor the reservoirs pressure or the brake pipe pressure.

The auxiliary reservoir is the car component that provides the pressurized air required for service brake application. The auxiliary reservoir, in other words, is one of the main CCU compressed air storage components where the air coming from the brake pipe is stored. The compressed air transfers from the brake pipe to the auxiliary reservoir during the recharging phase. Similarly, the emergency reservoir is the other main air storage component that provides additional compressed air for emergency brake application, when occasionally needed.

The brake cylinder is the car component that transmits the force required for brake application to the brake rigging and the brake shoes. As shown in Fig 8 inside the brake cylinder, there is a piston connected to a spring used to return the piston to its release position during the brake recharge/release. In the simplified model developed in this study, the brake cylinder is filled with the pressurized air coming from the auxiliary reservoir during service brake; while during the emergency brake, it is filled from the air of both the emergency and auxiliary reservoirs. This pressure pushes the piston against the spring producing braking force that is transmitted to the wheels through the brake rigging and the brake shoes.

The brake rigging is a common term used to refer to the mechanical system that consists of rods, levers, and connecting elements. The function of the brake rigging is the magnification of the brake cylinder force and the transmission of this force to the brake shoes. The car brake shoe, usually made of cast iron, sintered iron, or composite materials, produces frictional braking force when pressed against the wheel tread during brake application. During brake release, the brake shoe normal forces are relieved on the wheels when the air in the brake cylinder is vented.

2.3 ECP OPERATION

As mentioned before the main characteristic of an ECP system is that the information of a desired pressure in the brake cylinder is not bounded to the brake pipe pressure drop as in the conventional air brake but is brought from an electric signal that arrives from the Head End Unit through the ECP trainline. This signal is designed for be easily understood by the microprocessor inside the CCD. To provide the different possible situations in which the system have to work there are several types of signal, in this work will be considered only some of the possible types of signals that the operator could use for the control of the braking system. First of all will be considered if the system ECP is enabled or disabled, in the case of disabled will consider the system is identical to a conventional system and will therefore be controlled by the automatic valve locomotive. In case of enabled system are considered four possible cases: application, release, emergency and lap.

To every signal type corresponds a different action of CCD microprocessor on the solenoid actuator that controls the four (*cut out, vent, auxiliary and emergency*) valves inside the ECP manifold shown in Fig. 11.

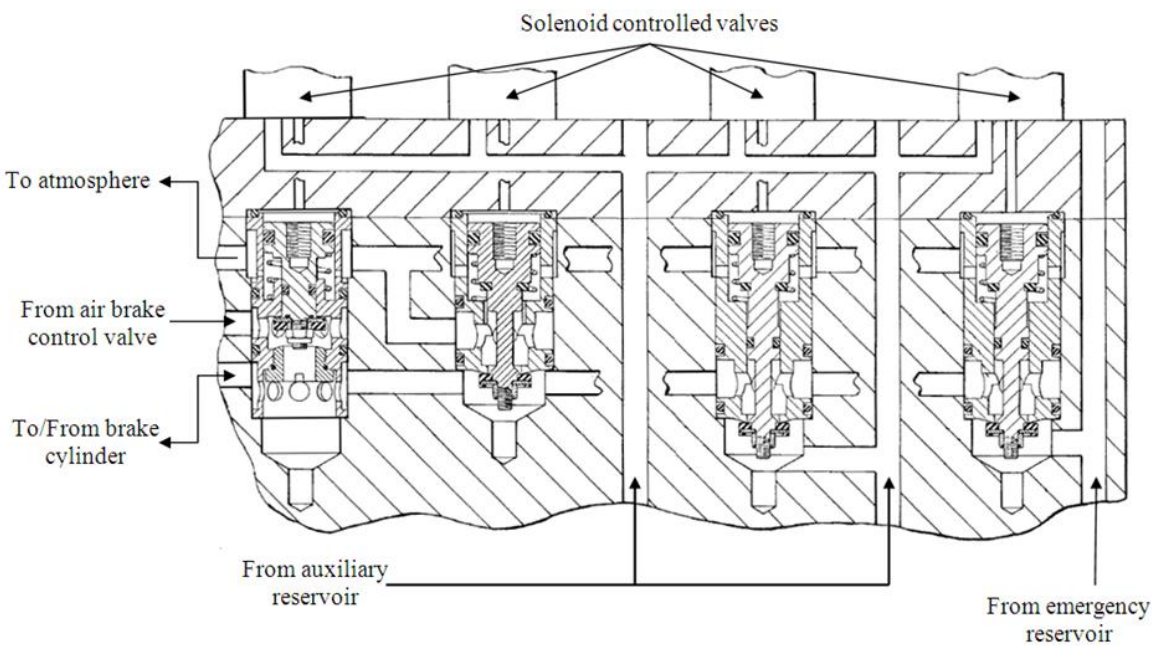

Figure 11 ECP manifold [7]

In this paragraph it is explained how the CCD respond to different signal from the HEU; as a logic controller is important to keep in mind that the CCD has different inputs in addition to the signal from the HEU, first of all the pressure in the brake cylinder and then the pressure in the reservoirs and in the brake pipe. So from a certain set of inputs there will be a corresponding action implemented in the CCD logic.

On a freight train equipped with both types of brake control systems, the train operator in the locomotive can thus select whether the conventional brake control system or the ECP brake control system will be used to operate the brakes. When the conventional braking mode is selected, the brake pipe is used to convey the brake commands pneumatically to the pneumatic brake equipment on each railcar. When the ECP braking mode is selected, the ECP trainline conveys the brake commands electrically to the ECP brake equipment on the railcars, with the brake pipe also being used to convey emergency brake commands as a safety measure.

Mounted to the top of cover plate are four solenoids as shown in Fig. 11. Above each valve insert, one solenoid communicates with the pilot airway and the pilot passage for its corresponding borehole. Each solenoid has an armature stem around which lies an energizable coil. At its head end, the armature stem has a seal. When the coil is de-energized, the armature stem has its head end biased against the top of cover plate above the valve insert. This seals off the pilot passage from the pilot airway and the auxiliary reservoir connected thereto, and thereby prevents pressurized air from acting against the top of the valve insert.

Enabled and Disabled mode

In selecting which brake control system will direct control of the brakes, the train operator in the locomotive ultimately determines the state of the cut-out valve insert in ECP manifold. When the conventional braking mode is selected, the CCD on each railcar is not commanded via the ECP trainline to energize the solenoid of the cut-out valve. This leaves cut-out valve in its cut-out state, i.e., its lower valve closed and its upper valve open. Consequently, whenever the conventional brake control system conveys a brake application command along the brake pipe, the cut-out valve will allow pressurized air to flow through its upper valve and into the brake cylinder. When the ECP braking mode is selected, the CCD on each railcar receives a signal via the ECP trainline to energize the solenoid. When energized, solenoid electromagnetically compels its armature stem upward, and thereby interconnects the pilot passage of the valve upper chamber to the pilot airway. Pilot air from the auxiliary reservoir then acts against the top of the piston. As the pilot pressure builds, the hollow shaft encompasses the knob and soon pushes insert piston downward against the bias of spring. This forces cut-out valve into its cut-in state, its upper valve closes. In this state, the cut-out valve disconnects the brake cylinder from the passage in the service portion of the brake control valve.

With the ECP system enabled the operator has the possibility to control the brake system sending different signals, in this paragraph it will be explained which kind of signal can be sent and what that means for the CCD. As explained in AAR standard S-4200 “the train brake commands (TBC) determine the level of brake application for electronically controlled brake systems and shall be expressed as a percentage from 0% to 100% of full-service pressure in 1% increments. A 100% TBC shall be for full service, and 0% shall be for full release. Minimum service shall be at 10%, and an emergency brake application (whether intentional or the result of a fault or penalty) shall result in a TBC of 120% (of the full-service brake cylinder pressure setting).” Between the minimum and full service positions lies the service zone wherein each incremental movement of the handle toward the full service position causes an even stronger service application of the brakes. The force with which the service brakes will apply depends on how far towards the full service position the automatic brake handle is moved. For the release mode the command is similar, the engineer can decide the desired pressure of the brake cylinder between a full release pressure (atmospheric pressure) and a minimum release (between 85 and 90 percent of the service pressure).

Service and Emergency brake application mode

Whenever the ECP brake control system conveys a brake application (service mode) command along the ECP trainline, the CCD – will confront the value of pressure from the brake cylinder transducer, if the brake cylinder pressure is lower than the desired it will energize the solenoid above auxiliary valve. Pilot air from the auxiliary reservoir then acts against the top of the piston. As the pilot pressure builds, the piston moves downward against the bias of spring. This forces the auxiliary valve into its energized state, its upper valve closed and its lower valve opened. In this state, the auxiliary insert allows pressurized air to flow from the auxiliary reservoir through its lower valve and into the brake cylinder. When the pressure in the brake cylinder reach the desired pressure, according to the TBC received from the HEU the CCD will deenergize the solenoid and close the passage in order to seal the brake cylinder at the desired pressure. In this situation the CCD keep monitoring the brake cylinder in order to maintain the desired pressure against leakage or other causes. In case of emergency application both the solenoids above both auxiliary and emergency valve are energized, and so both valves permit air to flow from the reservoirs to the brake cylinder in order to reach the required emergency pressure of 120% of the full service application pressure in the brake cylinder in the shorter time possible.

Release mode

Whenever the ECP brake control system conveys a brake release command along the ECP trainline, the CCU will energize the solenoid above vent valve. Pilot air from the auxiliary reservoir then acts against the top of insert piston. As the pilot pressure builds, the piston moves downward against the bias of spring. This forces the vent valve into its energized state, i.e., its upper valve closed and its lower valve opened. In this state, the vent allows the pressurized air previously developed within the brake cylinder to flow through its lower valve to atmosphere. Also in this situation the CCD keep monitoring the brake cylinder pressure

Recharge mode

The AAR Standard S-4200 provides for the ECP system a system of continuous charging. This means that in any status the system is the reservoirs must be recharged until the operating pressure required, in most cases the operating pressure is set at 90 psig). The air required for charging is drawn from the brake pipe which, in the ECP system, is used only as a link between the main reservoir located in the locomotive and car unit along the train. The most widely used constructive solutions provide to admit the incoming flow to the reservoirs automatically only if the pressure falls below a certain threshold. The threshold is usually set in a way to start recharging after a minimum service application.

Safety

The ECP system as required by AAR S-4200 must be designed and installed in accordance with the principle of failsafe due to the extreme importance of safety in the railway and in particular braking systems. The conventional system, as is well known in the railway, applying the brake due to a pressure drop in the brake pipe is structurally built with this logic of failsafe. The ECP uses instead its peculiarities to structure its logic failsafe mainly in two ways. The first is to exploit the information network, which by its nature, the system has to provide the operator with a greater amount of information about the status of each car unit. For example in a train equipped with an ECP system the operator has available the information of the service of each wagon including the possible faults on board, and the greater amount of information provided to the operator as a result certainly have a greater driving safety. The second mode in which the system structure ECP logic failsafe is to have an automatic system in which the information collected from the individual car unit are analyzed continuously and become critical in case an emergency application is commanded in an automatic way.

In fact the HEU send a beacon message every second to all network devices in the train to check their status and receives an up-dated status report from each CCD. As part of the failsafe operation of the ECP system the EOT broadcasts a beacon message every second. If a CCD confirmed a loss of 3 consecutive EOT beacon messages and 2 other CCDs also sensed a similar loss then the devices broadcast a critical loss message to all other devices and apply and emergency brake application as well the HEU will command an ECP emergency brake application.

In addition, for the system equipped with both ECP and conventional system ,as a safety measure, emergency brake commands are conveyed to the railcars not only electrically along the ECP trainline but also pneumatically along the brake pipe. By moving the handle into the emergency position, the train operator in the locomotive causes the pressure in the brake pipe to drop at an emergency rate. This drop in pressure then quickly propagates along the brake pipe to each railcar in the train. Should the ECP equipment lose power or otherwise fail electrically, it will still respond pneumatically to the telltale reduction in pressure that occurs in the brake pipe during an emergency. The ECP brake equipment is designed to respond to the emergency pressure drop by supplying pressurized air from both the auxiliary and emergency reservoirs to the brake cylinder and thereby cause an emergency application of the brakes.

3. ECP MATHEMATICAL MODEL

Now it will be developed a mathematical model CCU in the case of ECP brake system. The principal components are the same of the conventional air brake, in fact are still present the auxiliary and emergency reservoirs, the brake cylinder, the brake rigging and the brake shoes. For these components will be used the models already explained in section 2.3, in particular for the brake cylinder.

The most relevant part of the model will be the formulation of the electro pneumatic valves that are included in the ECP manifold (Fig.12). For the model of the valves is useful to recall the mathematical formulation for the calculation of the mass flow rates between to components, the pressure rates in a constant (or variable) volume component and the equivalent connecting areas reported in Appendix.

It will be used the following notation, all the variables referred to the cut-off valve are marked with number *1*, *2* for the vent valve, *3* for the auxiliary valve and *4* for the emergency valve. For the others components will be used the same letters as before, *bp*, *x*, *bc*, *em*, and *a* denote, respectively, the brake pipe, the auxiliary reservoir, the brake cylinder, emergency reservoir, and the atmosphere.

3.1 AIR MASS FLOW FLUID NETWORK MODEL

In this paragraph is described the trend of the air flows in the possible status in which the ECP system can be found in the normal operation. It will be neglected in this section the how the air passage will be opened or closed because it will be discussed in depth in the next paragraphs. First it will be defined the possible status: application, release and commanded emergency. The air flow network is represented in Fig 12.

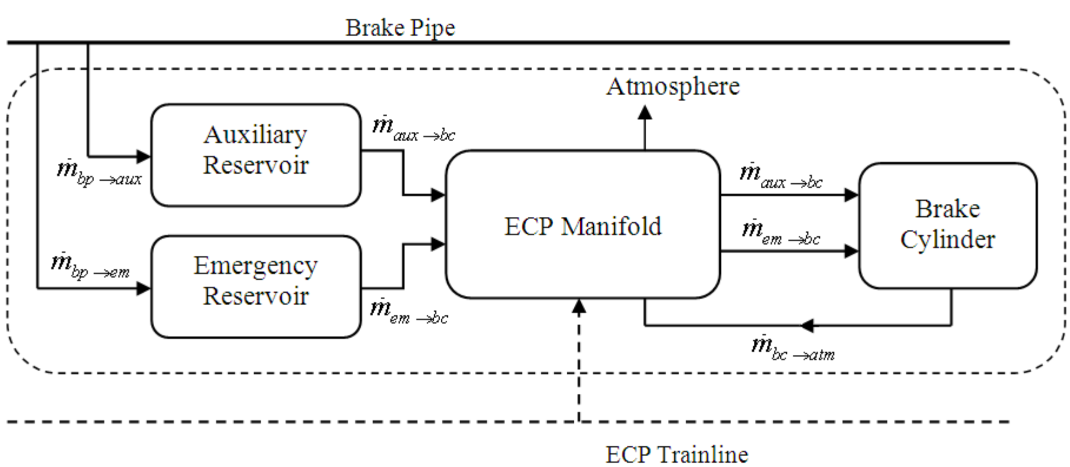

Figure 12 The mass flow rate between the brake pipe and the CCU and between the reservoirs, the ECP manifold and the brake cylinder

In the application mode the brake cylinder has to increase its pressure in order to apply a certain amount of brake, so the air will be conveyed from the auxiliary reservoir to the brake cylinder opening the corresponding passage in the ECP manifold. The corresponding mass air flow is called $\dot{m}_{(bc-x)}$ and how it is calculate it will be explained in paragraph 4.4. At this point it is possible to write the pressure rate of the brake cylinder in the same as it is done in paragraph 2.3:

$$\frac{dP_{bc}(t)}{dt} = \frac{1}{V_{bc}}\left(R_g\Theta\frac{dm_{(bc-x)}(t)}{dt} - P_{bc}\frac{dV_{bc}}{dt}\right)$$

The pressure in the brake cylinder will be used to calculate the brake force as shown in paragraph 2.3.1.

In the release mode the brake cylinder has to vent in order to release the brake, for this the brake cylinder has to be connected with the atmosphere opening the corresponding orifice by the vent valve mounted in the ECP manifold. The corresponding air flow is called $\dot{m}_{(a-bc)}$ and it is shown in Fig 12. The detail process to calculate this air mass flow will be treated in paragraph 4.3. As before it is possible to write the pressure rate of the brake cylinder:

$$\frac{dP_{bc}(t)}{dt} = \frac{1}{V_{bc}}\left(R_g\Theta\frac{dm_{(a-bc)}(t)}{dt} - P_{bc}\frac{dV_{bc}}{dt}\right)$$

The pressure in the brake cylinder will be used to calculate the brake force as shown in paragraph 2.3.1.

In the emergency mode both the air from the auxiliary reservoir and the emergency has to be conveyed to the brake cylinder. For this reason two different passages will be opened in the ECP manifold, the mass flow rate will be the sum of $\dot{m}_{(bc-x)}$ and $\dot{m}_{(bc-em)}$. The pressure rate in the brake cylinder will be:

$$\frac{dP_{bc}(t)}{dt} = \frac{1}{V_{bc}}\left(R_g\Theta\frac{d\left(m_{(bc-x)} + m_{(bc-em)}\right)}{dt} - P_{bc}\frac{dV_{bc}}{dt}\right)$$

The pressure in the brake cylinder will be used to calculate the brake force as shown in paragraph 2.3.1.

In any status the system is the CCD will check the pressure in the auxiliary reservoir and the emergency reservoir; if the pressure is under a certain threshold the control logic provide to open a connection between the brake pipe and the reservoirs. The two mass flow rates in this case are completely separate and can be written as:

$$\begin{cases} \dot{m}_{(bp-x)} = 0.6 A_{bp-x} P_x \sqrt{\dfrac{|r^2-1|}{R_g \Theta}} \dfrac{|r-1|}{r-1} \\ \dot{m}_{(bp-em)} = 0.6 A_{bp-em} P_{em} \sqrt{\dfrac{|r^2-1|}{R_g \Theta}} \dfrac{|r-1|}{r-1} \end{cases}$$

where in the first expression $r = P_{bp} / P_x$ and in the second $r = P_{bp} / P_{em}$.

As before is possible to write the pressure rate for the reservoirs:

$$\begin{cases} \dfrac{dP_x(t)}{dt} = \dfrac{1}{V_x} \left(R_g \Theta \dfrac{dm_{(bp-x)}(t)}{dt} - P_x \dfrac{dV_x}{dt} \right) \\ \dfrac{dP_{em}(t)}{dt} = \dfrac{1}{V_{em}} \left(R_g \Theta \dfrac{dm_{(bp-em)}(t)}{dt} - P_{em} \dfrac{dV_{em}}{dt} \right) \end{cases}$$

At every time steps the proper (with respect to the status) set of pressure rates will be given into the integrator which will restitute the value of pressure for the next time step.

3.2 CUT OUT VALVE MATHEMATICAL MODEL

The main function of the cut out valve is to enabled-disabled the ECP brake system on a single car. A drawing of the valve is shown in Fig. 13

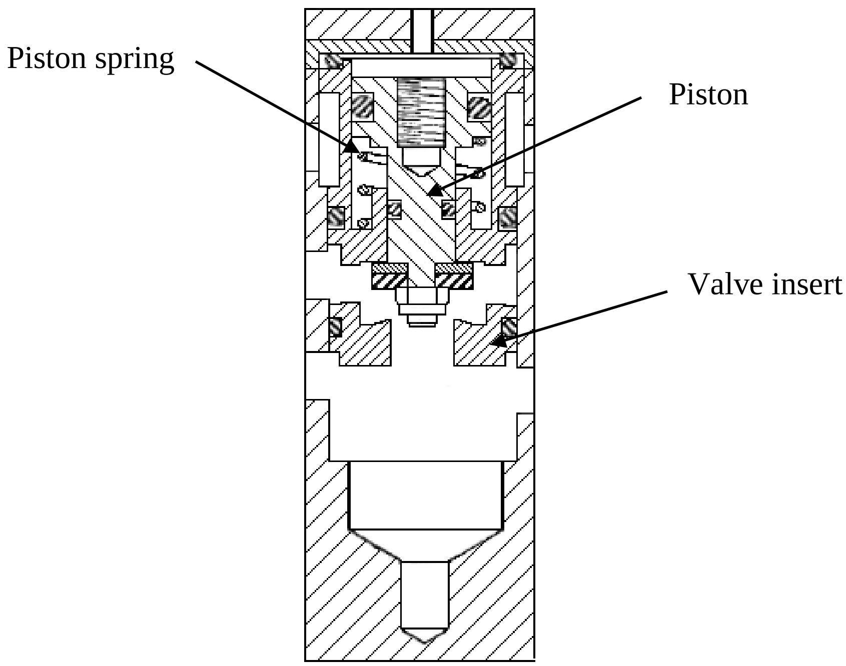

Figure 13 Cut out valve scheme

This valve is controlled by a solenoid valve that has only two possible positions *on* and *off*. The solenoid above the valve itself controls the flow of air from the auxiliary reservoir to the upper chamber of the valve cylinder; this air flow passes through a small orifice which is called in this formulation $A_{1,1}$. The fluid network for the valve is shown in Fig.14.

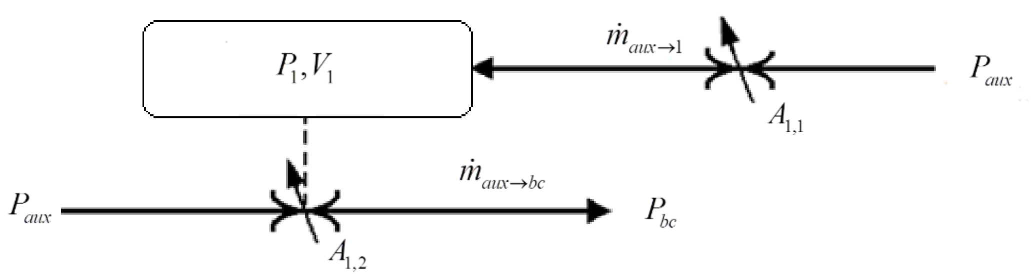

Figure 14 Cut out valve fluid network

If the solenoid position is *off* the value of area $A_{1,1}$ is zero, which means that the passage is shut and the mass flow rate is zero, in this way the pressure in the upper chamber will be not sufficient to move the valve piston downwards. When the position of the solenoid valve is *off*, the task of the valve is to put in communication the auxiliary reservoir, after a passage in the pneumatic control valve, with the brake cylinder in order to bypass the ECP system. It is clear from the figures 11 and 13a that if the valve is in its rest position allows the passage of air from the air brake control valve to the brake cylinder. Otherwise if the position of the solenoid valve is *on* the cut out valve has to close the passage, called $A_{1,2}$ in this formulation, which put in communication the pneumatic control valve with the brake cylinder, and in this way enable the ECP brake system.

If the solenoid position is *on* the value of the area $A_{1,1}$ is not zero and it is possible to determinate the air mass flow rate from the auxiliary reservoir to the upper chamber as:

$$\dot{m}_{(x-1)} = 0.6 A_{1,1} P_1 \sqrt{\frac{\left|r^2 - 1\right|}{R_g \Theta}} \frac{\left|r - 1\right|}{r - 1} \tag{21}$$

where $r = \frac{P_x}{P_1}$.

As the pressure in the chamber P_1 increase the piston which is composed the valve start to move, for this system it is possible to write the following equation about the pressure rate.

$$\frac{dP_1}{dt} = \frac{1}{V_1}\left(R_g \Theta \frac{dm_{(x-1)}}{dt} - P_1 \frac{dV_1}{dt} \right) \tag{22}$$

And V_1 is a not constant volume but as it is known that the cross section of the cylinder is constant it is clear that: $V_1 = V_{1,0} + S_1 x_1(t)$

So it is also clear that the pressure rate equation became:

$$\frac{dP_1}{dt} = \frac{1}{V_{1,0} + S_1 x_1(t)}\left(R_g \Theta \frac{dm_{(x-1)}}{dt} - P_1 S_1 \frac{dx_1(t)}{dt} \right) \tag{23}$$

It is necessary to determinate the equation which control the displacement $x_1(t)$ and its derivative.

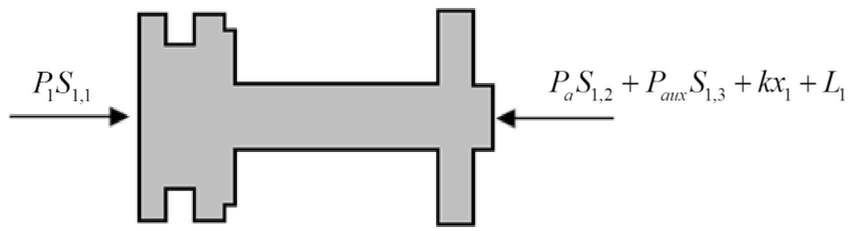

Figure 15 Cut out valve free body diagram

Using the free body diagram for the piston shown in Fig. 15, the equilibrium equation is:

$$m_1 \ddot{x}_1 = P_1 S_{1,1} - P_{atm} S_{1,2} - P_x S_{1,3} - k_1 x_1 - L_1 \tag{24}$$

Where k_1 is the stiffness of the spring valve, L_1 is the preload force of the spring, $S_{1,1}$ is the area of the piston that face the upper chamber, $S_{1,2}$ is the area of the middle part of the piston, $S_{1,3}$ is the smaller area of the piston in the lower chamber and m_1 is the mass of the piston.

Because the small mass of the piston and the very little displacement in which the piston is involved, one can assume that the inertial force $m_1 \frac{d^2 x_1(t)}{dt^2} \cong 0$ and lead to a approximate equation for the calculation of x_1:

$$x_1 = \frac{P_1 S_{1,1} - P_{atm} S_{1,2} - P_x S_{1,3} - L_1}{k_1} \tag{25}$$

And to calculate $\dot{x}_1$ differentiating the previous equation;

$$\dot{x}_1 = \frac{\dot{P}_1 S_{1,1} - \dot{P}_x S_{1,3}}{k_1} \tag{26}$$

Now is possible to write as well the mass flow rate from the auxiliary reservoir to the brake cylinder.

$$\dot{m}_{(bc-x)} = 0.6 A_{1,2} P_x \sqrt{\frac{\left|r^2 - 1\right|}{R_g \Theta}} \frac{\left|r-1\right|}{r-1} \tag{27}$$

Where $r = \frac{P_{bc}}{P_x}$

But $A_{1,2}$ is not a constant area but is as well function of x_1:

$$A_{1,2} = \pi D_1 (x_{1,\max} - x_1) \tag{28}$$

With there x_1 can be $0 < x_1 < x_{1,\max}$, x is equal to zero when the pressure P_1 is equal to atmospheric pressure and x_1 is equal to $x_{1,\max}$ if P_1 is equal to P_x.

3.3 VENT VALVE MATHEMATICAL MODEL

The main function of the vent valve is to connect the brake cylinder to atmosphere in case of release mode. A drawing of the valve is shown in Fig. 16.

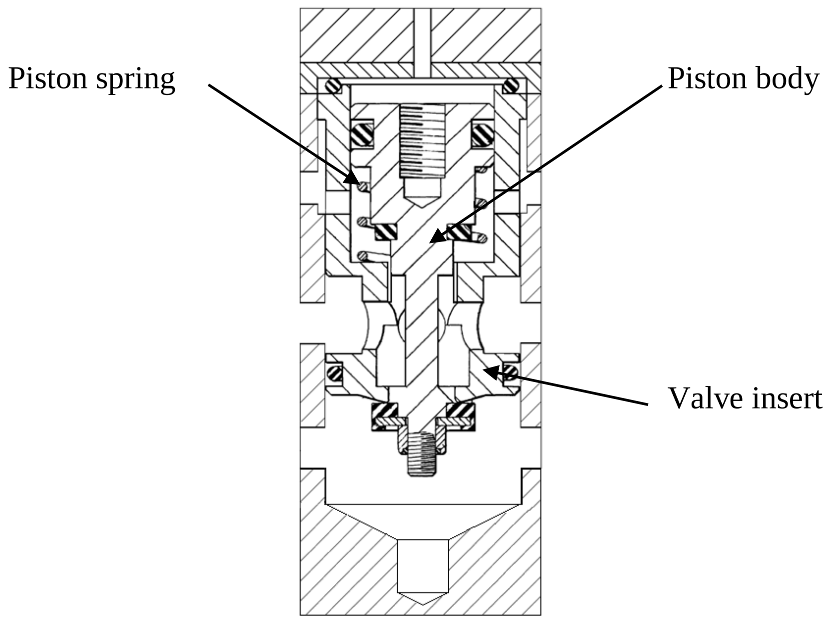

Figure 16 Vent valve scheme

This valve is controlled by a solenoid valve that is assumed only two possible position *on* and *off*. The solenoid valve controls the flow of air from the auxiliary reservoir to the upper chamber of the valve, this air flow passes through a small orifice which is called in this formulation $A_{2,1}$. The fluid network for the valve is shown in Fig.17.

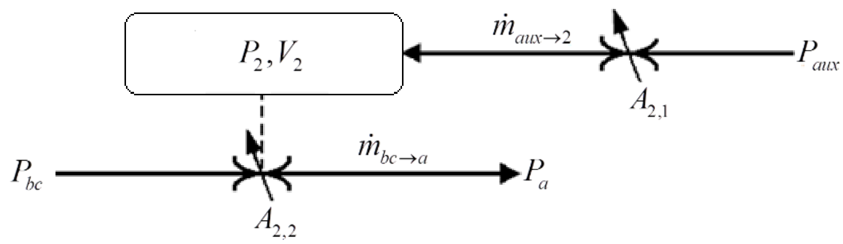

Figure 17 Vent valve fluid network

If the solenoid position is *off* the value of area $A_{2,1}$ is zero, which means that the passage is shut and the mass flow rate is zero. So when the position of the solenoid valve is *off*, the vent valve has no effect on the air flow and the connection between the brake cylinder and the atmosphere is closed.

If the position of the solenoid valve is *on* the vent valve has to open the passage, called $A_{2,2}$ in this formulation, which put in communication the brake cylinder with the atmosphere causing a drop in the cylinder which cause the release of the brake. This will happen increasing the pressure in the upper chamber of the valve (P_2) until the valve piston will move downwards opening the passage between the brake cylinder and the atmosphere, the passage area is called in this formulation $A_{2,2}$.

In order to increase the pressure in the upper chamber the orifice that connects the auxiliary reservoir with the upper chamber has to be open by the solenoid valve. This area is called $A_{2,1}$ and its value is not zero when the solenoid status is *on*. Thus it is possible to determinate the air mass flow rate as:

$$\dot{m}_{(x-2)} = 0.6 A_{2,1} P_2 \sqrt{\frac{|r^2 - 1|}{R_g \Theta}} \frac{|r-1|}{r-1} \tag{29}$$

Where $r = \dfrac{P_x}{P_2}$

As the pressure in the chamber P_2 increase the piston which is composed the valve's piston start to move, for this system it is possible to write the following equation:

$$\frac{dP_2}{dt} = \frac{1}{V_2}\left(R_g \Theta \frac{dm_{(x-2)}}{dt} - P_2 \frac{dV_2}{dt} \right) \tag{30}$$

And V_2 is a not costant volume but as it is known that the cross section of the cylinder is constant it is clear that: $V_2 = V_{2,0} + S_2 x_2(t)$

So it is also clear that the pressure rate equation became:

$$\frac{dP_2}{dt} = \frac{1}{V_{2,0} + S_2 x_2(t)} \left(R_g \Theta \frac{dm_{(x-2)}}{dt} - P_2 S_2 \frac{dx_2(t)}{dt} \right) \tag{31}$$

It is necessary to determinate the equation which control the displacement $x_2(t)$ and its derivative.

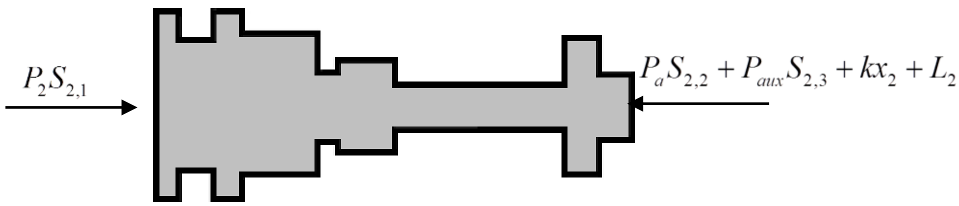

Figure 18 Vent valve free body diagram

Using the free body diagram for the piston shown in Fig. 18, the equilibrium equation is:

$$m_2 \ddot{x}_2 = P_2 S_{2,1} - P_a S_{2,2} - P_x S_{2,3} - k_2 x_2 - L_2 \tag{32}$$

Where k_2 is the stiffness of the spring valve, L_2 is the preload force of the spring, $S_{2,1}$ is the area of the piston that face the upper chamber, $S_{2,2}$ is the area of the middle part of the piston, $S_{2,3}$ is the smaller area of the piston in the lower chamber and m_2 is the mass of the piston.

Because the small mass of the piston and the very little displacement in which the piston is involved, one can assume that the inertial force $m_2 \frac{d^2 x_2(t)}{dt^2} \cong 0$ and lead to an approximate equation for the calculation of x_2:

$$x_2 = \frac{P_2 S_{2,1} - P_a S_{2,2} - P_x S_{2,3} - L_2}{k_2} \tag{33}$$

And to calculate $\dot{x}_2$ differentiating the previous equation;

$$\dot{x}_2 = \frac{\dot{P}_2 S_{2,1} - \dot{P}_x S_{2,3}}{k_2} \tag{34}$$

Now is possible to write as well the mass flow rate from the brake cylinder to the atmosphere.

$$\dot{m}_{(a-bc)} = 0.6 A_{2,2} P_a \sqrt{\frac{|r^2 - 1|}{R_g \Theta}} \frac{|r-1|}{r-1} \tag{35}$$

Where $r = \frac{P_{bc}}{P_a}$

But $A_{2,2}$ is not a constant area but is as well function of x_2: $A_{2,2} = \pi D_2 x_2$

where x_2 can be $0 < x_2 < x_{2,\max}$, x_2 is equal to zero when the pressure P_2 is equal to atmospheric pressure and x_2 is equal to $x_{2,\max}$ if P_2 is equal to P_x.

3.4 AUXILIARY VALVE MATHEMATICAL MODEL

The main function of the auxiliary valve is to connect the auxiliary reservoir to the brake cylinder in case of brake application. A drawing of the valve is shown in Fig. 19.

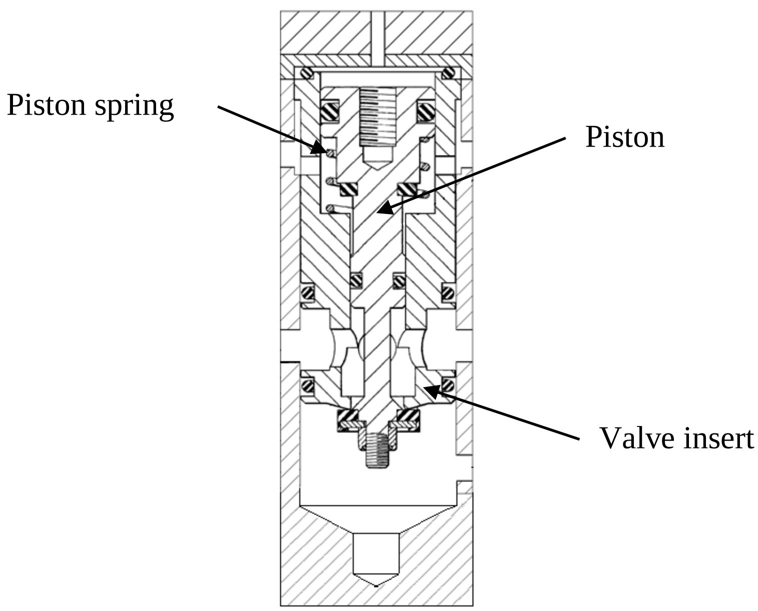

Figure 19 Auxiliary valve scheme

This valve is controlled by a solenoid valve that has only two possible positions *on* and *off*. The solenoid valve controls the flow of air from the auxiliary reservoir to the upper chamber of the valve cylinder; this air flow passes through a small area which is called in this formulation $A_{3,1}$.

The fluid network for the valve is shown in Fig. 20.

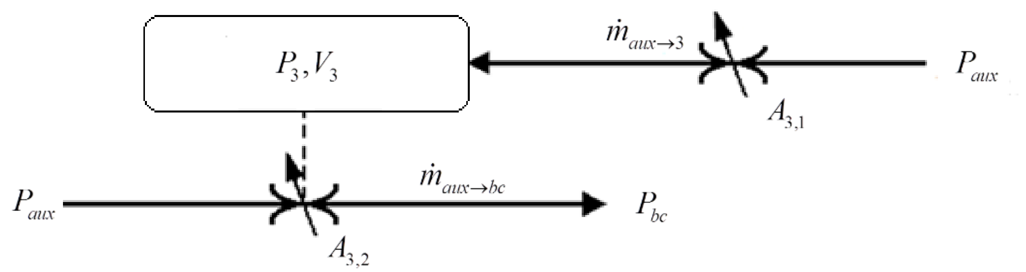

Figure 20 Auxiliary valve fluid network

If the solenoid position is *off* the value of area $A_{3,1}$ is zero, which means that the passage is shut and the mass flow rate is zero. When the position of the solenoid valve is *off*, the auxiliary valve remain in its rest position and the air flow between the auxiliary reservoir and the brake cylinder is closed.

If the solenoid position is *on* the value of the area $A_{3,1}$ is not zero and it is possible to determinate the air mass flow rate as:

$$\dot{m}_{(x-3)} = 0.6 A_{3,1} P_3 \sqrt{\frac{\left|r^2-1\right|}{R_g \Theta}\frac{\left|r-1\right|}{r-1}} \quad (36)$$

Where $r = \frac{P_x}{P_3}$.

As the pressure in the chamber P_3 increase the piston which is composed the valve start to move, for this system it is possible to write the following equation about the pressure rate.

$$\frac{dP_3}{dt} = \frac{1}{V_3}\left(R_g \Theta \frac{dm_{(x-3)}}{dt} - P_3 \frac{dV_3}{dt}\right) \quad (37)$$

But V_3 is a variable volume and as it is known that the cross section of the cylinder is constant it is clear that: $V_3 = V_{3,0} + S_3 x_3(t)$

So it is also clear that the pressure rate equation became:

$$\frac{dP_3}{dt} = \frac{1}{V_{3,0} + S_3 x_3(t)} \left(R_g \Theta \frac{dm_{(x-3)}}{dt} - P_3 S_3 \frac{dx_3(t)}{dt} \right) \qquad (38)$$

It is necessary to determinate the equation which control the displacement $x_3(t)$ and its derivative.

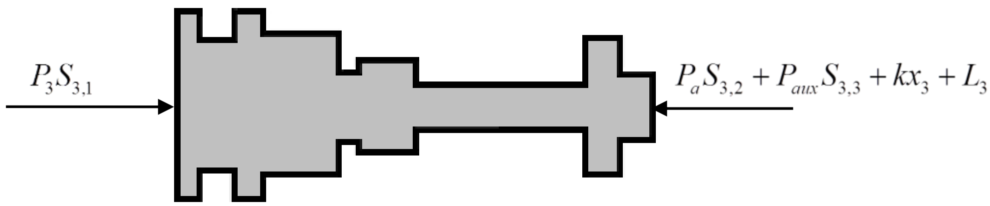

Figure 21 Auxiliary valve free body diagram

Using the free body diagram for the piston shown in Fig. 21, the equilibrium equation is:

$$m_3 \ddot{x}_3 = P_3 S_{3,1} - P_a S_{3,2} - P_x S_{3,3} - k_3 x_3 - L_3 \qquad (39)$$

Where k_3 is the stiffness of the spring valve, L_3 is the preload force of the spring, $S_{3,1}$ is the area of the piston that face the upper chamber, $S_{3,2}$ is the area of the middle part of the piston, $S_{3,3}$ is the smaller area of the piston in the lower chamber and m_3 is the mass of the piston. Because the small mass of the piston and the very little displacement in which the piston is involved, one can assume that the inertial force $m_3 \frac{d^2 x_3(t)}{dt^2} \cong 0$, and lead to an approximate equation for the calculation of x_3:

$$x_3 = \frac{P_3 S_{3,1} - P_a S_{3,2} - P_x S_{3,3} - L_3}{k_3} \qquad (40)$$

And to calculate $\dot{x}_3$ differentiating the previous equation;

$$\dot{x}_3 = \frac{\dot{P}_3 S_{3,1} - \dot{P}_x S_{3,3}}{k_3} \qquad (41)$$

Now is possible to write as well the mass flow rate from the auxiliary reservoir to the brake cylinder.

$$\dot{m}_{(bc-x)} = 0.6A_{3,2}P_{bc}\sqrt{\frac{\left|r^2-1\right|}{R_g\Theta}\frac{\left|r-1\right|}{r-1}} \tag{42}$$

Where $r = \dfrac{P_x}{P_{bc}}$

But $A_{3,2}$ is not a constant area but is as well function of x_3:

$$A_{3,2} = \pi D_3\left(x_3\right) \tag{43}$$

So x_3 can be $0 < x_3 < x_{3,max}$ x_3 is equal to zero when the pressure P_3 is equal to atmospheric pressure and x_3 is equal to $x_{3,\max}$ if P_3 is equal to P_x.

3.5 EMERGENCY VALVE MATHEMATICAL MODEL

The main function of the emergency valve is to connect the emergency reservoir to the brake cylinder to increase the pressure in it in order to apply faster higher forces in emergency application. A drawing of the valve is shown in Fig. 22.

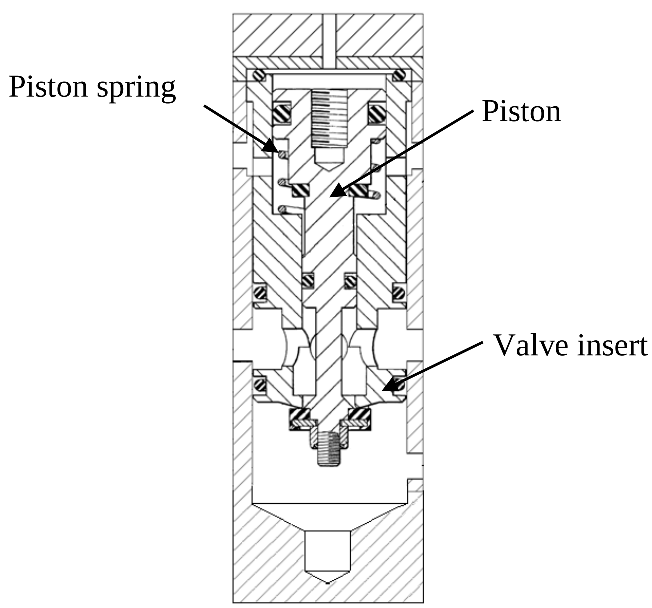

Figure 22 Emergency valve scheme

This valve is controlled by a solenoid valve which has only two possible position *on* or *off*. The solenoid valve controls the flow of air from the auxiliary reservoir to the upper chamber of the valve cylinder, this air flow passes through a small area which is called in this formulation $A_{4,1}$.

The fluid network for the valve is shown in Fig.23.

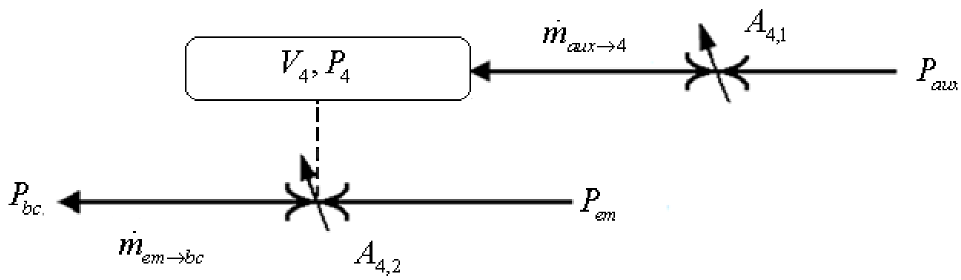

Figure 23 Emergency valve Fluid network

If the solenoid position is *off* the value of area $A_{4,1}$ is zero, which means that the passage is shut and the mass flow rate is zero.

When the position of the solenoid valve is *off*, the emergency valve has no effect on the air flow and on air brake system.

If the solenoid position is *on* the value of the area $A_{4,1}$ is not zero and it is possible to determinate the air mass flow rate as:

$$\dot{m}_{(x-4)} = 0.6 A_{4,1} P_4 \sqrt{\frac{\left|r^2 - 1\right|}{R_g \Theta} \frac{\left|r-1\right|}{r-1}} \tag{44}$$

Where $r = \frac{P_x}{P_4}$

As the pressure in the chamber P_4 increase the piston which is composed the valve start to move, for this system it is possible to write the following equation about the pressure rate.

$$\frac{dP_4}{dt} = \frac{1}{V_4}\left(R_g \Theta \frac{dm_{(x-4)}}{dt} - P_4 \frac{dV_4}{dt}\right) \tag{45}$$

And V_4 is a not constant volume but as it is known that the cross section of the cylinder is constant it is clear that:

$$V_4 = V_{4,0} + S_4 x_4(t) \tag{46}$$

So it is also clear that the pressure rate equation became:

$$\frac{dP_4}{dt} = \frac{1}{V_{4,0} + S_4 x_4(t)} \left(R_g \Theta \frac{dm_{(x-4)}}{dt} - P_4 S_4 \frac{dx_4(t)}{dt} \right) \tag{47}$$

It is necessary to determinate the equation which control the displacement $x_4(t)$ and its derivative.

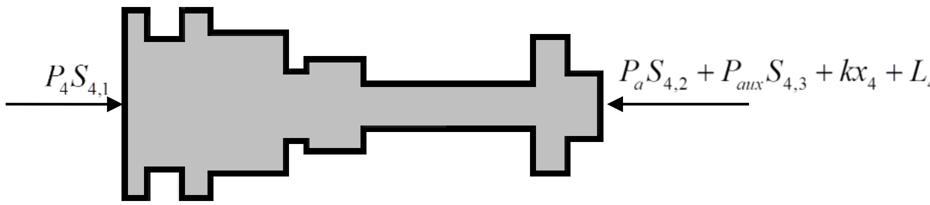

Figure 24 Emergency valve free body diagram

Using the free body diagram for the piston shown in Fig. 24, the equilibrium equation is:

$$m_4 \ddot{x}_4 = P_4 S_{4,1} - P_a S_{4,2} - P_x S_{4,3} - k_4 x_4 - L_4 \tag{48}$$

Where k_3 is the stiffness of the spring valve, L_4 is the preload force of the spring, $S_{4,1}$ is the area of the piston that face the upper chamber, $S_{4,2}$ is the area of the middle part of the piston $S_{4,3}$ is the smaller area of the piston in the lower chamber and m_4 is the mass of the piston. Because the small mass of the piston and the very little displacement in which the piston is involved, one can assume that the inertial force $m_4 \frac{d^2 x_4(t)}{dt^2} \cong 0$ and lead to a approximate equation for the calculation of x_4 :

$$x_4 = \frac{P_4 S_{4,1} - P_{atm} S_{4,2} - P_{aux} S_{4,3} - L_4}{k} \tag{49}$$

And to calculate $\dot{x}_4$ differentiating the previous equation;

$$\dot{x}_4 = \frac{\dot{P}_4 S_{4,1} - \dot{P}_x S_{4,3}}{k_4} \tag{50}$$

Now is possible to write as well the mass flow rate from the emergency reservoir to the brake cylinder.

$$\dot{m}_{(bc-em)} = 0.6A_{4,2}P_{bc}\sqrt{\frac{\left|r^2-1\right|}{R_g\Theta}}\frac{\left|r-1\right|}{r-1} \tag{51}$$

Where $r = \frac{P_{em}}{P_{bc}}$

But $A_{4,2}$ is not a constant area but is as well function of x_4 :

$$A_{4,2} = \pi D_4\left(x_4\right) \tag{52}$$

So x_4 can be $0 < x_4 < x_{4,max}$, x_4 is equal to zero when the pressure P_4 is equal to atmospheric pressure and x_4 is equal to $x_{4,\max}$ if P_4 is equal to P_x.

4. TRAIN NONLINEAR DYNAMIC EQUATIONS

In this section, the nonlinear dynamic equations of the train cars are developed using the trajectory coordinates. It is assumed that rail vehicle dynamics has no effect on the air flow in the brake pipe, while the braking forces can have a significant effect on the train longitudinal forces.

4.1 POSITION, VELOCITY, AND ACCELERATION

In order to develop the nonlinear dynamic equations of motion of the train, the global position vector of an arbitrary point on a car body is first defined.

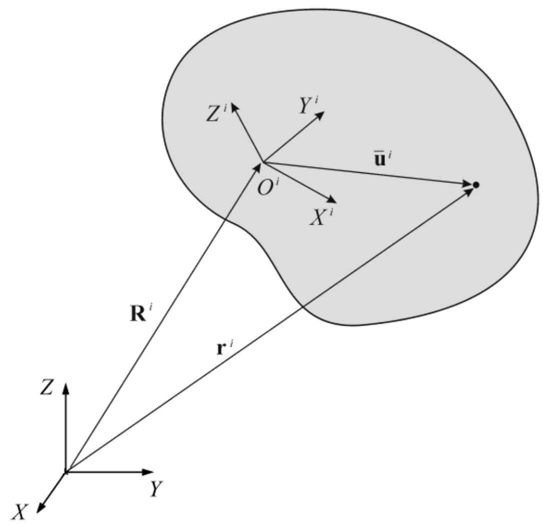

Figure 25 Coordinate systems

The position vector $\mathbf{r}^i$ of an arbitrary point on body i with respect to the global coordinate system can be defined as shown in Fig. 25 as in [8] .

$$\mathbf{r}^i = \mathbf{R}^i + \mathbf{A}^i\bar{\mathbf{u}}^i \tag{53}$$

where $\mathbf{R}^i$ is the global position vector of the origin of the body coordinate system, $\bar{\mathbf{u}}^i$ is the position vector of the arbitrary point on the body with respect to the local coordinate system, and $\mathbf{A}^i$ is the rotation matrix that defines the orientation of the local coordinate system with respect to the global system. In rigid body dynamics, $\bar{\mathbf{u}}^i$ is constant and does not depend on time. Differentiating Eq. 55 with respect to time, one obtains the absolute velocity vector defined as

$$\dot{\mathbf{r}}^i = \dot{\mathbf{R}}^i + \boldsymbol{\omega}^i \times \mathbf{u}^i \tag{54}$$

where $\boldsymbol{\omega}^i$ is the absolute angular velocity vector defined in the global coordinate system, and $\mathbf{u}^i = \mathbf{A}^i\bar{\mathbf{u}}^i$. The absolute acceleration vector is obtained by differentiating the preceding equation with respect to time, leading to

$$\ddot{\mathbf{r}}^i = \ddot{\mathbf{R}}^i + \boldsymbol{\alpha}^i \times \mathbf{u}^i + \boldsymbol{\omega}^i \times \left(\boldsymbol{\omega}^i \times \mathbf{u}^i\right) \tag{55}$$

where $\boldsymbol{\alpha}^i$ is the angular acceleration vector of body i. The preceding equation can also be written in the following alternate form:

$$\ddot{\mathbf{r}}^i = \ddot{\mathbf{R}}^i + \mathbf{A}^i\left(\bar{\boldsymbol{\alpha}}^i \times \bar{\mathbf{u}}^i + \bar{\boldsymbol{\omega}}^i \times \left(\bar{\boldsymbol{\omega}}^i \times \bar{\mathbf{u}}^i\right)\right) \tag{56}$$

where $\boldsymbol{\alpha}^i = \mathbf{A}^i\bar{\boldsymbol{\alpha}}^i$ and $\boldsymbol{\omega}^i = \mathbf{A}^i\bar{\boldsymbol{\omega}}^i$. The angular velocity vectors defined, respectively, in the global and body coordinate systems can be written in terms of the time derivatives of the orientation coordinates $\boldsymbol{\theta}^i$ as follows:

$$\boldsymbol{\omega}^i = \mathbf{G}^i\dot{\boldsymbol{\theta}}^i, \qquad \bar{\boldsymbol{\omega}}^i = \bar{\mathbf{G}}^i\dot{\boldsymbol{\theta}}^i \tag{57}$$

where $\mathbf{G}^i$ and $\bar{\mathbf{G}}^i$ can be expressed in terms of the orientation parameters $\boldsymbol{\theta}^i$ [14].

5.2 TRAJECTORY COORDINATES

The trajectory coordinate formulation is suited for the study of the train longitudinal force dynamics since the car body degrees of freedom can be systematically reduced to a set that can be related to the track geometry. A centroidal body coordinate system is introduced for each of the railroad vehicle components. In addition to the centroidal body coordinate system, a *body/track coordinate system* that follows the motion of the body is introduced. The location of the origin and the orientation of the body/track coordinate system are defined using one geometric parameter s^i that defines the distance travelled by the body along the track. The body coordinate system is selected such that it has no displacement in the longitudinal direction of motion with respect to the body/track coordinate system. Two translational coordinates, y^{ir} and z^{ir}; and three angles, ψ^{ir}, ϕ^{ir}, and θ^{ir}, are used to define the position and orientation of the body coordinate system with respect to the body/track coordinate system $X^{ti}Y^{ti}Z^{ti}$, as shown in Fig. 26.

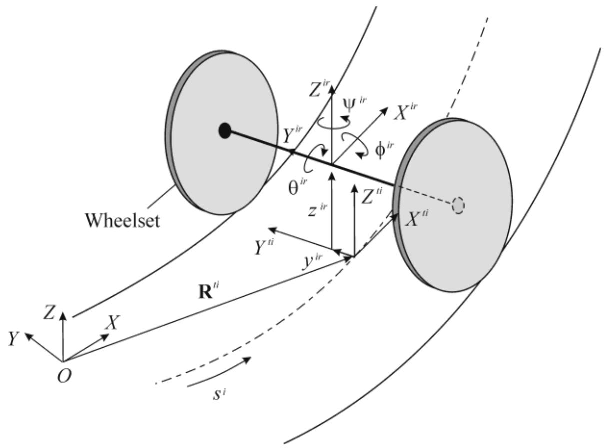

Figure 26 Trajectory coordinates

Therefore, for each body i in the system, the following six trajectory coordinates can be used:

$$\mathbf{p}^i = [s^i \quad y^{ir} \quad z^{ir} \quad \psi^{ir} \quad \phi^{ir} \quad \theta^{ir}]^T \tag{58}$$

In terms of these coordinates, the global position vector of the centre of mass of body i can be written as

$$\mathbf{R}^i = \mathbf{R}^{ti} + \mathbf{A}^{ti}\bar{\mathbf{u}}^{ir} \tag{59}$$

where $\bar{\mathbf{u}}^{ir}$ is the position vector of the center of mass with respect to the body/track coordinate system, $\mathbf{R}^{ti}$ is the global position vector of the origin of the trajectory coordinate system, and $\mathbf{A}^{ti}$ is the matrix that defines the orientation of the body/track coordinate system and is a function of three predefined Euler angles ψ^{ti}, ϕ^{ti}, and θ^{ti} which are used to define the track geometry. The vector $\mathbf{R}^{ti}$ and the matrix $\mathbf{A}^{ti}$ are functions of only one time dependent arc length parameter s^i. For a given s^i, one can also determine the three Euler angles $\boldsymbol{\theta}^{ti}\left(s^i\right) = \left[\psi^{ti}\left(s^i\right) \quad \theta^{ti}\left(s^i\right) \quad \phi^{ti}\left(s^i\right)\right]^T$ that enter into the formulation of the rotation matrix $\mathbf{A}^{ti}$ [14] (Shabana et al., 2008). The vector $\bar{\mathbf{u}}^{ri}$ can be written as

$$\bar{\mathbf{u}}^{ir} = [0 \quad y^{ir} \quad z^{ir}]^T \tag{60}$$

The matrix $\mathbf{A}^{ir}$ that defines the orientation of the body coordinate system with respect to the body/track coordinate system can be expressed in terms of the three time dependent Euler angles $\boldsymbol{\theta}^{ir} = [\psi^{ir} \quad \theta^{ir} \quad \phi^{ir}]^T$ previously defined.

5.3 EQUATIONS OF MOTION

A velocity transformation matrix that relates the absolute Cartesian accelerations to the trajectory coordinate accelerations can be systematically developed. Using the velocity transformation and the Newton-Euler equations that govern the spatial motion of the rigid bodies, the equations of motion of the car bodies expressed in terms of the trajectory coordinates can be developed. The following form of the Newton-Euler equations is used in this investigation as in [8]:

$$\begin{bmatrix} m^i\mathbf{I} & \mathbf{0} \\ \mathbf{0} & \bar{\mathbf{I}}^i_{\theta\theta} \end{bmatrix} = \begin{bmatrix} \ddot{\mathbf{R}}^i \\ \bar{\boldsymbol{\alpha}}^i \end{bmatrix} = \begin{bmatrix} \mathbf{F}^i_e \\ \bar{\mathbf{M}}^i_e - \bar{\boldsymbol{\omega}}^i \times \left(\bar{\mathbf{I}}^i_{\theta\theta}\bar{\boldsymbol{\omega}}^i\right) \end{bmatrix} \tag{61}$$

where m^i is the mass of the rigid body; $\mathbf{I}$ is a 3×3 identity matrix; $\bar{\mathbf{I}}^i_{\theta\theta}$ is the inertial tensor defined with respect to the body coordinate system; $\mathbf{F}^i_e$ is the resultant of the external forces applied on the body defined in the global coordinate system; and $\bar{\mathbf{M}}^i_e$ is the resultant of the external moments acting on the body defined in the body coordinate system. The forces and moments acting on the body include the effect of the gravity, braking forces, coupler forces, and tractive effort and motion resisting forces. If $\mathbf{a}^i$ is the vector of absolute Cartesian accelerations of the body, one can use the kinematic description given in this section to write the Cartesian accelerations in terms of the trajectory accelerations as

$$\mathbf{a}^i = \mathbf{B}^i\ddot{\mathbf{p}}^i + \boldsymbol{\gamma}^i \tag{62}$$

In this equation, $\mathbf{a}^i = \begin{bmatrix} \ddot{\mathbf{R}}^{iT} & \bar{\boldsymbol{\alpha}}^{iT} \end{bmatrix}^T$, $\mathbf{B}^i$ is a velocity transformation matrix, and $\boldsymbol{\gamma}^i$ is a quadratic velocity vector. Substituting Eq. 64 into Eq. 63 and pre-multiplying by the transpose of the velocity transformation matrix $\mathbf{B}^i$, one obtains the dynamic equations expressed in terms of the trajectory coordinates, as described in detail in [14].

5. THREE DIMENSIONAL COUPLER MODEL

As shown in Fig.27, the coupler element consists of a head and shank that can be connected to a flexible unit such as a draft gear or an end-of-car-cushioning (EOC) device that are attached to the car body.

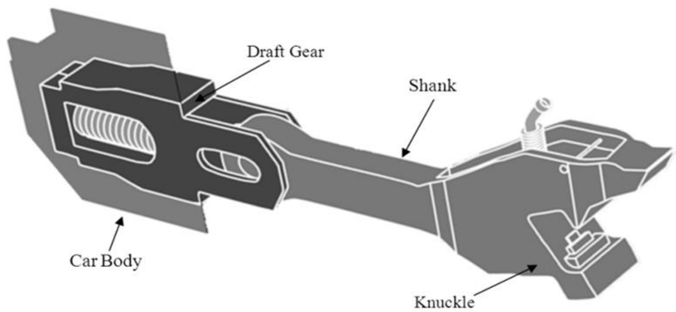

Figure 27 Automatic coupler

EOC devices generally differ from draft gears in the manner that damping is achieved. While draft gears generally use dry friction, EOC devices generally utilize dashpots. In most coupler models reported in the literature in [15], the coupler is represented using a discrete massless spring-damper element which has no kinematic degrees of freedom. This simple model does not capture geometric nonlinearities resulting from the relative motion between the coupler components as well as the relative motion of the coupler with respect to the car body. In order to be able to develop accurate longitudinal train force models, it is important to take into account the relative motion between the coupler components including the relative rotations, the slack action sliding, and the motion due to the deformation of the coupler compliant components. In this investigation a new coupler model which captures the geometric nonlinearities due to the three-dimensional kinematic motion of the car bodies as well as the motion of the coupler components is developed. In order to develop an efficient formulation and avoid increasing the number of coordinates and differential equations of motion, the effect of the inertia of the coupler has been neglected. The use of this assumption is also necessary in order to avoid having a stiff system of differential equations due to the relatively small coupler mass. The effect of neglecting the inertia of the coupler in both the computational time and the results have been discussed in [16], where neglecting of the coupler inertia has dramatic effects in increasing the computational time with excellent agreement of the results obtained. Using this assumption, one can identify two distinct sets of coordinates; inertial and non-inertial coordinates. *Inertial coordinates*, which describe three-dimensional arbitrary displacements of the car bodies, has inertia forces and coefficients associated with them. On the other hand, no inertia forces are associated with the *non-inertial coordinates*, which are used to describe the coupler kinematics. Using the principle of virtual work, one obtains a coupled system of differential/algebraic equations that must be solved simultaneously for the inertial and non-inertial coordinates. The differential equations govern the motion of the car bodies, while the resulting algebraic force equations are the result of the quasi-static equilibrium of the coupler. Knowing the inertial coordinates and velocities, the algebraic coupler force equations can be solved for the non-inertial coordinates using an iterative Newton-Raphson algorithm. In this section, the kinematic equations of the coupler components are developed in terms of independent relative coordinates [15].

5.1 DRAFT GEAR/EOC DEVICE

The draft gear or EOC device can be presented by the slider block B^i, shown in Fig.28.

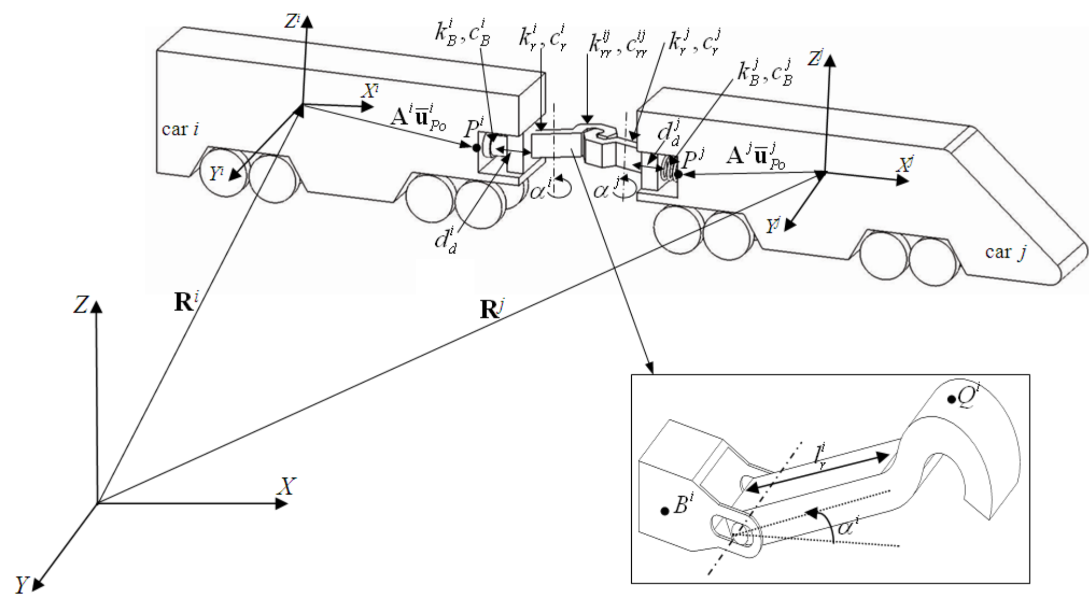

Figure 28 Two-car system

The global position vector of the center of this block, which has relative displacement d_d^i with respect to the car body i, can be written as

$$\mathbf{r}_B^i = \mathbf{R}^i + \mathbf{A}^i\left(\bar{\mathbf{u}}_{Po}^i + \bar{\mathbf{u}}_d^i\right) \tag{63}$$

Where $\mathbf{R}^i$ is the global position vector of the origin of the coordinate system of car body i, $\mathbf{A}^i$ is the transformation matrix that defines the orientation of the coordinate system of car body i, $\bar{\mathbf{u}}_{Po}^i$ is the local position vector of point P^i, $\bar{\mathbf{u}}_d^i = \left(l_o^i + d_d^i\right)\hat{\bar{\mathbf{d}}}_B^i$, $\hat{\bar{\mathbf{d}}}_B^i$ is a unit vector that defines the block sliding axis, l_o^i is the initial distance between point P^i and the center of the block B^i,and d_d^i is the relative displacement of the sliding block with respect to the car body i. The virtual displacement of the position vector of Eq. 1 can then be written as

$$\begin{aligned}\delta\mathbf{r}_B^i &= \delta\mathbf{R}^i - \mathbf{A}^i\left(\tilde{\bar{\mathbf{u}}}_o^i + \tilde{\bar{\mathbf{u}}}_d^i\right)\bar{\mathbf{G}}^i\delta\boldsymbol{\theta}^i + \mathbf{A}^i\hat{\bar{\mathbf{d}}}_B^i\delta d_d^i \\ &= \mathbf{L}_B^i\delta\mathbf{q}^i + \mathbf{L}_{Bd}^i\delta d_d^i\end{aligned} \tag{64}$$

Where

$$\mathbf{L}_B^i = \begin{bmatrix}\mathbf{I} & -\mathbf{A}^i\left(\tilde{\bar{\mathbf{u}}}_{P0}^i + \tilde{\bar{\mathbf{u}}}_d^i\right)\bar{\mathbf{G}}^i\end{bmatrix}, \quad \mathbf{L}_{Bd}^i = \mathbf{A}^i\hat{\bar{\mathbf{d}}}_B^i \tag{65}$$

The kinematic equations of the slider block will be used to define the draft gear and EOC kinematics.

5.2 SHANK

As shown in Fig. 20, the shank is allowed to rotate by the angle α^i with respect to the car body i. The location of the end point Q^i of the shank with respect to the origin of the car body coordinate system is defined by the vector $\bar{\mathbf{u}}_Q^i = \bar{\mathbf{u}}_{P0}^i + \bar{\mathbf{u}}_d^i + \bar{\mathbf{u}}_r^i$, where, $\bar{\mathbf{u}}_r^i$ is a vector defined along the rotating arm which is assumed to have length l_r^i. It follows that:

$$\bar{\mathbf{u}}_r^i = l_r^i\begin{bmatrix}\cos\alpha^i & \sin\alpha^i & 0\end{bmatrix}^T \tag{66}$$

So, the global position vector of point Q^i shown in Fig. 20 as

$$\mathbf{r}_Q^i = \mathbf{R}^i + \mathbf{A}^i\bar{\mathbf{u}}_Q^i \tag{67}$$

And the virtual change in this position vector can be written as

$$\delta\mathbf{r}_Q^i = \mathbf{L}_Q^i\delta\mathbf{q}^i + \mathbf{L}_{Bd}^i\delta d_d^i + \mathbf{L}_r^i\delta\alpha^i \tag{68}$$

where

$$\mathbf{L}_Q^i = \begin{bmatrix}\mathbf{I} & -\mathbf{A}^i\tilde{\bar{\mathbf{u}}}_Q^i\bar{\mathbf{G}}^i\end{bmatrix}, \quad \mathbf{L}_r^i = \mathbf{A}^i\left(\bar{\mathbf{u}}_r^i\right)_{\alpha^i} \tag{69}$$

and $\left(\bar{\mathbf{u}}_r^i\right)_{\alpha^i} = l_r^i\begin{bmatrix}-\sin\alpha^i & \cos\alpha^i & 0\end{bmatrix}^T$.

5.3 NON-INERTIAL GENERALIZED FORCES

As we mentioned before, neglecting the effect of the inertia of the coupler components, a quasi-static equilibrium conditions that define a set of nonlinear algebraic equations can be developed. These nonlinear equations can be solved iteratively using a Newton-Raphson algorithm to determine the non-inertial coordinates d_d^i and α^i introduced in the preceding section. In this section the nonlinear force model for both the draft gear and EOC device will be presented.

5.3.1 DRAFT GEAR FORCE MODEL

The draft gear force displacement relationship is usually highly non-linear [9], [10]. The model of any particular draft gear is based on force-displacement relationships determined using empirical formulas. Figure 29 depicts a force displacement diagram for a Mark 50 draft gear. This force displacement relationship can be closely approximated by treating it as being composed of four separate segments, as shown.

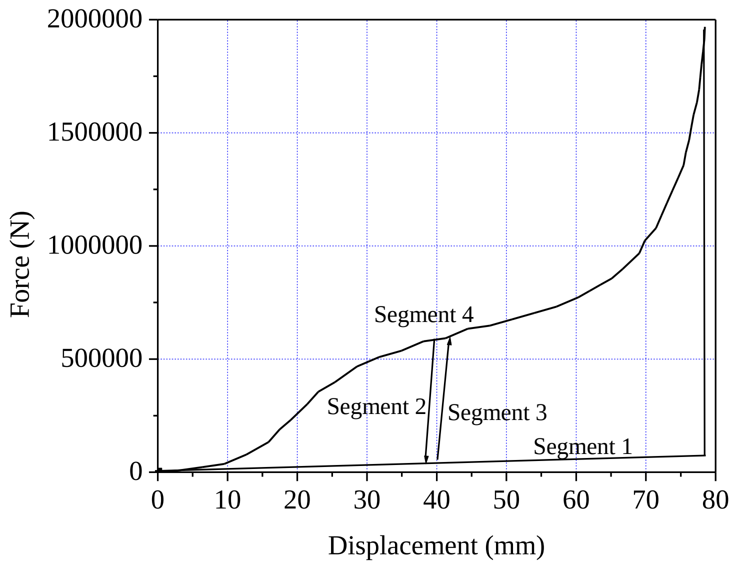

Figure 29 Force displacement curve for mark 50 Draft gear

The force of the spring between the car body i and its coupler slider component that represent the draft gear is denoted as $\mathbf{f}_B^i$ is determined in the following manner. For coupler i, let $\mathbf{f}_{Bs}^i(d_d^i)$ be the force, which can be defined as a cubic spline, for segment s, where s is segment 1 through 4, d_d^i is the current displacement, and let S^i be the slack range, h^i be the maximum coupler displacement, and k_C^i be the chassis stiffness of the cars associated with coupler i. If $d_d^i \le S^i$, then $\mathbf{f}_B^i = 0$,because the coupler is in the slack range. If $d_d^i \ge h^i$, the maximum displacement of the coupler is exceeded and now the rail car chassis themselves are deflecting. In this case, the force $\mathbf{f}^i_{Bs}$ can be calculated as

$$\mathbf{f}^i_B = (k^i_C(d^i_d - h^i) + \mathbf{f}^i_{Bs}(h^i) + c^i_C \dot{d}^i_d)\hat{\mathbf{d}}^i_B \tag{70}$$

Where c^i_C is the chassis damping coefficient and $\hat{\mathbf{d}}^i_B$ is unit vector a long which the draft gear slides. If neither of the above conditions is meet, then the coupler is in the active range of the draft gear. The draft gear's force is found in the same manner whether in draft or in buff. Therefore, only the draft condition will be described here. The buff condition is found in the same manner, except that the displacements are negative and the sign of the resultant force is negative as well. When in the active range of the draft gear, the force is determined as :

$$\mathbf{f}^i_B = (\mathbf{f}^i_{Bs}(d^i_d) + \mathbf{f}^i_{Bd}(\dot{d}^i_d))\hat{\mathbf{d}}^i_B \tag{71}$$

Where $\mathbf{f}^i_{Bd}$ is the friction damping force associated with the draft gear i, and $\dot{d}^i_d$ is the time derivative of the draft gear's displacement. To use Eq. 73, we have to determine $\mathbf{f}^i_{Bs}$ and $\mathbf{f}^i_{Bd}$, To determine $\mathbf{f}^i_{Bs}$, the segment which represents the current force displacement relationship must be determined. The force can only be read from segment 1 when the displacement is decreasing, and it can only be read from segment 4 when the displacement is increasing. If the force was being read from segment 1 or 4 in the previous time step but the direction of the motion of the displacement changes, the segment from which to read the force does not immediately switch from segment 1 to segment 4 or vice versa. It smoothly travels across the gap in between them. A segment is created between segment 1 and segment 4 whenever this condition occurs. This segment is called the hysteresis segment and is shown in Fig. 29 as segment 2 when it travels from segment 1 to segment 4 , or segment 3 when it travels segment 4 to segment 1. Whereas segments 1 and 4 are fixed and do not change with time, the hysteresis segment is repositioned whenever the force was being read from segment 1 or 4 and the direction of the motion of the displacement changes. The hysteresis segment's slope is very steep, which would cause the coupler to oscillate violently when the force is read from the hysteresis.

In this section the draft gear is modeled using the friction wedge model, where the friction wedge model gives a model that is dependent on the impact conditions as displacement and velocity. While $\mathbf{f}^i_{Bs}$ depend on the displacement d^i_d, the friction wedge adds a velocity dependent friction force $\mathbf{f}^i_{Bd}$. The friction properties of the wedge are approximated to function as :

$$\left.\begin{array}{lll} \mu = \mu_s & \text{for} & \dot{d}^i_d = 0 \\ \mu = \mu(\dot{d}^i_d) & \text{for} & 0 < \dot{d}^i_d < \mathrm{V}_f \\ \mu = \mu_k & \text{for} & \dot{d}^i_d \geq \mathrm{V}_f \end{array}\right\} \tag{72}$$

Where $\mu, \mu_s, and\ \mu_k$ are respectively the fiction coefficient, static friction coefficient, and dynamic friction coefficient, while V_f is the kinetic friction coefficient. Therefore the friction damping force can be determined as

$$\mathbf{f}_{Bd}^{i} = \mu N \hat{\mathbf{d}}_{B}^{i} \tag{73}$$

Where N is the surface normal force.

5.3.2 EOC DEVICE FORCE MODEL

The data for a generic EOC device extracted from experimental tests in draft and in buff, where EOC device exhibits different forces as well as different maximum displacements in draft and in buff. In this investigation, the force $\mathbf{f}_{B}^{i}$ acting on the coupler is found from the force-displacement curve and from known constant spring stiffness. The spring force is found by the linear relationship $\mathbf{f}_{Bk}^{i} = k_{B}^{i} d_{d}^{i} \hat{\mathbf{d}}_{B}^{i}$, where $\mathbf{f}_{Bk}^{i}$ is the force from the spring and k_{B}^{i} is the spring constant. The damping force is found by subtracting the spring force $\mathbf{f}_{Bk}^{i}$ from $\mathbf{f}_{Bc}^{i}$, where $\mathbf{f}_{Bc}^{i}$ the force interpolated from the force-displacement curve shown in Fig. 30 and Fig. 31.

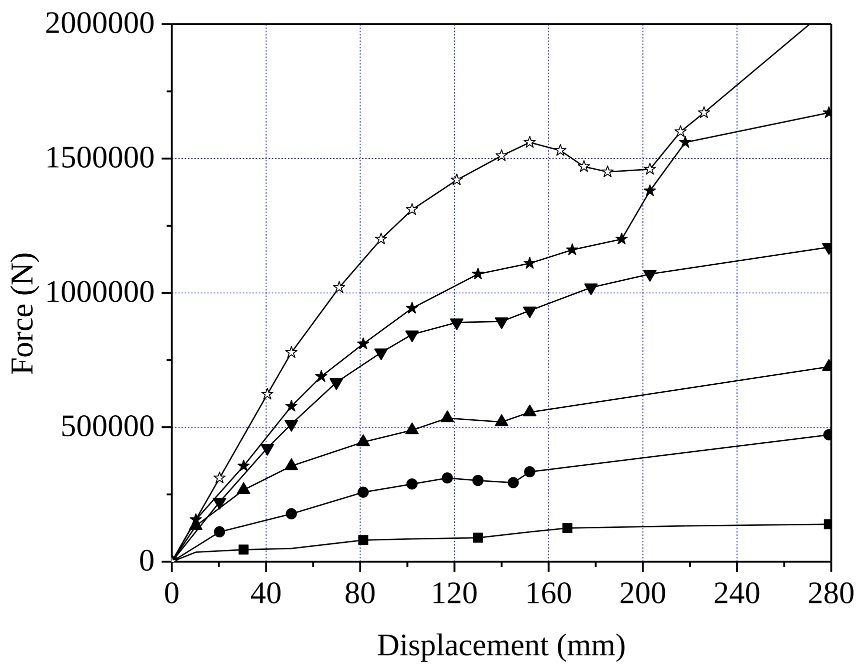

Figure 30 Force displacement curve for EOC device in draft ─■─ 0.42 m/s, ─●─ 0.916 m/s, ─▲─ 1.29 m/s, ─▼─ 1.814 m/s, ─★─ 2.02 m/s, ─☆─ 2.56 m/s

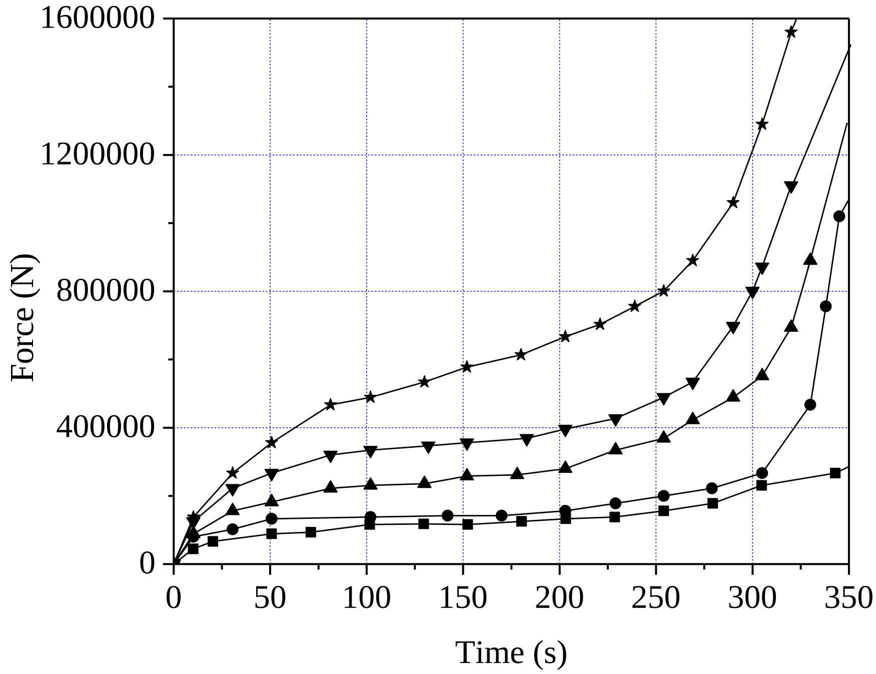

Figure 31 Force displacement curve for EOC device in buff
—■— 0.473 m/s, —●— 0.867 m/s, —▲— 1.31 m/s, —▼—1.774 m/s, —★— 2.244 m/s

For a given displacement velocity of the EOC device $\dot{d}_d^i$, $\mathbf{f}_{Bc}^i$ is found from linear interpolation between the force-displacement curves

$$\mathbf{f}_{Bc}^i = \frac{v_{s+1} - \dot{d}_d^i}{v_{s+1} - v_s}\mathbf{f}_{B(s+1)}^i(d_d^i) + \frac{\dot{d}_d^i - v_s}{v_{s+1} - v_s}\mathbf{f}_{B(s)}^i(d_d^i) \tag{74}$$

where $\mathbf{f}_{B(s)}^i(d_d^i)$ is the force at displacement d_d^i for the curve for displacement velocity v_s. If $\dot{d}_d^i$ lies below the minimum curve, $\mathbf{f}_{B(\min)}^i(d_d^i)$ then $\mathbf{f}_{Bc}^i = \frac{\dot{d}_d^i}{v_{\min}}\mathbf{f}_{B(\min)}^i(d_d^i)$ where $v_{\min}$ is the velocity of the minimum curve. If $\dot{d}_d^i$ is greater than the highest curve, $\mathbf{f}_{B(\max)}^i(d_d^i)$, then the force $\mathbf{f}_{Bc}^i$ is found by linear extrapolation $\mathbf{f}_{Bc}^i = \frac{\dot{d}_d^i}{v_{\max}}\mathbf{f}_{B(\max)}^i(d_d^i)$, where $v_{\max}$ is the velocity of the maximum curve. The magnitude of the damping force $\left|\mathbf{f}_{Bc}^i\right|$ can then be found using the difference $\mathbf{f}_{Bc}^i - \mathbf{f}_{Bk}^i$.The damping force is then determined from $\left|\mathbf{f}_{Bc}^i\right|$ according to the sign of the velocity $\dot{d}_d^i$ as follows:

$$\mathbf{f}_{Bc}^{i}=\begin{cases}\left|\mathbf{f}_{Bc}^{i}\right| & \text{if } \dot{d}_{d}^{i}>0\\ -\left|\mathbf{f}_{Bc}^{i}\right| & \text{if } \dot{d}_{d}^{i}<0\end{cases} \tag{75}$$

The total force acting on the coupler is then $\mathbf{f}_{B}^{i}=\mathbf{f}_{Bc}^{i}+\mathbf{f}_{Bk}^{i}$.If the EOC device has different force characteristics in draft and in buff, then different sets of curves are used for $\mathbf{f}_{B(s)}^{i}(d_{d}^{i})$.

The virtual work of the forces given for both the draft gear and EOC device can be written as $\delta W_{B}^{ij}=\mathbf{f}_{B}^{i\,T}\delta\mathbf{r}_{P}^{i}-\mathbf{f}_{B}^{i\,T}\delta\mathbf{r}_{B}^{i}+\mathbf{f}_{B}^{jT}\delta\mathbf{r}_{P}^{j}-\mathbf{f}_{B}^{jT}\delta\mathbf{r}_{B}^{j}$. Using this equation and the expressions of the virtual displacements, one obtains

$$\delta W_{B}^{ij}=\mathbf{Q}_{B}^{i\,T}\delta\mathbf{q}^{i}+\mathbf{Q}_{B}^{j\,T}\delta\mathbf{q}^{j}+\left(\mathbf{Q}_{B}^{ij}\right)_{ni}^{T}\delta\mathbf{q}_{ni}^{ij} \tag{76}$$

In this equation, $\mathbf{q}_{ni}^{ij}$ is the vector of the coupler non-inertial coordinates defined as

$$\mathbf{q}_{ni}^{ij}=\begin{bmatrix}d_{d}^{i} & \alpha^{i} & d_{d}^{j} & \alpha^{j}\end{bmatrix}^{T} \tag{77}$$

and

$$\left.\begin{aligned}&\mathbf{Q}_{B}^{i}=\left(\mathbf{L}_{P}^{i}-\mathbf{L}_{B}^{i}\right)^{T}\mathbf{f}_{B}^{i},\quad \mathbf{Q}_{B}^{j}=\left(\mathbf{L}_{P}^{j}-\mathbf{L}_{B}^{j}\right)^{T}\mathbf{f}_{B}^{j},\\ &\left(\mathbf{Q}_{B}^{ij}\right)_{ni}=\begin{bmatrix}-\mathbf{L}_{Bd}^{i\ T}\mathbf{f}_{B}^{i} & 0 & -\mathbf{L}_{Bd}^{j\ T}\mathbf{f}_{B}^{j} & 0\end{bmatrix}^{T}\end{aligned}\right\} \tag{78}$$

5.3.3 SHANK CONNECTION FORCES

For the revolute joint between the coupler shank and the draft gear/EOC of each car, a torsional spring with stiffness k_{r}^{i} and damping c_{r}^{i} is introduced at this joint. The generalized forces associated with the non-inertial coordinates α^{i} and α^{j} can be written, respectively, as

$$Q_{r}^{i}=-k_{r}^{i}\left(\alpha^{i}-\alpha_{o}^{i}\right)-c_{r}^{i}\dot{\alpha}^{i},\quad Q_{r}^{j}=-k_{r}^{j}\left(\alpha^{j}-\alpha_{o}^{j}\right)-c_{r}^{j}\dot{\alpha}^{j} \tag{79}$$

Where $\hat{\mathbf{d}}_{r}^{i}$ and $\hat{\mathbf{d}}_{r}^{j}$ are unit vectors along the shank and draft gear/EOC joint axis of car bodies i and j, respectively. This leads to the following generalized force vector associated with the non-inertial coupler coordinates

$$\left(\mathbf{Q}_{r}^{i}\right)_{ni}=\begin{bmatrix}0 & Q_{r}^{i} & 0 & Q_{r}^{j}\end{bmatrix}^{T} \tag{80}$$

The force at the knuckle due to the interaction between the two couplers that connect the two cars is denoted as $\mathbf{f}_{rr}^{ij}$. This force vector can be written as

$$\mathbf{f}_{rr}^{ij} = \left(k_{rr}^{ij} \left(l_r^{ij} - l_{ro}^{ij} \right) + c_{rr}^{ij} \dot{l}_r^{ij} \right) \hat{\mathbf{d}}_{rr}^{ij} \tag{81}$$

In this equation, k_{rr}^{ij} and c_{rr}^{ij} are the spring stiffness and damping coefficients, l_r^{ij} is the current spring length, l_{ro}^{ij} is the un-deformed length of the spring, and $\hat{\mathbf{d}}_{rr}^{ij}$ is a unit vector along the line connecting points Q^i and Q^j, that is, $\hat{\mathbf{d}}_{rr}^{ij} = \left(\mathbf{r}_Q^i - \mathbf{r}_Q^j \right) \big/ \left| \mathbf{r}_Q^i - \mathbf{r}_Q^j \right|$. The virtual work of the force $\mathbf{f}_{rr}^{ij}$ can be written as $\delta W_{rr}^{ij} = -\mathbf{f}_{rr}^{ijT} \delta \mathbf{r}_Q^i + \mathbf{f}_{rr}^{ijT} \delta \mathbf{r}_Q^j$. This equation upon using the kinematic equations previously developed in this study can be written as

$$\delta W_{rr}^{ij} = \mathbf{Q}_{rr}^{i\,T} \delta \mathbf{q}^i + \mathbf{Q}_{rr}^{j\,T} \delta \mathbf{q}^j + \left(\mathbf{Q}_{rr}^{ij} \right)_{ni}^T \delta \mathbf{q}_{ni}^{ij} \tag{82}$$

In this equation,

$$\left. \begin{aligned} &\mathbf{Q}_{rr}^i = -\mathbf{L}_Q^{i\,T} \mathbf{f}_{rr}^{ij}, \quad \mathbf{Q}_{rr}^j = \mathbf{L}_Q^{i\,T} \mathbf{f}_{rr}^{ij}, \\ &\left(\mathbf{Q}_{rr}^{ij} \right)_{ni} = \left[-\mathbf{L}_{Bd}^{i\,T} \mathbf{f}_{rr}^{ij} \quad -\mathbf{L}_r^{i\,T} \mathbf{f}_{rr}^{ij} \quad \mathbf{L}_{Bd}^{j\,T} \mathbf{f}_{rr}^{ij} \quad \mathbf{L}_r^{j\,T} \mathbf{f}_{rr}^{ij} \right]^T \end{aligned} \right\} \tag{83}$$

5.4 GENERALIZED INERTIAL AND NON-INERTIAL FORCES

From the forces developed in previous section, the generalized coupler forces associated with the inertial coordinates of the car bodies i and j can be written as

$$\left. \begin{aligned} \mathbf{Q}_c^i &= \mathbf{Q}_B^i + \mathbf{Q}_{rr}^i = \left(\mathbf{L}_P^i - \mathbf{L}_B^i \right)^T \mathbf{f}_B^i - \mathbf{L}_Q^{i\,T} \mathbf{f}_{rr}^{ij}, \\ \mathbf{Q}_c^j &= \mathbf{Q}_B^j + \mathbf{Q}_{rr}^j = \left(\mathbf{L}_P^j - \mathbf{L}_B^j \right)^T \mathbf{f}_B^j + \mathbf{L}_Q^{i\,T} \mathbf{f}_{rr}^{ij} \end{aligned} \right\} \tag{84}$$

The forces associated with the non-inertial coupler coordinates are

$$\left(\mathbf{Q}_c^i \right)_{ni} = \left(\mathbf{Q}_B^i \right)_{ni} + \left(\mathbf{Q}_{rr}^i \right)_{ni} + \left(\mathbf{Q}_r^i \right)_{ni} = \begin{bmatrix} -\mathbf{L}_{Bd}^{i\,T} \left(\mathbf{f}_B^i + \mathbf{f}_{rr}^{ij} \right) \\ -\mathbf{L}_r^{i\,T} \mathbf{f}_{rr}^{ij} + Q_r^i \\ -\mathbf{L}_{Bd}^{j\,T} \left(\mathbf{f}_B^j - \mathbf{f}_{rr}^{ij} \right) \\ \mathbf{L}_r^{j\,T} \mathbf{f}_{rr}^{ij} + Q_r^j \end{bmatrix} \tag{85}$$

The generalized forces associated with the car body inertial coordinates od Eq. 87 can be introduced to the dynamic equations of motion, while the four dimensional force vector associated with the coupler non-inertial coordinates can be used to solve for non-inertial coordinates d_d^i, α^i, d_d^j, and α^j using an iterative procedure described in [15].

6. NUMERICAL RESULTS

In this section will be presented several numerical results in order to give to the model proposed in this study, a strong experimental support and then to present the improvement of the ECP braking system in respect to the conventional air brake.

For this first reason it will be presented the results of obtained with the developed model that follow the standard proposed by AAR for testing of cable based ECP system (S-4200) ("Performance Requirements for Testing Electronically Controlled Pneumatic (ECP) Cable-Based Freight Brake System") [1].

These results has the aim to show that the system meets the performance requirements specified in the standard and furthermore the results will be compared with the experimental results of the same test reported in [11] in order to provide a sort of validation of the model described before.

In the second part of the chapter, numerical results will be exposed in order to evaluate the effects of the ECP system in the field of the longitudinal dynamic for long trains. In order to accomplish this task will be studied at first the stopping distance with the ECP system and the conventional air brake system, to verify the benefits of the ECP system claimed in the literature. Then it will be studied the in-train forces with the two system in order to evaluate the effects of simultaneous braking compared to those of the delay time of the pressure drop in the brake pipe. Finally a comparison between the two systems in the charging phase will be made.

6.1 PNEUMATIC PERFORMANCE TEST

As previously specified in this section will be provided the results of some of the test described in "Performance Requirements for Testing Electronically Controlled Pneumatic (ECP) Cable-Based Freight Brake System", AAR S-4200 standard [1].

To be consistent with the experimental result with which it will compared the developed model we now provide a brief description of the equipment used in the test and subsequently will be explained what will be the conditions in which it will be performed the simulations, in order to make clear the differences and similarities between the two configurations.

Description of the test condition for TSM system

The TSM systems consist of a Car Control Device (CCD) and a manifold. The manifold contains the solenoids valves and the pressure transducers which are used to fill and vent the brake cylinder and monitor brake pipe and reservoir pressure. The manifold is mounted between the pipe bracket and the service portion of the pneumatic control valve. When the ECP is system is energized, the manifold cuts off communication between the service portion and the brake cylinder, but the service portion continues its function of charging the reservoir. The system is controlled by the head end unit (HEU) which is mounted on the top of the engineer's control stand. The HEU consist of a control box which has push buttons and soft keys.

Brake applications are made as a percent of full service pressure, with full service being a 100-percent application, a minimum service being a 15-percent application, and an emergency being a 120-percent application. The brake can be applied and released in 1-percent increments from 0 to 100 percent. The car brake systems are connected to each other by a shielded two-conductor gage cable. The cable carries both power and signal. The system allows the engineer to directly control the brake cylinder pressure on every car in the train. The brake pipe is used only to charge the reservoirs. Fifty TSM manufactured ECP brake CCDs were installed on the 150-car brake rack. The TSM CCDs were installed on every third air-brake control valve. Unequipped air-brake control valves were cut out. This setup resulted in the equivalent of a 7500-foot train comprised of fifty 150-foot cars.

Train model for the simulation

In order to obtain comparable results it will be build a 50-car train model in which every car will be "equipped" with the ECP brake system. In this series of simulation the dynamic of the train is ignored because the aim of this part is to evaluate the pneumatic performance of the system. Every ECP unit in the train model is composed as well by a CCD and of the four valves (cut-out, vent, auxiliary, emergency) described before. In the model the CCD is a logical controller, as described in chapter 3 of this study, and so is not affected by any errors or inaccuracy that can affect a real CCD. The simulated system assumes for the brake pipe model and for the brake cylinder model the one proposed in [5] and [6]. In Table 1 are reported the parameter of brake pipe and the detailed parameters of the CCU are reported in Table 2.

The tests that it will be made are described in the standard "Performance Requirements for Testing Electronically Controlled Pneumatic (ECP) Cable-Based Freight Brake System", AAR Specification S-4200. The aim of these tests is to verify the performance of the electro-pneumatic system, especially in order to estimate the time required to apply brakes o to release on a single car and in the following cars. The test plan consisted of testing to Section 4 and 5 of the S-4200 specification. Section 4 describes the single car test rack requirements, and Section 5 describes the performance requirements during test testing on an AAR approved 150-car test rack. The performance requirements cover the normal operation of the system.

Full-Service Brake Application and Release Test

The first test is a "Full-Service Brake Application and Release Test" performed on the 50-car model. The test consist in apply a full service brake force; hold the pressure in the brake cylinder for 20 seconds and then a full release is commanded. The requirements for the successful completion of the test are as follows, the correct pressure (64 psig, 542589.47 Pa) in the brake cylinder must be achieved in 10 seconds with a maximum inaccuracy of ±2 psig for at least 10 seconds in all the units. The full release (in which the threshold is assumed to be 5 psig (135798.7 Pa)) must be reached within 15 seconds of the time at which the command is given.

In Fig. 32 is shown the pressure in the brake cylinder and the auxiliary reservoir in cars 1 and 50, in order to show the worst possible case in the simulation test. From Figure 24 is possible to appreciate that the system fulfills the requirements, the build up time is about 5 second for every car and it is also evident that the pressure increase simultaneously in all the brake cylinders. As well the requirement for the release time is achieved; with the threshold pressure of 5 psig is reached after 12 seconds.

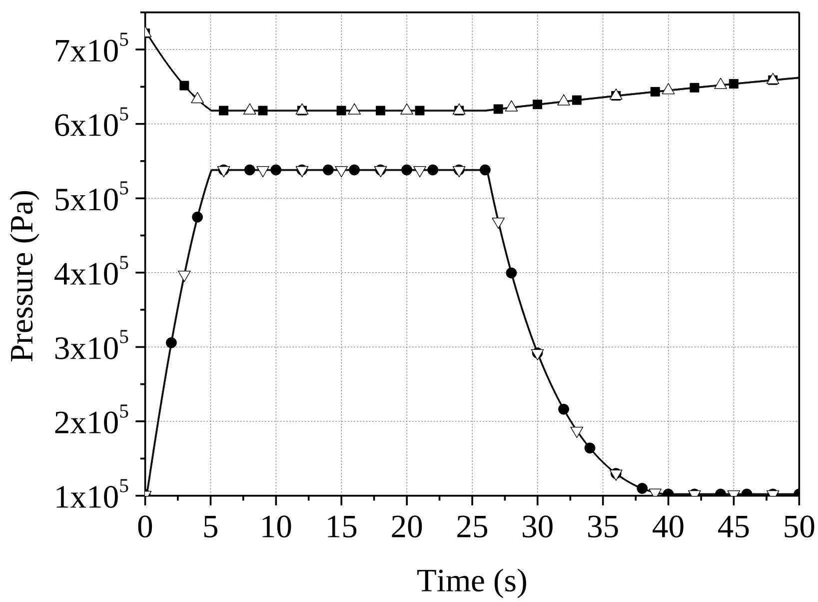

Figure 32: Full service application scenario.
Brake cylinder car 1 Brake cylinder car 50 Auxiliary reservoir car Auxiliary reservoir car 50

In Fig. 33 is reported the experimental results of the previously cited paper and the numerical results. From the comparison is possible to appreciate that the behavior of the tested system is reasonably similar to the one of the simulation.

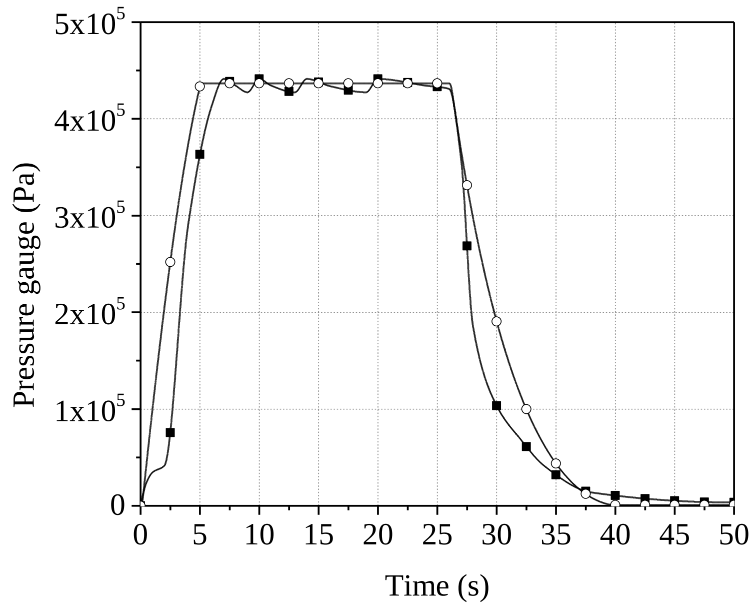

Figure 33: Full service application scenario comparison.
—■— Experimental results —○— Simulation results

It is important to keep in mind that the system in the proposed model is not exactly the system tested because the detail parameters of the TSM system are not available. The main difference is in the phase in which the pressure of the brake cylinder has to be maintained to the desired value, in this phase the TSM brake cylinder appear to have some leakage and so the system's control center fill it in order to re-establish the desired pressure. In the simulated system there is no leakage on the brake cylinder and so the pressure is stable when has reached the desired level of application.

Minimum Service Application and Release Test

Minimum service requirements were tested in accordance with Section 4.1 of S-4200. With the reservoirs fully charged, a minimum service brake application is commanded. The pressure is maintained for 20 seconds and then the complete release is commanded. The only requirement for this test is to reach the desired pressure (9.6 psig, 167514.6 Pa) and maintain it in the tolerance of ±2 psig for 20 seconds.

In Fig. 26 is shown that the simulated model meets the requirements and as before mentioned all the units reach the desired pressure in the same time.

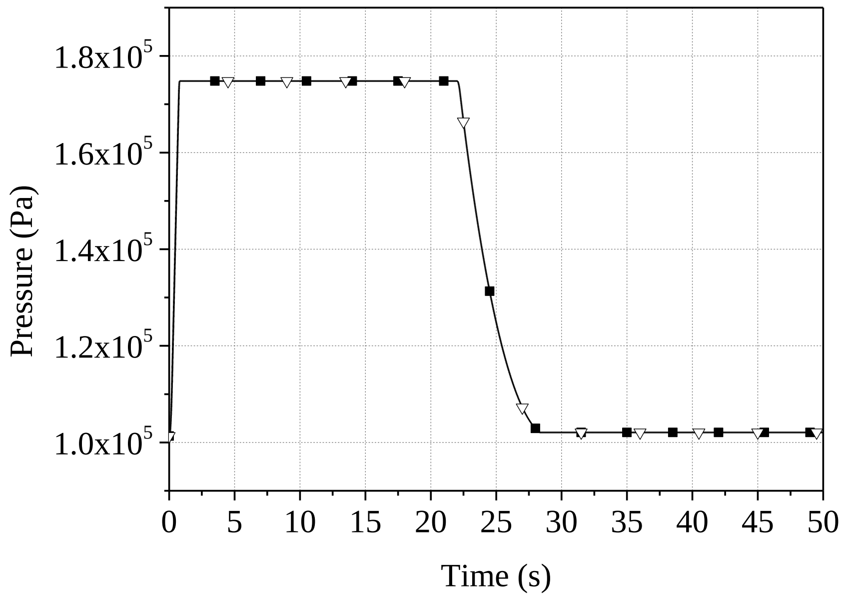

Figure 34: Minimum service application scenario.
Brake cylinder car 1 Brake cylinder car

The experimental data showed in Fig. 27 behave in a good way but suffer a problem of over-pressure which is quickly corrected by the controller, still the over-pressure has to be eliminated as the report said "this over-pressure condition is undesirable and is being addressed by the equipment manufacturer".

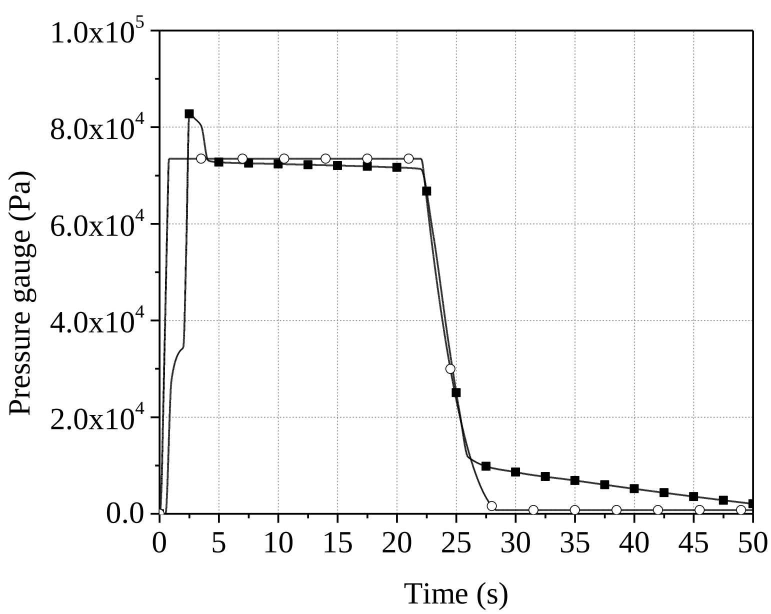

Figure 35: Minimum service application scenario comparison.
Experimental results Simulation results

Emergency Application

Emergency application is tested in accordance with Section 4.3 of S-4200. An emergency application is commanded immediately after a release from full service, as specified in the S-4200, no release command is given. To be successful in this test the brake cylinder should reach the 120-percent of the full service application pressure (76.8 psig, 630842.36 Pa) within 10 seconds and hold this pressure indefinitely. In Fig. 28 is shown the results of this test, the requirement were fulfilled with a build up time of approximately 2 second. The numerical results for this test are not presented because the TSM system does not fulfill the requirements.

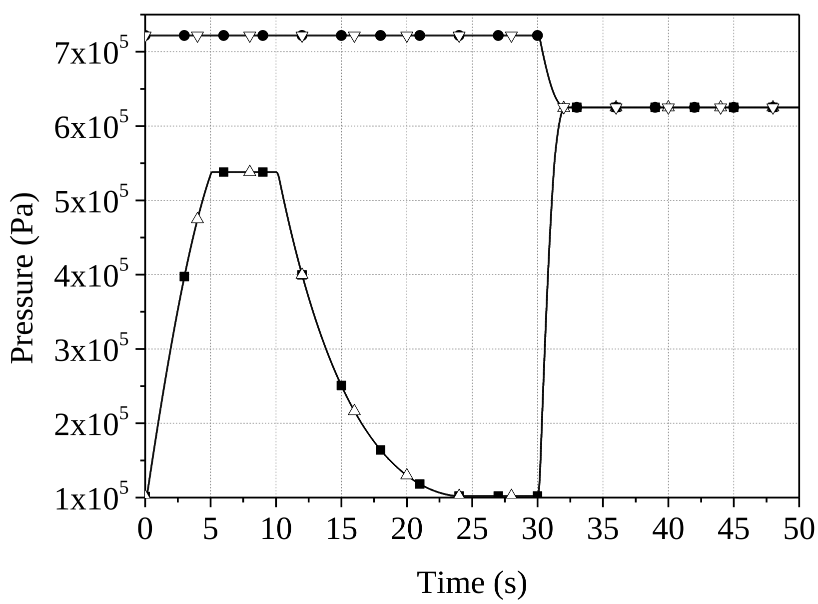

Figure 36: Emergency application scenario.
Brake cylinder car 1 Brake cylinder car 50 Emergency reservoir car 1 Emergency reservoir car 50

Graduated Application and release

The graduated application and release test is performed in accordance with Section 5.2 of S-4200. Starting with the reservoirs fully charged, a minimum service application is commanded (as explained before means 15 percent of the full service brake pressure), then the pressure is reduced to 10 percent of full service. Then every 5 seconds, the commanded brake application is increased by 10-percent of full service until a full service brake application is reached. Afterwards the commanded brake application is reduced by 10 percent of full service at 5 seconds intervals until the brakes are fully released. The S-4200 standard requires that the pressure within the brake cylinder follow commands quickly and ensure the required pressure with a tolerance of ±2 psig.

As pointed out in [2] and [3] the gradual release of the brake is the new possibilities that the ECP system allows in respect to the conventional brake system. Graduated or incremental release of a brake application is a major benefit on North America where existing equalization type systems are direct release only. In fact, with the conventional air brake system was not possible to carry out a partial release of the brake, and this meant that once started braking was not possible to reduce the intensity but only release the brake completely or continue with the intensity selected. With this new capability is possible to improve braking efficiency by ensuring greater control of braking maneuvers by the engineer. It follows also the ability to reduce the fuel consumption and requires a lesser amount of air increasing the availability of reservoirs in brake application. The simulated system meets the requirements of the standard as is shown in figure 37 and figure 38. The TSM system also follows the indication of standard with more inaccuracy than the proposed model.

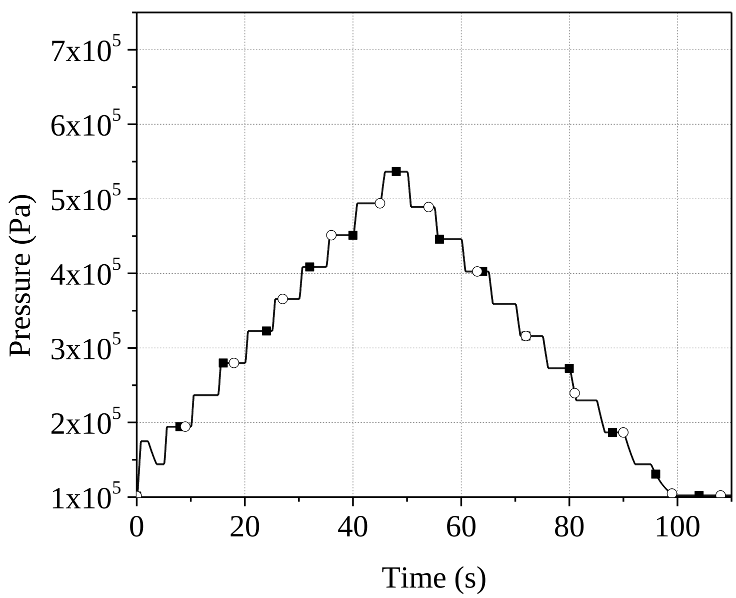

Figure 37: Graduated application and release scenario.
(—■— Brake cylinder car 1 —○— Brake cylinder car 50)

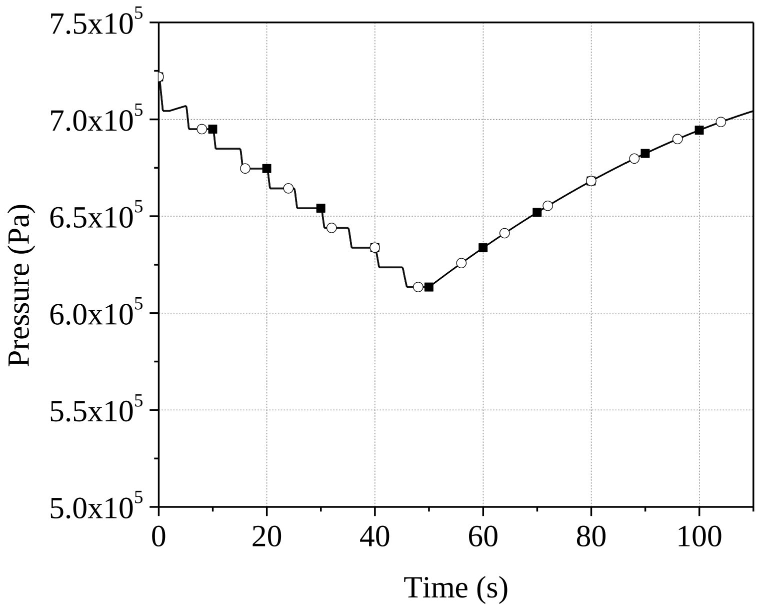

Figure 38: Graduated application and release scenario.
(—■— Auxiliary reservoir car 1 —○— Auxiliary reservoir car 50)

Repeated Full Service Brake Application Test

The repeated Full service brake application test is performed in accordance with section 5.3 of S-4200. With the reservoir completely charged a full-service application is commanded, when the desired pressure (64 psig, 542589.47 Pa) is reached a complete release is commanded. After fifteen second another full-service application is made. The standard requires that both the first and the second application to reach the full-service pressure. In Fig. 39 is shown that the proposed model is able to fulfill the requirements. Figure 32 shows that also the test system fulfills the requirements of the standard, it also shows that the simulated system and the tested system have a very similar behavior.

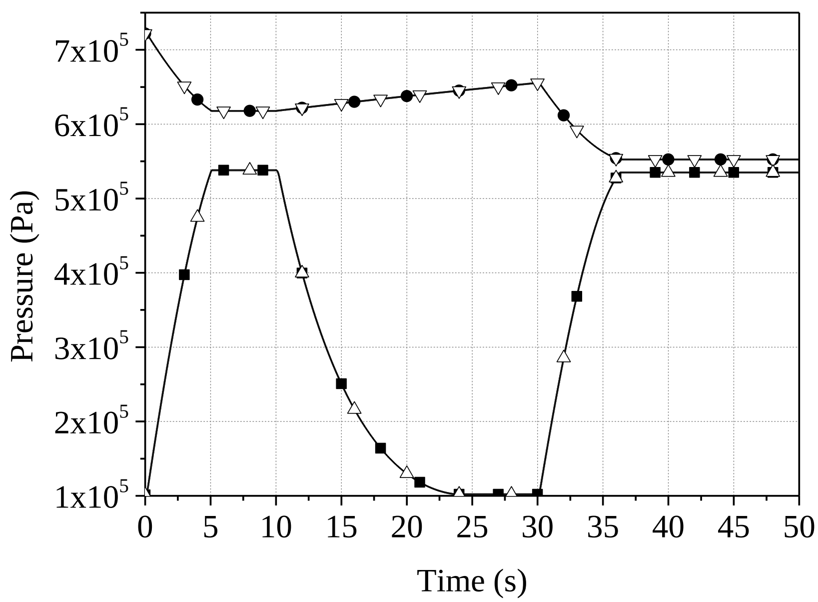

Figure 39: Repeated full service application scenario.
(—■— Brake cylinder car 1 —△— Brake cylinder car 50 —●—Auxiliary reservoir car 1
—▽—Auxiliary reservoir car 50)

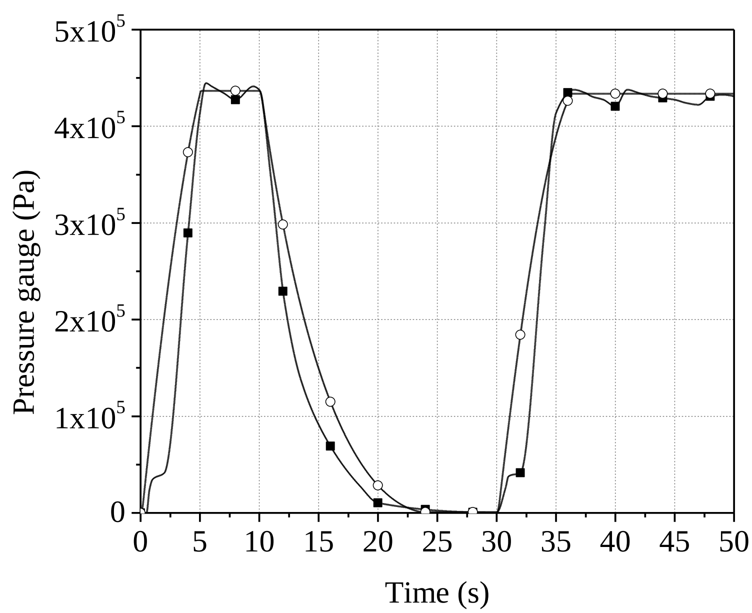

Figure 40: Repeated full service application scenario comparison.
(—■— Experimental results —○— Simulation results)

With this test is ended the part about the pneumatic performance of the system. By the results presented it is possible to conclude that the developed model with the features provided meets the requirements of the standard S-4200 and by comparison with the test found in the literature may also conclude that the behavior is reasonably consistent with an ECP system currently installed on freight trains in North America. Finally is important to remember that the system parameters have not been taken from an actual prototype but based on the information gathered and experience gained, which means that a system with different parameters may result in more or less significant differences with results presented in this work.

6.2 BRAKING PERFORMANCE OF ECP SYSTEM

In this section it will be tested the performance of the ECP braking system in respect to the conventional air brake system. As is well known the application of conventional pneumatic brakes is dependent on the pressure differential between the auxiliary reservoir and the brake pipe, and the rate at which the brake pipe pressure drop being sensed by the triple valve. Due to this dependency on the triple valve detecting these changes in the brake pipe pressure results in a delay from when the driver enables a brake application till the triple valves in the train are consecutively activated. Thus the brake delay period varies with the train length, so the longer the train the longer the delay. The consequences of this delay are critical mainly in two aspects, the stopping distance and the longitudinal forces exchanged between a carriage and the adjacent absorbed almost entirely by couplers.

With ECP the factor of train length affecting brake delay is removed since all CCDs in the train receive the broad cast Train Brake Command (TBC) from the HEU with any delay.

The analysis of the performance will consider several aspects; first the stopping distance difference between an ECP equipped train and a conventional air brake equipped train, second the in-train force distribution along the train. It will be also shown how the continuous recharging will affect the charging time in a long train.

Stopping distance

The first result presented will be a confrontation of the stopping distance of the same train with the two different braking systems proposed. A 75-car model for a train with 3 locomotives travelling on a tangent track is considered. It is assumed that all the cars and the locomotives have initial forward velocity of 29.1 m/s (65.0 mph), and the brake pipe length is 1059.5 m (3476.05 ft), which is modeled using 150 finite elements, the characteristics of it such mass, number of wheelset, dimension of the cars and locomotives are shown in Table 4. The train will start with the reservoirs at the operative pressure of 90 psig (721853.15 Pa), after 5 seconds a full service application is made then at 80 seconds a full release is commanded. The simulation will continue until all the auxiliary reservoirs are fully recharged at the operative pressure. In the Figures 33 and 34 is shown the distance traveled and the velocity in respect to time by the train equipped with the conventional air brake compared with the one traveled by a ECP equipped train, the results represent the position and the velocity of center of mass of the trains. From the results obtained for the same train, as previously explained, the stopping distance and is reduced by approximately 40%. The train runs 1395.6 m before stopping with conventional brake as the train equipped with the ECP stops after about 895.4 m. These results confirm what is said in several scientific papers like [2] and [3] about the decreasing of the stopping distance.

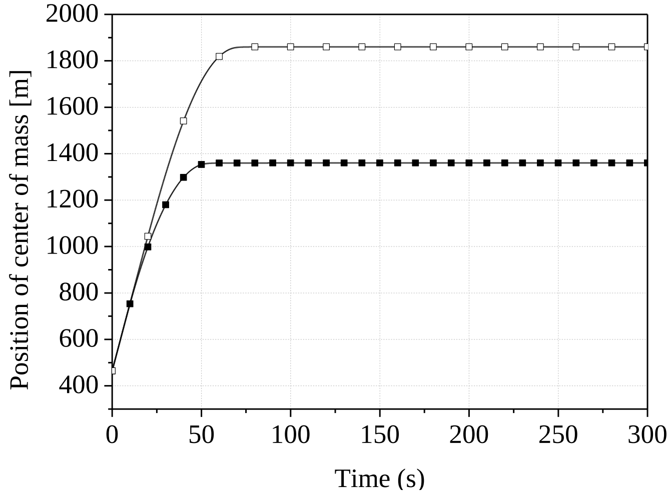

Figure 41 Stopping distance
ECP Conventional air brake

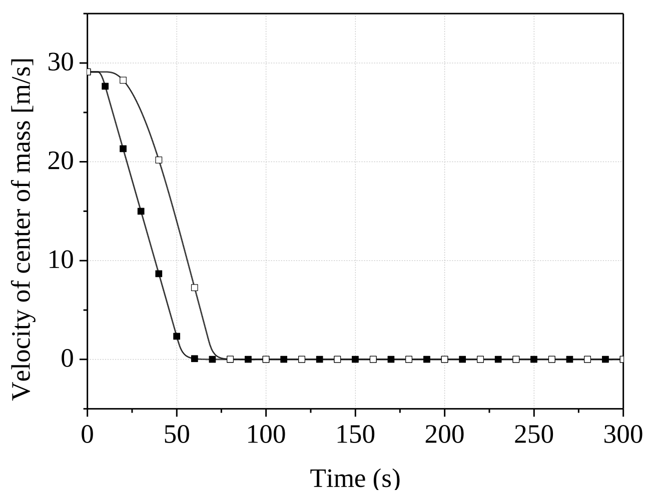

Figure 42 Velocity of the center of mass
ECP Conventional air brake

Longitudinal Couplers Force

In the next simulation we will show you how in a situation of long freight train braking system as proposed ECP substantially reduces the forces acting in the couplers. The simulation is conducted on the same train model previously used for the simulations about the stopping distance. A 75-car model for a train with 3 locomotives travelling on a tangent track is considered. It is assumed that all the cars and the locomotives have initial forward velocity of 29.1 m/s (65.0 mph), and the brake pipe length is 1059.5 m (3476.05 ft), which is modeled using 150 finite elements, the characteristics of it such mass, number of wheelset, dimension of the cars and locomotives are shown in Table 3. The train will start with the reservoirs at the operative pressure of 90 psig (721853.15 Pa), after 5 seconds a full service application is made then at 80 seconds a full release is commanded. The simulation will continue until all the auxiliary reservoirs are fully recharged at the operative pressure. For the conventional air brake train is well known that the longitudinal force in a braking situation like the one simulated are for the most part compression forces caused by the delay in the brake application, another numerical study of this phenomenon can be found in [18]. The coupler force depend also by the type of couplers used in the simulation , in the presented results is used an End of Car Cushioning Device force model (see chapter 5).The ECP model as it was said before completely eliminates the problem of the delay in application thanks to the electronic communication system.

In figures 43, 44 and 45 are presented the behavior the of the conventional air system equipped train in the previously described scenario. It is possible to see how the well-known phenomenon of the delay time affects the performance of the system resulting in a less efficient application of the brake.

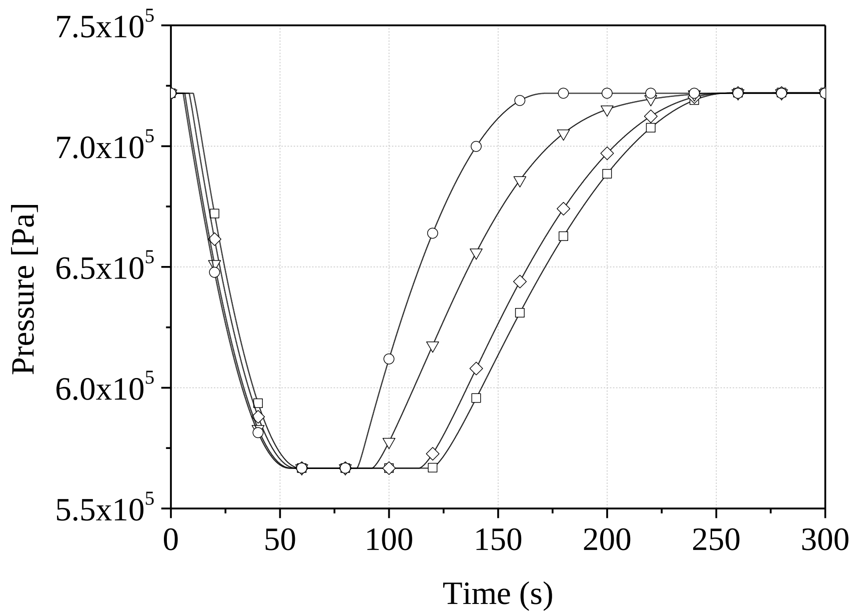

Figure 43 Pressure in auxiliary reservoirs
car 1 —○— car 25 —▽— car 50 —◇— car 75 —□—

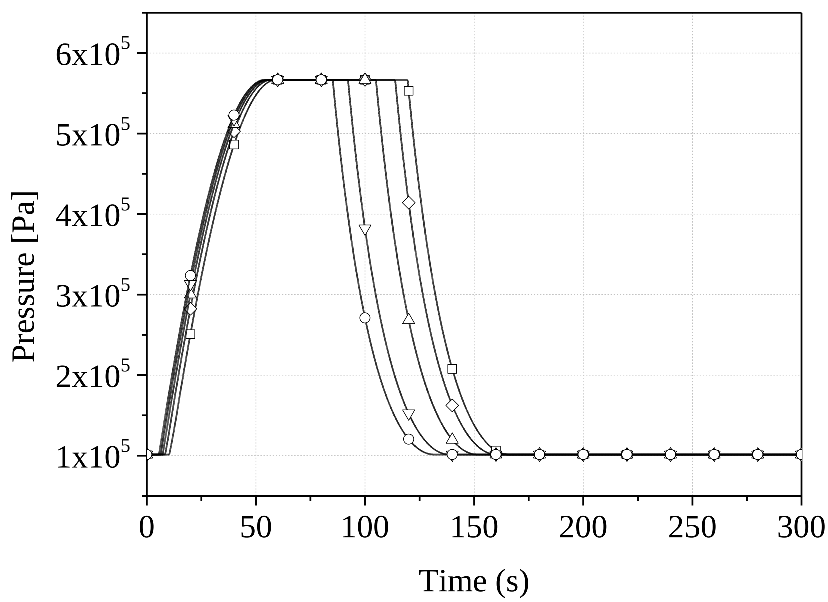

Figure 44 Pressure in the brake cylinders
car 1 —○— car 25 —▽— car 35 —△— car 50 —◇— car 75 —□—

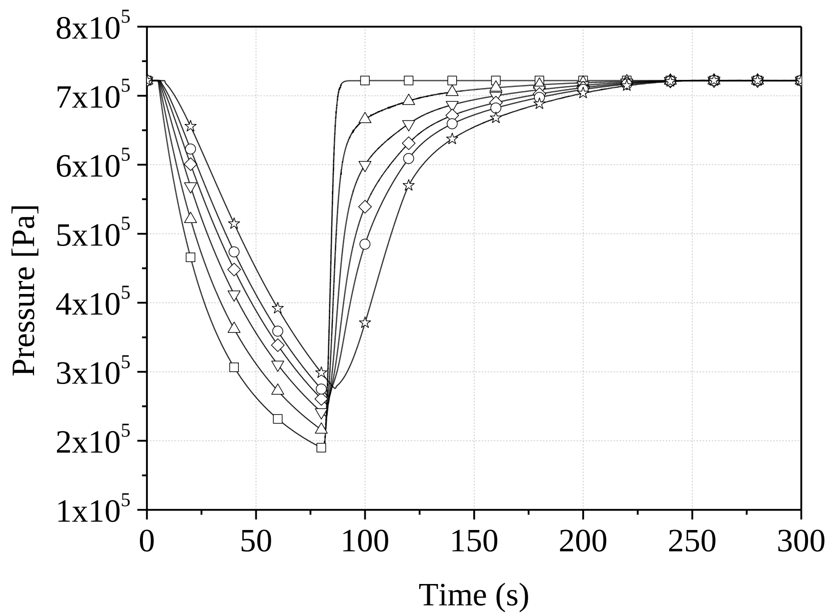

Figure 45 Pressure in the brake pipe
node 1 —□— node 20 —△— node 60 —▽— node 80 —◇— node 90 —○— node 150 —☆—

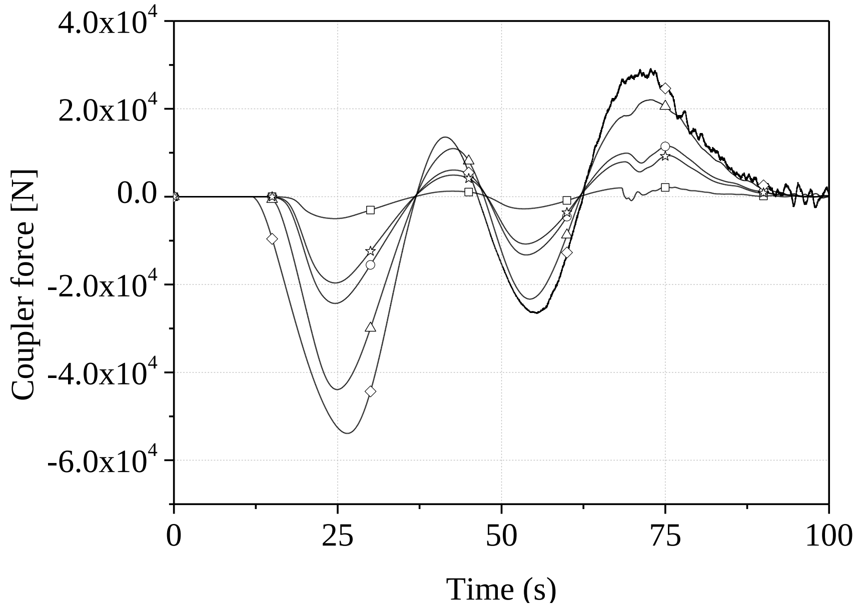

Figure 46 Couplers forces of conventional air brake train
coupler 1 —□— coupler 25 —☆— coupler 35 —◇— coupler 40 —△— coupler 60 —○—

On the other side, as showed in figures 47 and 48, the delay time is approximately zero for the ECP equipped train with all the cars applying brake at the same moment.

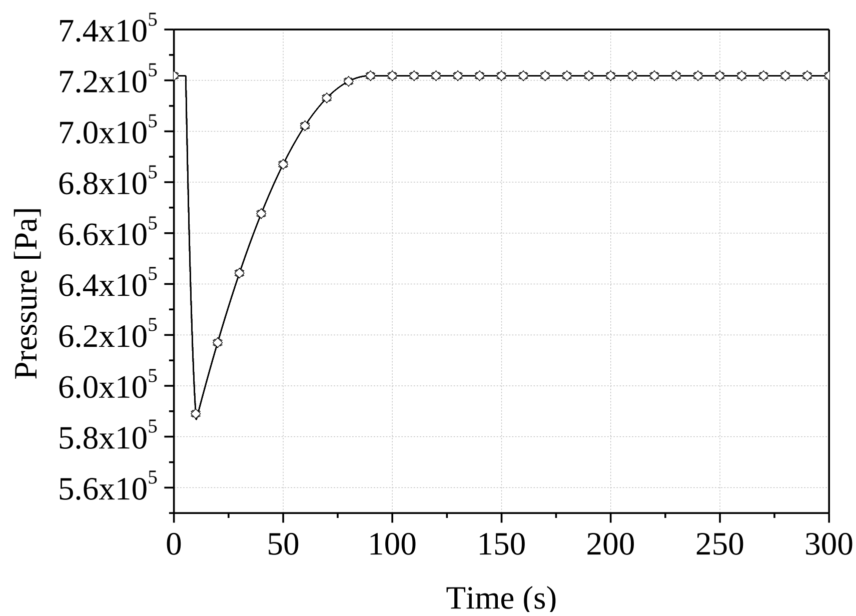

Figure 47 Auxiliary reservoirs pressure (ECP system)
car 1 —○— car 25 —▽— car 35 —△— car 50 —◇— car 75 —□—

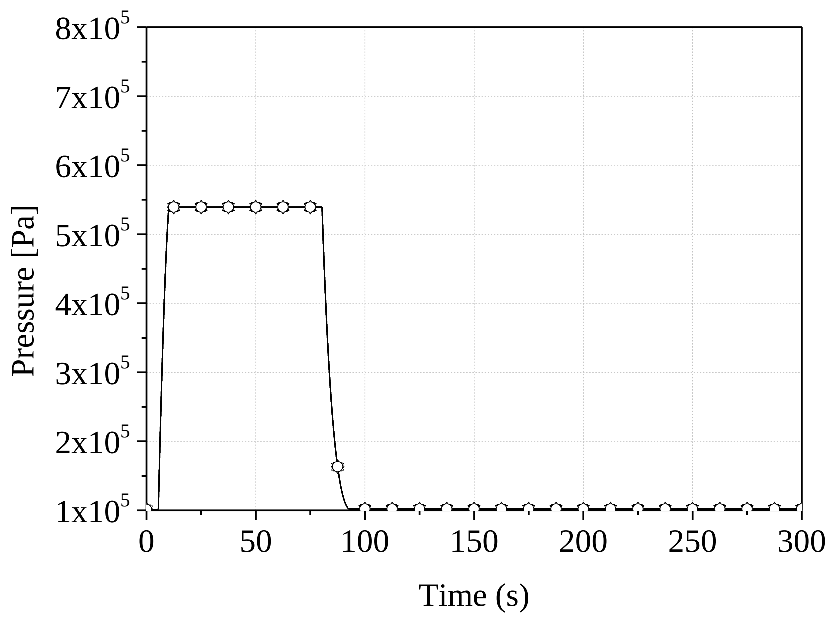

Figure 48 Brake cylinder pressure
car 1 —○— car 25 —▽— car 35 —△— car 50 —◇— car 75

An analysis of the couplers force distribution along the train will be now made. As a reference is useful to recall the study of Nasr et al, 2010 [18] who studied as well the distribution of the couplers along the train in order to study the longitudinal dynamic of a freight train equipped with a conventional air brake system. In Nasr model the delay of application of the braking force was an input of the system and in his paper he tries to determine the correct delay time comparing the couplers force distribution along the train. In this study the delay time is determined by the finite elements model of the brake pipe in a systematical way.

The figures 49 and 50 represents the couplers force along the train, on the x-axis is represented the position of the *i*-th couplers normalized on the length of the train, on y-axis the maximum value reached of compression and traction forces are represented. As is well known in the railroad area, in a train equipped with the conventional air brake system the higher forces should be in the central couplers of the train because the suffer the most the compression force caused by the longer delay time of the last cars. The results obtained confirmed this well-known phenomenon.

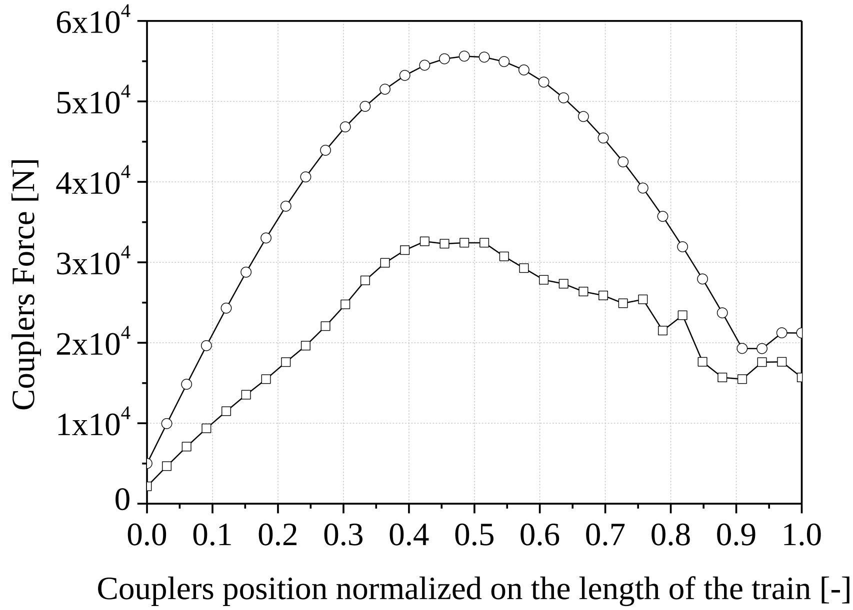

Figure 49 Maximum couplers forces in conventional train
—○— Compression force —□—Traction force

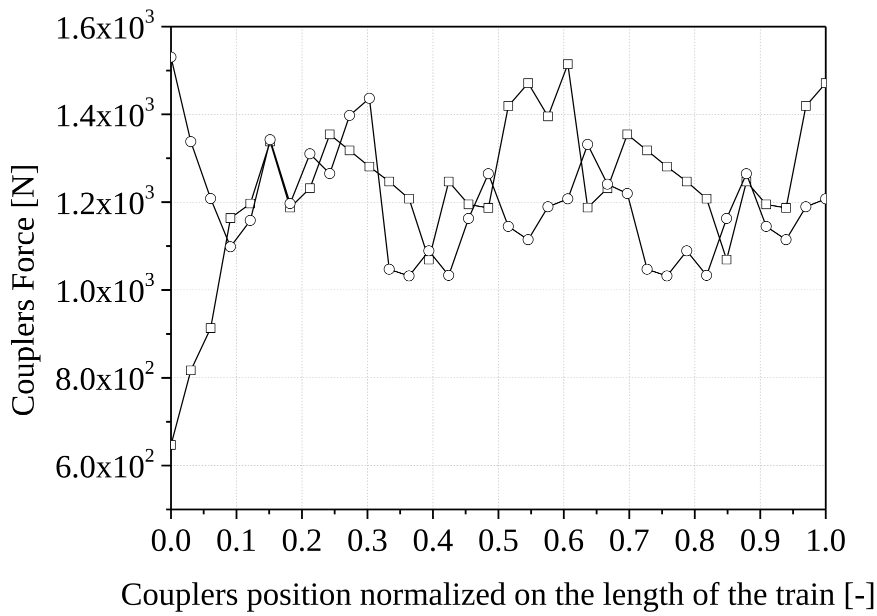

Figure 50 Maximum couplers forces in ECP train
—○— Compression force —□—Traction force

In the ECP train a complete different scenario is observed; thanks to the simultaneous application of the brake force in all the cars the couplers force along the train are significantly lower than in the previous case. Moreover the distribution of the couplers force along the train is more or less constant along the train, or at least with smaller variation of the values than the previous conventional air brake system equipped train.

Charging

The executed simulation shows also the different behavior of the system in the charging phase. As showed in Fig 35 the conventional system starts charging of the reservoirs when the release command is given, it is also affect by the delay time of because the pressure in the auxiliary reservoirs present on the *i*-th car can starts to increase only when the pressure in the brake pipe at the corresponding connecting point is higher than the actual auxiliary pressure. As a result the time necessary to fill all the reservoirs of a 75-car train for the conventional air brake system is about 170 seconds. The ECP instead (Fig 39), not using a brake pipe drop to transmit the signal, can start to charge the reservoirs as soon as the pressure in the auxiliary become lower than a fixed threshold, so the charging start in an automatic way, without any specific command from the HEU. This result in faster recharging evaluate in about 90 seconds, with a reduction of about 50% in respect to the conventional system.

Table 1 Brake Pipe properties (conventional air brake system)

Parameter description	Value
Air temperature	300 ^{o}K
Air viscosity	1.95×10^{-5} Pa.s
Atmospheric pressure	101.325 kPa (14.7 psia)
Brake pipe diameter (1¼” Schedule 80 extra heavy pipe)	3.246 cm (1.278 inches)
Operating pressure	620.5 kPa gage (90 psig)
Main reservoir pressure	951.48 kPa gage (138 psig)

Table 2 Car control unit properties

Parameter description	Value
Number of brake cylinders per car	1
Number of brake shoes per car	8
Brake rigging leverage ratio	10:1
Brake rigging efficiency at full service brake	0.65
Brake shoe/wheel friction coefficient	0.35
Brake cylinder spring stiffness	14593 N/m
Brake cylinder maximum swept volume	10296 cm3
Brake piston effective frontal area	506.7 cm^2
Brake cylinder and auxiliary reservoir equivalent connecting area	0.0236 cm^2
Brake cylinder and emergency reservoir equivalent connecting area	0.0400 cm^2
Brake cylinder and atmosphere equivalent connecting area	0.0446 cm^2
Brake cylinder piping volume	4839.3 cm^3
Auxiliary reservoir to brake valve piping volume plus quick service volume in pipe bracket	4439.1 cm^3
Emergency reservoir to brake valve piping volume	3186.6 cm^3
Auxiliary reservoir volume	40967 cm^3
Auxiliary reservoir and brake pipe equivalent connecting area	0.0201 cm^2
Emergency reservoir volume	57354 cm^3
Auxiliary Reservoir and Cut-Out Valve upper chamber connecting area	0.00314 cm^2
Diameter of the passage section Cut-Out Valve	1 cm
Maximum Displacement of the Cut-out Valve	0.1 cm
Upper chamber frontal area Cut-Out Valve	0.5 cm^2
Lower chamber frontal area Cut-Out Valve	0.085 cm^2
Initial Volume of the upper chamber of the Cut-Out Valve	7.6 cm^3
Auxiliary Reservoir and Vent Valve upper chamber connecting area	0.0314 cm^2
Diameter of the passage section Vent Valve	0.5 cm
Maximum Displacement of the Vent Valve	0.15 cm
Upper chamber frontal area Vent Valve	0.5 cm^2
Lower chamber frontal area Vent Valve	0.085 cm^2
Initial Volume of the upper chamber of the Vent Valve	7.6 cm^3
Auxiliary Reservoir and Auxiliary and Emergency Valve upper chamber connecting area	0.0314 cm^2
Diameter of the passage section Auxiliary and Emergency Valve	0.5 cm

Maximum Displacement of the Auxiliary and Emergency Valve	0.15 cm
Upper chamber frontal area Auxiliary and Emergency Valve	0.5 cm^2
Lower chamber frontal area Auxiliary and Emergency Valve	0.085 cm^2
Initial Volume of the upper chamber of the Auxiliary and Emergency Valve	7.6 cm^3
Stiffness of the piston spring in the ECP valves	3500 N/m

Table 3 Train model data

Parameter description	Value
Number of cars	75
Number of locomotives	3
Cars mass (full loaded)	129727.42 Kg
Locomotives mass	166921.99 Kg
Number of wheelsets for car	4
Number of wheelsets for locomotive	6

BIBLIOGRAPHY

[1] American Association of Railroads, 2011A, Manual of Standards and Recommended Practices-Section E-II, Electronically controlled brake system, Association of American Railroads.

[2] Chris Formenton, 2009, Improving Operational Performance of Freight Trains using Electronically Controlled Pneumatic (ECP) Braking, IRSE Australasia Technical Meeting: Sydney

[3] Brian Smith, Fred Carlson, 1999, Electronically Controlled Pneumatic (ECP) brake systems, Railway Age, Vol. 200 Issue 9,Transportation Technology Center, Inc. (TTCI), Pueblo, Colorado

[4] Mark Dingler, Yung-Cheng (Rex) Lai, Christopher P.L. Barkan, 2010, A Review of the Effects of CBTC and ECP Brakes on Railroad Capacity, Transportation Research Record: Journal of the Transportation Research Board

[5] Specchia S., Afshari A. and Shabana A. A., 2011, "A Train Air Brake Force Model: Locomotive Automatic Brake Valve and Brake Pipe Flow Formulations", Proceedings of the Institution of Mechanical Engineers, Part F: Journal of Rail and Rapid Transit January 2013 vol. 227 no. 1 19-37

[6] Afshari, A., Specchia, S., Shabana, A. A., 2011, "A Train Air Brake Force Model: Car Control Unit and Numerical Results", Proceedings of the Institution of Mechanical Engineers, Part F: Journal of Rail and Rapid Transit January 2013 vol. 227 no. 1 38-55

[7] US 6422531 Ecp manifold valve inserts, 2002, Gary M. Sich and Wabtec Corporation

[8] Shabana, A. A., 2010, *Computational Dynamics*, Third Edition, John Wiley and Sons.

[9] Sanborn, G., Heineman, J., and Shabana, A.A., 2007, "A Low Computational Cost Nonlinear Formulation for Multibody Railroad Vehicle Systems", Proceedings of the 2007 ASME Design Engineering Technical Conferences, Paper # DETC2007-34522, Las Vegas, Nevada, September 4 – 7, 2007.

[10] Sanborn, G., Heineman, J., and Shabana, A.A., 2007, "Implementation of Low Computational Cost Nonlinear Formulation for Multibody Railroad Vehicle Systems", Proceedings of the 2007 ASME Design Engineering Technical Conferences, Paper # DETC2007-34525, Las Vegas, Nevada, September 4 – 7, 2007.

[11] Safety Evaluation of TSM Prototype Electronically Controlled Pneumatic train brake system on brake rack, 1998, Federal Railroad Administration

[12] Shabana, A.A., 2008, *Computational Continuum Mechanics*, Cambridge University Press.

[13] Abdol-Hamid, K.S., 1986, “Analysis and Simulation of the Pneumatic Braking System of Freight Trains”, Ph.D. Dissertation, Department of Mechanical Engineering, University of New Hampshire, Durham, New Hampshire.

[14] Shabana, A. A., Zaazaa, K. E., and Sugiyama, H., 2008, *Railroad Vehicle Dynamics: A Computational Approach*, Francis & Taylor/RC.

[15] Shabana, A. A., Ahmed K. Aboubakr., and Lifen Ding., 2012, “Use of the Non-Inertial Coordinates In the Analysis of Train Longitudinal Forces”, Computational and Nonlinear Dynamics,7,pp. 1-10.

[16] Massa, A., Stronati, L., Ahmed K. Aboubakr, Shabana A. A., and Bosso, N.,2011., Study Of The Effect of Train Coupler Inertia ., Nonlinear Dynamics Volume 68, Issue 1-2 , pp 215-233

[17] Cole, C., and Sun, Y.Q., 2006, “Simulated Comparisons of Wagon Coupler Systems in Heavy Haul Trains”, IMechE Journal of Rail and Rapid Transit, Vol. 220, pp. 247- 256.

[18] Nasr, A., and Mohammad, S., 2010, “The effects of train brake delay time on in-train forces”, Proceedings of the Institution of Mechanical Engineers, 224, Part F: Journal of Rail and Rapid Transit, pp. 523-534

[19] John, J. E., and Keith, T. G., 2006, *Gas dynamics*, Third Edition, Pearson Education, Inc.

[20] White, F.M., 2008, *Fluid Mechanics*, Sixth Edition, McGraw Hill Book Company.

APPENDIX

In order to be able to develop the valve equations, several basic thermodynamics relationships must be used in [19] and [20] . The first is the universal law of gases for a volume V_f of a component f given by

$$P_f V_f = m_f R_g \Theta_f \tag{A1}$$

where P_f is the absolute pressure inside the volume (N/m^2), V_f is the volume (m^3), m_f is the mass (Kg), R_g is the gas constant (J/(Kg °K)) and Θ_f is the temperature (°K). Differentiating the preceding equation with respect to time and assuming isothermal process ($\Theta_f = \Theta$ is constant), one obtains

$$\frac{dP_f}{dt} = \frac{1}{V_f}\left(R_g \Theta \frac{dm_f}{dt} - P_f \frac{dV_f}{dt} \right) \tag{A2}$$

There are different formulas for calculating the rate of mass flow through orifices. For more detail see [13], [19] and [20].

In this paper, the total mass flow rate to component e is denoted by $dm_e/dt = \dot{m}_e$, while the mass flow rate from component f to component e as shown in Fig. A1, is denoted by $\dot{m}_{e-f}$ calculated using the following formula:

$$\dot{m}_{e-f} = \frac{dm_{e-f}}{dt} = -\dot{m}_{f-e} = 0.6 A_{e-f} P_e \sqrt{\frac{|r^2 - 1|}{R_g \Theta}} \frac{|r-1|}{r-1} \tag{A3}$$

where P_e is be the pressure inside component e, r is the pressure ratio ($r = P_f / P_e$), R_g and Θ are the gas universal constant and gas temperature, respectively, and A_{e-f} is the equivalent area of the two areas connecting the two components (i.e. A_e and A_f). As reported in the literature [13], the difference between different formulas is always less than 10%, which can be less than the error in calculating the geometric area of the orifice. The preceding equation, however, is simpler to use because it is valid for any value of the pressure ratio r (sonic or subsonic), while using other formulas requires a check of the value of r against the critical pressure ratio $r_c = 1.893$ that defines whether the flow is sonic or subsonic.

With the assumption of a series connection, A_{e-f} can be calculated as follows:

$$A_{e-f} = \frac{1}{\sqrt{\frac{1}{A_e^2} + \frac{1}{A_f^2}}} = \frac{A_e A_f}{\sqrt{A_e^2 + A_f^2}} \tag{A4}$$

While Eq. A1 is based on the assumption that the two components, schematically shown in Fig. A1, have constant volumes, this equation is applicable to any CCU part.

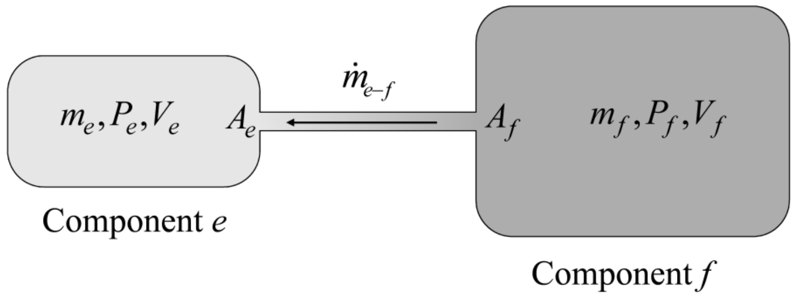

Figure A1 The mass flow rate between components *e* and *f*